Master Thesis in Geosciences

Recent changes in glacier area in the Central Southern Alps of New Zealand

- Mapped from ASTER satellite imagery

Endre Før Gjermundsen

UNIVERSITY OF OSLO

FACULTY OF MATHEMATICS AND NATURAL SCIENCES

UNIVERSITY *of* OTAGO

Te Whare Wānanga o Otāgo

Recent changes in glacier area in the Central Southern Alps of New Zealand

- Mapped from ASTER satellite imagery

Endre Før Gjermundsen

Master Thesis in Geosciences

Discipline: Physical Geography and Geomatics

Department of Geosciences

Faculty of Mathematics and Natural Sciences

UNIVERSITY OF OSLO

[January 2007]

Recent changes in glacier area in the Central Southern Alps of New Zealand

- Mapped from ASTER satellite imagery

Endre Før Gjermundsen

This work was carried out in collaboration with:

UNIVERSITY *of* **OTAGO**

Te Whare Wānanga o Otāgo

School of Surveying

UNIVERSITY OF OTAGO

[January 2007]

Background

In 2002 I spent a year at the University of Otago in Dunedin, New Zealand, doing papers in Remote Sensing, climatology and GIS. I attended some papers with Renaud Mathieu at the School of Surveying and with Blair Fitharriz at the Department of Geography. I also did a small project with Renaud on remote sensing of glaciers. In addition to studying, I was introduced to New Zealand's amazing nature and mountains. A few years later, when I was about to start on my masters, I wasn't quite sure where to go. I wanted to go abroad again, maybe to South-America, but back to New Zealand sounded attractive too. I had stayed in touch with Renaud since I left in 2002, and after strong encouragements from him to come back, and with all the familiar settings in New Zealand (I knew what I would get), this seemed more and more like the right thing to do. When Jon Ove made sure that I could go to the University of Otago and do my work down there as part of my Norwegian degree, and John Hannah (Dean of School of Surveying at that time) welcomed me to his Department, there was no reason not stay home. There were still lots of mountains I wanted to climb in the Southern Alps….

Acknowledgements

Abstract

Change in glacier extent is a good indication of climate change. Inventories for glaciated areas should therefore be made at certain intervals. For New Zealand a digitized glacial inventory including both the two main islands' glaciers was made from aerial photographs recorded in 1978. This inventory needed an update.

One Aster scene (60*60km) recorded 14. February 2002 covering the central Southern Alps of New Zealand is used for the updating. The area covered by the image contained, in 1978, 41% of the glaciated areas in New Zealand. The image was orthorectified using a combination of points collected in field and points from the New Zealand topographic database and DEM made from 20-meter contour intervals in PCI. Due to the problems often involved in automatic methods for glacier extraction, the glacier areas on the image were manually digitized. For validation of the digitizing, field work was conducted during late summer of 2005 (Feb-April). Glacier outlines were mapped for 9 individual glaciers using a differential GPS. These data were later corrected to a base antenna giving sub-meter accuracy. 5 of these 9 glaciers were so called 'Index glaciers' that had been annually photographed since 1977 as a part of the New Zealand Annual Snowline Survey. Aerial photographs of the 5 field work Index glaciers, were used to adjust for eventual changes in the glacier outlines between image acquisition and the in-situ recordings. Automatic classifications were tested on the entire image and on 3 zoomed in study areas to give an estimate of the efficiency of these automatic methods in the New Zealand setting. Band ratio of ATER3/ASTER4 proved to be the most efficient automatic classification method, with the threshold set around 2.0. However, as a result of the large debris cover on many glaciers in New Zealand, automatic glacier extraction would require significant manual post processing. The manually digitized glacier map was used to calculate the change in glacier area since 1978. An overall reduction of 16.6% was found, more specifically 14.3% for the western and 18.3% eastern side of the Main Divide of the Southern Alps. The large and fast flowing western glaciers, Fox and Franz Josef Glaciers, were pulsing back and forward in the study period, but showed an overall advance, whereas the large low-gradient heavily debris covered valley glaciers developed proglacial lakes and have shown a rapidly increasing retreat due to calving. The smaller high elevated alpine glaciers in the area show only slight changes.

TABLE OF CONTENS

TABLE OF CONTENTS

TABLE OF CONTENTS

1. INTRODUCTION

1.1 General background

Glaciers are sensitive indicators of climate change, growing and wasting in response to changes in temperature and precipitation (Fitzharris, 1992). Thus, the past and present glacier fluctuations serve as a valuable source of information for understanding global and local climate change patterns. In turn, large glaciers and ice sheets exert their own influence on regional climate, altering pressure systems and wind directions, and serving to keep vast areas locked in perpetual cold. They also influence the sea currents, and a retreat of the world's glaciers will lead to a rise in the global sea level (Oerlemans, 1989). The potential economic impact of sea-level rise is enormous. High altitude glaciers are also important for managing local water resources as glaciers are a significant water source from mid- to late-summer water for either direct consumption, agricultural use, or for hydro-electric power generation.

Approximately 10% of the earth land surface is covered by glaciers. The ice sheet of Antarctica contributes to 84% of the total, the ice sheet of Greenland to 13% and the remaining 3% or 500,000 km² exists as ice caps and glaciers located at high latitudes or in mountainous regions around the world (Benn & Evans, 1998). These are located predominantly in the northern hemisphere, specifically around the Arctic Ocean basin, in mountainous maritime localities like Norway, Alaska and the Andes in the southern hemisphere, and in continental high mountain terrains like the European Alps and the Himalayas (Benn & Evans, 1998). New Zealand glaciers only represent about 0.2% of the total area of the worlds glaciers and ice caps (Fitzharris et al., 1997). While relatively insignificant in term of surface, the glaciers of the Southern Alps of New Zealand are the most significant in the Southern Hemisphere outside Antarctica and South America. Thus, the nature and behaviour of New Zealand's glaciers are of wide scientific interest, because they are highly sensitive, high input-output systems that represent the temperate, maritime end of the glacier behaviour continuum (Fitzharris et. al., 1999).

More knowledge about glacier area and volume changes is essential in order to get a better understanding of the changes in today's climate and be able to better predict future changes as

a result of global warming. The Intergovernmental Panel on Climate Change considers that with anthropogenic global warming, temperate glaciers will make an important contribution to sea-level rise over the next century (IPCC, Climate Change, 2001). Hence, the responses of New Zealand glaciers to climate changes should be placed in this wider global context. There have also been an increase research interest in global-scale linkages in response to climate change and the role of the southern hemisphere (Clare et al, 2002).

1.2 Background on the glaciers in New Zealand

The Southern Alps of New Zealand lie athwart the prevailing westerly weather systems, and generate a strong west-east orographic precipitation gradient with and associated steep eastward rise of glacier equilibrium line altitudes. Extremely maritime glaciers occur west of the Main Divide, with "dry" balance glaciers and rock glaciers lying to the east. Norway, Alaska and Chile also have glaciers lying in the prevailing westerlies. Thus, more knowledge about the glaciers in New Zealand will gain the general knowledge of these glacier systems. Both Norway and New Zealand experienced recent glacial advances, commencing in the early 1980s and ceased around 2000, which were more extensive than any other since the end of the Little Ice Age. Common to both countries, the positive glacier balances are associated with an increase in the strength of westerly atmospheric circulation which brought increased precipitation (Chinn et al, 2005).

In 1978 a complete and unique inventory of New Zealand glaciers was carried out by T. Chinn using aerial photographs. T. Chinn identified 3144 glaciers covering a total area of 1158 km² (Chinn, 1991). Except for some glaciers on the volcano Mount Ruhapehu in the North Island all glaciers are distributed along the Southern Alps, from 42 to 45 degrees south latitude (Chinn, 1991). The number of individual glaciers in New Zealand is relatively high, but the average size is very small because of a steep topography, which favours individual small cirque glaciers and ice patches on separate peaks (Chinn, 2000). The bulk of this ice is located in the icefields of the Mt Cook area of the Southern Alps at around 43.5º south.

Chinn's inventory is now over 25 years old and needs to be updated. Paul, 2003, recommends that national inventory glacier data should be updated at approximately a decadal scale. An

urgent need for an update of the 1978 inventory was also pointed out by the New Zealand's Snow and Ice Research Group (Annual Workshop, January 2005). Glacier research in New Zealand has typically concentrated on only a few key glaciers such as Franz Josef and Tasman glaciers and has focused on understanding glacier change (Fitzharris et al., 1999). This fact also highlights the need for a new glacier inventory in order to get a broader picture on the development of New Zealand glaciers.

Satellite remote sensors have the capability to image large areas of the earth's surface at a relatively low cost compared to aerial photographs. Recent glacier inventories using satellite imagery have been made in Switzerland, the New Swiss Glacier Inventory 2000 (Paul, 2003). The moderate spatial resolution of earlier satellites (e.g. Landsat MSS 1 and 2, with 80 m spatial resolution) was not appropriate in the New Zealand context where glaciers are typically small and steep. By contrast, the "Advanced Spaceborne Thermal Emission & Reflection Radiometer" (ASTER) instrument, with a spatial resolution ranging from 15 to 30 m, has good potential to meet the necessary accuracy requirements for glacier mapping in the New Zealand context. ASTER satellite images are currently used by scientist working in the international program "Global Land Ice Measurements from Space" (GLIMS) (Kargel et al., 2005). The GLIMS program was initiated in 1999 by the US Geological Survey with the aim of mapping world glaciers and extracting glaciological information through the use of satellite imagery. Over 60 institutions across the globe are involved in GLIMS, including New Zealand.

1.3 Objectives

The overall aim of this thesis is to quantify the glacier area change in the Central Southern Alps of New Zealand over the last approx 25 years. In order to reach this aim various approaches to inventory New Zealand glaciers using ASTER imagery are tested. More specific objectives are:

- Map and quantify the glacier area in the Central Southern Alps by photo-interpreting and manual digitizing a multi-spectral ASTER satellite imagery.

- Compare this photo interpretation with field data and semi-automatic per-pixel classifications.

- Compute the area of the 1978 GIS glacier map within the boarders of the chosen 2002 ASTER image.

- Quantify the glacier area change between 1978 and 2002 and discuss on the possible reasons behind these changes.

1.3 Structure of the thesis

The thesis is presented in six main chapters. In chapter 2 general theoretical background of glaciers, their characteristics and their fluctuations according to climate change are covered. It reviews glacier research in New Zealand, and describes techniques for glacier inventories. A full understanding of this chapter might require a basic knowledge in glaciology and remote sensing.

Chapter 3 describes the methodological framework of the study. It covers the data used and the satellite image processing and the extraction of glacier area using different approaches, including field work, photo image interpretation and classification.

Chapter 4 compares the manual digitizing of the image to the fieldwork conducted to get an estimation of the accuracy of this digitizing. It presents the results of the various classification techniques tested.

Chapter 5 gives the overall glacier area change in the study area between 1978 and 2002 and a more specific description of some characteristic glaciers.

Chapter 6 discusses the results and the accuracy of the different approaches. The findings are compared to other parts of the world.

2. Literature review

2.1 Glaciers

2.1.1 What is a glacier?

Professor H. Ahlman defined a glacier as such: "A glacier is a many year old mass of snow and ice in movement" (Liestøl, 2000). By including movement in the definition he excluded most snow patches. A similar expression of the same professor can be found in Brelære, by Atle Nesje, 1995; "A glacier is a mass of snow and ice, which mainly is bedded on land, and which is or has been in motion". People have had different opinions on what a glacier is, through the historic times, and one example is R. Fotherby, The Voyages of William Baffin (17th century) in The Physics of Glaciers, Paterson 1994; "This huge ice is, in my opinion, nothing but snow, which… is only a little dissolved to moisture, whereby it becomes more compact…". In the seventies the International Commission on Snow and Ice (ICSI, UNESCO) determined that the smallest area for a glacier or glacierette was 0.01 km² or one hectare (Chinn, 1988). This is a permanent patch of perennial snow and ice 100m by 100m. However, it was considered that it's not the size (area) alone that determined whether an area of snow and ice is a glacier or not. The snow patch has to survive all summers over a period of one or two decades. If, in this length of time, it does not have the substance to survive through the summer of greatest melt, then it can only be called a snow patch. This definition was adopted for mapping New Zealand glaciers. "Those ice bodies of 1 ha or greater in area which have remained in existence during the most negative balance years over the past two decades" were considered as glaciers (Chinn, 1991).

Winter-accumulation type glaciers are created where summer temperatures are not high enough to melt all the winter snowfall. Such conditions are found in high mountain areas and near the poles. Fresh snow accumulates year after year on the snow that did not melt during the summer. The snow pack eventually becomes so thick that the deepest layers turn into ice. The ice then begins flowing outwards and downwards in warmer areas where the ice melts (figure 2.1). Equilibrium is established on the glacier when the surplus in the higher areas is

balanced by a corresponding deficit in the lower areas of the glacier. The boundary between the accumulating areas and depleting areas is called the equilibrium line or snow line (figure 2.2). Snow remains above this line at the end of the summer while blue ice emerges below the line. The glacier is said to be in climatic equilibrium when the surplus and the deficit are equal, or in other words, when it keeps a constant volume from year to year (Liestøl, 2000). This description is not applicable to calving glaciers though, where temperatures are so low that the ice reaches the sea where it calves and melts in contact with the sea. The altitude of the equilibrium line depends on the amount of precipitation and the temperature. It rises from maritime areas where precipitation is high, to continental areas which are a lot dryer and colder (figure 2.2).
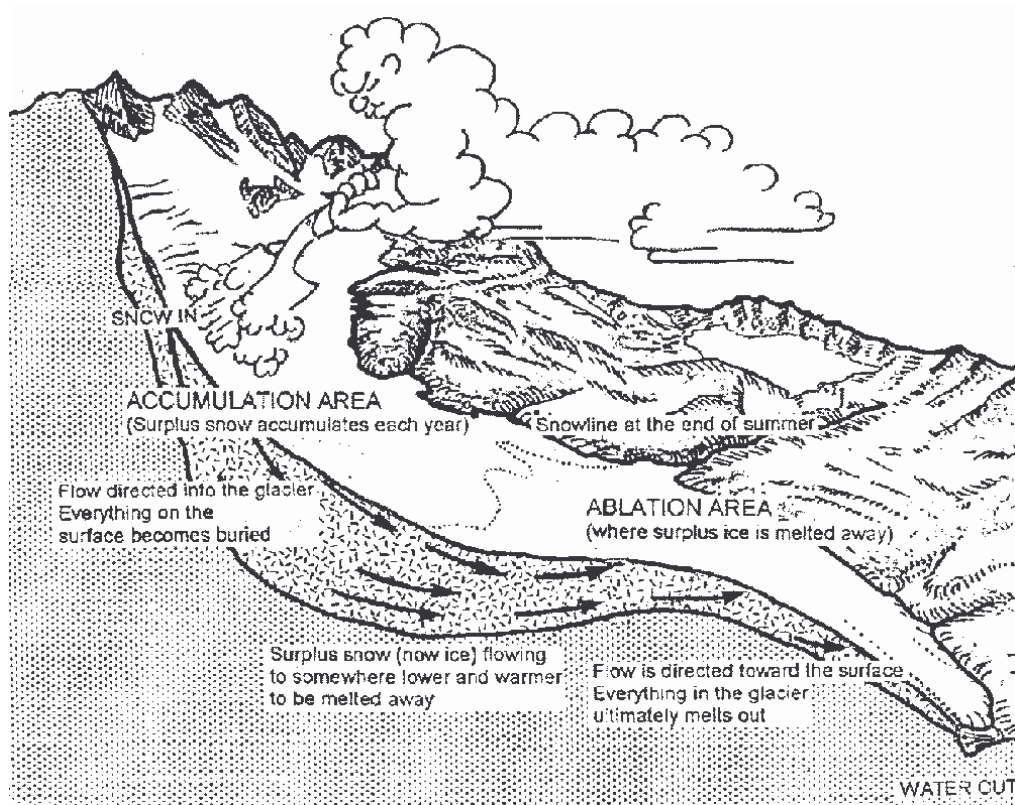
Figure 2.1 *Glacier basics, drawn by Trevor Chinn (printed in Chinn 2002)*
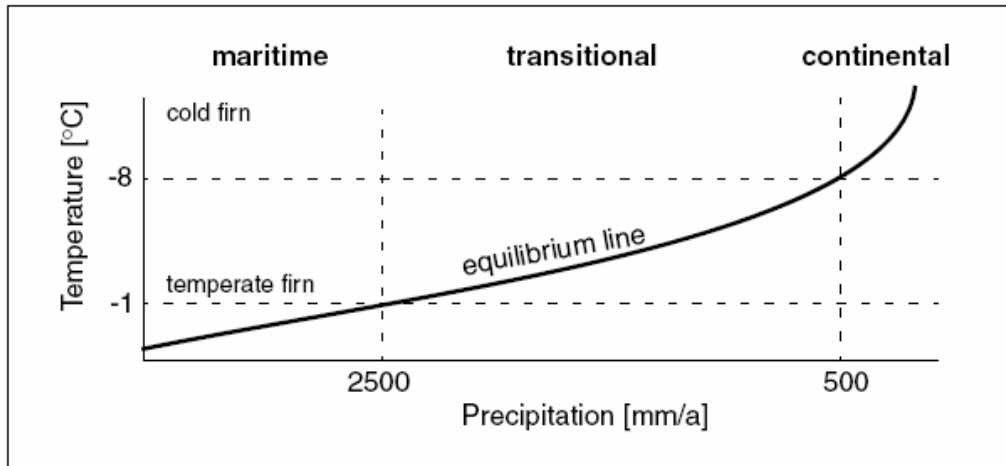
Figure 2.2 *The climate type of a glacier is governed by the annual precipitation and the average annual air temperature at the equilibrium line (after UNEP, 1992, in Paul 2000).*

Volume change for a glacier is expressed by the mass balance or the relation between ablation and accumulation through a year. This is measured from the minimum mass balance one year (the end of the melting season) to the minimum mass the following year (Liestøl, 2000). The ablation gradient and the accumulation gradient are the rates at which annual ablation and accumulation change with altitude. Together they define the mass balance gradient (Benn & Evans, 1998).

2.1.2 Glacier types

There are mainly two ways of classifying glaciers:

1. Morphologically, - which is mainly based on the three dimensional shape of the glacier.
2. Geophysically, - which is mainly based upon temperature conditions and other physical properties of the glacier mass.

Morphological classification; The glacier size and form will mainly be determined by the underlying relief and to which extent the area is glacierized which in turn mainly depend on the climate (Liestøl, 2000). How to morphologically divide glaciers into different classes has been a subject of debate amongst scientists, and different proposals have been suggested (Liestøl, 2000). Figure 2.3 shows examples of the morphological types found in New Zealand.

8

 In addition to these one could also include glaciers terminating lakes as a geomorphological class by its own or as a sub-class.

Geophysical classification; Ahlman, in Paterson (1994), proposed the geophysical classification of glaciers according to ice temperature and amount of surface melting. Ahlamn's categories were temperate, sub-polar/polythermal and polar. A temperate glacier is at the pressure melting point throughout the ice mass, while a polar glacier has its whole mass below pressure melting point. A sub-polar is a combination of the two. New Zealand glaciers are all temperate glaciers of high maritime type with precipitation at or well above 3m/yr. In the upper accumulation zones of some of the highest glaciers, above the permafrost limit (approx 3000 m.a.s.l), the nèvès will contain cold (or polar) firn and ice making the glacier polythermal to a small degree (Chinn, 1991). Very few glaciers can be fitted into a single category, because conditions vary from one point of a glacier to another.

Glaciers have also been classified according to *their response to climate* (Haeberli, 1995). To be able to compare glaciers with similar response times, three basic types based on specific shape and topography have been defined:

1. Small, low-shear-stress cirque glaciers reflecting changes in climate and mass balance almost without delay;

2. Large, high-shear-stress mountain glaciers reacting to decadal variations in climate and mass balance forcing with an enhanced amplitude after a delay of several years;

3. Valley glaciers with low gradient tongues give strong and most efficiently smoothed signals of secular trends with a delay of several decades (Chinn, 1991). All these glacier types are present in New Zealand.
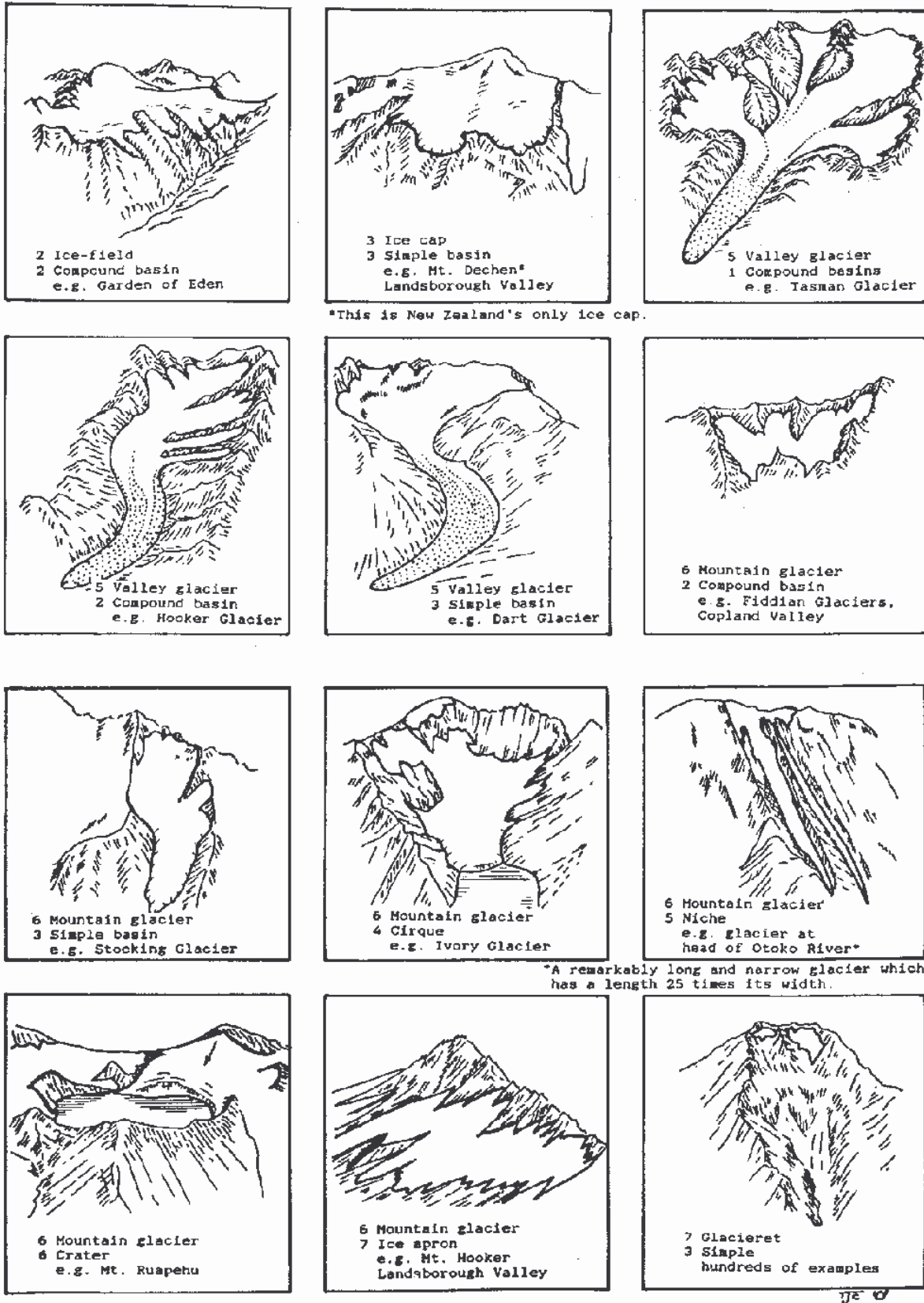
Figure 2.3 *Examples of glacier-types occurring in New Zealand according to the World Glacier Inventory classification. Figures drawn by Trevor Chinn. (printed in Chinn, 1988).*

2.1.3 Glacier physics

One of the most fundamental characteristics of ice is the ability to move. The deformation and sliding of glaciers under the force of gravity slowly transfers snow and ice from high-accumulation areas and continental interiors to areas of ablation, and allows glacial erosion and debris transport to take place (Benn and Evans, 1998).

Averaged over long periods, ice flow rates are governed by the climatic inputs (snow) and the geometry of the catchment. For an ideal glacier of constant size and shape, ice flow through a cross-section must exactly balance the accumulation and ablation taking place in the glacier. The ablation increases from zero at the equilibrium line to a maximum volume at the lower border of the glacier, producing a thinning wedge (figure 2.4). Similarly, accumulation increase from zero at the equilibrium line towards higher elevations, producing a thickening wedge. In order to maintain a steady state, the glacier must rectify the loss of the ablation wedge by transferring mass through the equilibrium line. The mass of each wedge is controlled by the snow or ice density, the mass balance gradient, and the width of the wedge. (Benn and Evans, 1998).
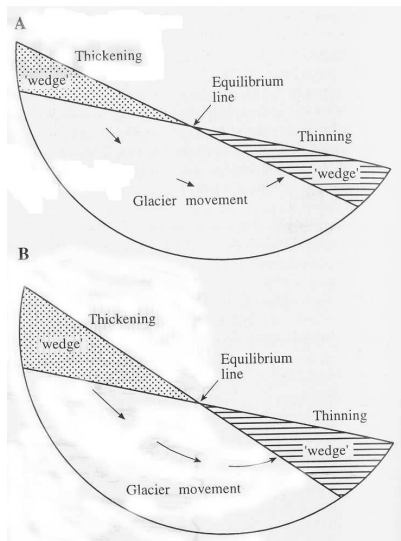
Figure 2.4 *The wedge model of glacier flow. Glacier B has a steeper mass balance gradient (typical maritime glacier, e.g. Fox and Franz Josef glaciers in New Zealand) than glacier A, so requires higher ice velocities to balance the mass gained and lost in the two wedges (Benn & Evans, 1998).*

The movement of glaciers results from permanent strain of the ice and the glacier bed in response to stress. Strain may occur by (a) deformation of the ice; (b) deformation of the glacier bed; or (c) sliding at the ice-bed interface (figure 2.5). Movement at the surface of a glacier is the cumulative effect of these processes acting singly or in combination (Benn and Evans, 1998).
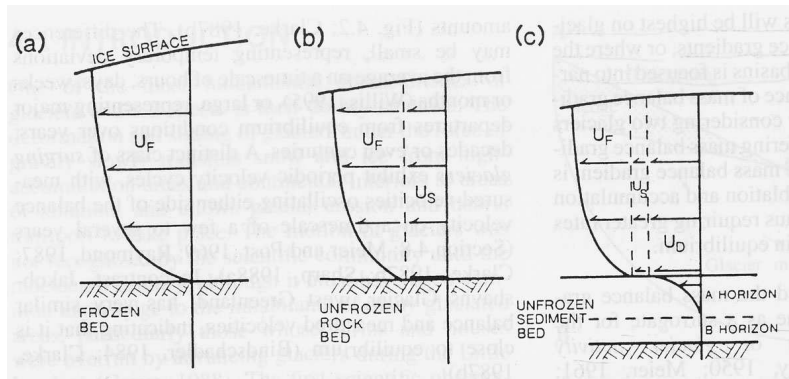
Figure 2.5 *Schematic diagrams showing the vertical distribution of velocity for glaciers moving by different mechanisms: (a) ice deformation only; (b) ice deformation and basal sliding; and (c) ice deformation, basal sliding and deformation of subglacial sediments. (Benn & Evans, 1998). B and C are the types that are found in New Zealand.*

2.1.4 Glaciers and environmental issues

2.1.4.1 Glaciers fluctuations and climate change

New Zealand glacier display a wide range of lag times in responding to changes in climate inputs (Chinn, 1996) (figure 2.6). The response time is the time a glacier takes to adjust to a change in its mass balance (Paterson, 1994). This is the same as the time the mass-balance perturbation takes to accumulate or remove the difference between the steady-state volumes of the glacier before and after the change in mass balance. The reaction time is the time it takes for the terminus to advance or retreat after a change in mass balance, this is also called the terminus response time. Salinger et al. (1983) believed that the reaction time for Stocking glacier was 2-5 years, and the Franz Josef glacier is generally thought to have a reaction time of 5-7 years (Fitzharris et al., 1999). The main valley glaciers on the eastern side of the NZ-Alps probably have response times of over a century (Chinn, 1996). In Norway similar reaction times occur, 5-6 years for Briksdalsbreen, 20 years for Nigardsbreen, and over 50 years for Tunsbergdalsbreen, all three outlets from Jostedalsbreen, i.e. being fed by the same accumulation basin (Jon Ove Hagen, personal communication). The reaction time depends on the hypsometry of the glacier (or the distribution of glacier area over its altitudinal range), the mean slope and the size of the glacier, and its climate sensitivity (determined by its mass balance gradient). The hypsometry of a glacier also informs on how vulnerable the glacier is

to a change in the cimate. The hypsometry of two completely different glaciers are shown in figure 2.6.
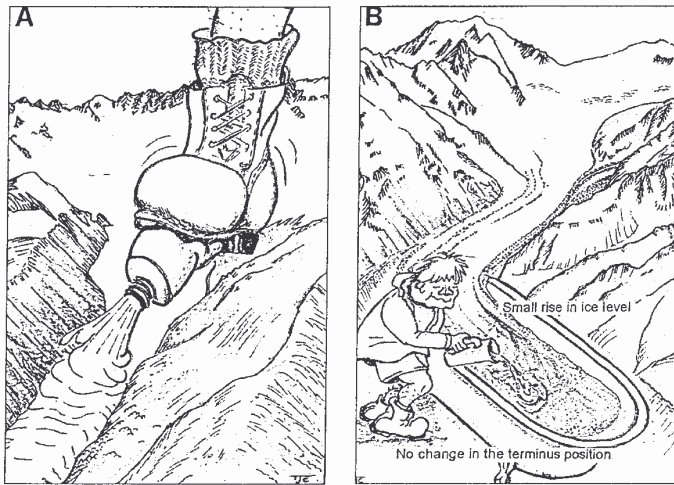
Figure 2.6 *Different responses of glaciers to the same climate of increased snow gain. (A) the enhanced response of glaciers like the Fox and Franz Josef, with wide accumulation areas funnelled into steep, narrow trunks causes ice to squirt down the valley in a fast response akin to stomping on a tube of toothpaste. (B) long, low gradient glaciers like the Tasman respond very slowly with a dampened effect akin to pouring a jug of water into a bath. Drawing by Trevor Chinn (from Chinn, 2002).*

2.1.4.2 Glaciers and natural hazards

Glacier outburst floods of various causes have been reported in New Zealand. Large floods, probably due to catastrophic release of rainwater stored in crevasses, occur regularly at the Franz Josef Glacier (Sara, 1968). On Mt Rupaheu in the North Island, glacier melt caused by geothermal heating periodically releases ice-dammed Crater Lake. During one such event in 1953, the resulting lahar (lahar is an Indonesian word used by geologists to describe a mudflow or a water-saturated debris flow on a volcano) caused 150 deaths (O'Shea, 1954). The rupture of the Tasman terminal moraine, and the release of the large terminal lake, would be dramatic for Lake Tekapo and the surrounding areas. Although the dam of Lake Tekapo is constructed to resist to such catastrophic events, it could potentially cause fatalities (Fitzharris, personal communication). Snow also contributes to hazards such as floods and avalanches, and its distribution has critical ecological implications for many protected natural areas, such as National Parks, a large number of which are located in the Southern Alps.

2.1.4.3 Glaciers and water resources

Land ice influences the water cycle in high mountains and is a crucial factor affecting water supply in some regions. Mountains cover about 25% of the Earth's continental area but provide roughly 40% of its fresh water supply (Kääb, 2005). Very little research has been done on glacier hydrological processes in New Zealand. Anderton (1973) quantified the significance of glaciers in the hydrological cycle, in terms of water storage for electricity generation. He found that while glaciers were significant for seasonal regulation of flow, they were generally insignificant in terms of their contribution to flow volume. However, in the large and heavily glacierized Hooker Catchment, runoff in the summer month of January alone accounts for 20% of annual flow (Fitzharris, 1999). The glaciers and snow cover of the Southern Alps provide a valuable resource for hydroelectric generation, agriculture and horticulture irrigation, the ski and tourism industry.

2.1.4.4 Glacier melt and sea level rise

The growth and decay of glaciers and ice sheets has a profound effect on regional and global sea-level changes over the course of glacial cycles. During the ice ages a vast amount of water was taken out of the Earth's hydrological cycle and stored in glaciers and ice sheets (Benn & Evans, 1998). The load of ice on the Earth's crust causes it to sink into the underlying mantle. Another mechanism of sea-level change relates to the change of water density. As fresh water is mixed with salt water the sea becomes less dense and expands. Further, as the water is heated above 4°C, the ocean warming will amplify the sea-level rise (Benn & Evans, 1998). During the last ice age maximum the sea level sank approximately 130 m due to water being stored as ice on the northern hemisphere, compared to today's level.

The potential economic and human impact of sea-level rise is enormous. Human systems that are sensitive to climate change include mainly water resources; agriculture (especially food security) and forestry; coastal zones and marine systems (fisheries); human settlements, energy, and industry; insurance and other financial services; and human health (IPCC,

Working Group 2, 2001). IPCC's Projected adverse impacts of climate change based on models and other studies include: A widespread increase in the risk of flooding for many human settlements, decreased water availability for populations in many water-scarce region etc.

2.1.5. Historical fluctuations and observations of New Zealand glaciers

The last glacial maximum was reached 18 000 years ago. The great Pleistocene glaciers finally collapsed about 13 500 years ago, but there were a few less dramatic resurgences in the following few thousand years. Around 6000 years ago there was a world wide warm period known as the climatic optimum. This interval was perhaps slightly warmer than today, and the pertinent point is that the glaciers which survived this time were (a) slightly smaller than today, and (b) lying in troughs carved during the ice age which have never been free of ice, thus preventing any infilling by gravel, while the ice free valleys and their lakes were being infilled by gravel (Chinn, 2002). About 5000 years ago, a mild new period of glaciation began associated with moderate climate cooling. This is often called the Neoglacial, which included a number of periods of ice expansion. These events left the tussock covered moraines surrounding the present glaciers in New Zealand. The last of these glacial expansions is known as the Little Ice Age (LIA), which was a cool period from the fifteenth century to the mid nineteenth century. The glaciers in New Zealand reached their maximum LIA extents between 1700s and late 1800s (Chinn, 2002).

The first published descriptions of New Zealand glaciers occurred in 1859. Early visitors made observations on positions of termini and rates of movement of the glaciers, and, in 1889, the first precise measurements were carried out (Chinn, 1989).

The first known sequences of vertical aerial photographs in New Zealand were taken around 1937 and 1938 by New Zealand Aerial Mapping, Ltd., but these were mainly of lowland areas. In autumn 1955 a set of oblique aerial photographs were taken by the Royal New Zealand Air Force along both sides of the Southern Alps (Chinn, 1989). Modern studies

began in the 1950's and included studies of flow, fluctuation, and mass and water balance on individual glaciers. The first topographic mapping of the entire country began in 1958 and was completed in the 1970's (Chinn, 1989).

A study using historical records, including maps, photographs, paintings and written accounts, to reconstruct the changing ice levels and terminal positions of the six main valley glaciers in Mt Cook National Park reported of a general still stand period is recorded by all of the glaciers in Mt Cook National Park was between 1900 and 1940 and this was followed by widespread glacial retreat which is still continuing at the present day (Gellatly, 1985).

2.1.6. Some characteristics of New Zealand glaciers

Debris cover

A major feature of many of the larger valley glaciers in New Zealand, is the mantle of bouldery debris covering their lower tongues. It has frequently been stated that this occurs predominantly on glaciers to the east of the Main Divide (e.g. Harper, 1893 in Chinn, 2001). However, Chinn (2001) demonstrated that the proportion of debris cover increased systematically with size, and was not dependent on which side of the Alps the glacier was located. He found that an average of over 25% of the surfaces of large valley glaciers were mantled with debris, while the alpine glaciers had an average of less than 10% debris cover (figure 2.7). Supraglacial debris are an effective insulator, reaching over 2 m in thickness towards the termini of the larger glaciers, and reducing melt rates of the underlying ice by up to 90%, even at the relatively low altitudes and high temperatures of the valley floors (Chinn, 1991). This insulation damps the response to climate forcing as it introduces inertia into the response of the glacier to negative balance while allowing rapid response to positive balance changes (Chinn, 1991).

Chinn (2001), mention 4 prerequisites which favour the accumulation of an extensive debris mantle on a glacier tongue:

    (1)   high ratio of debris to snow accumulation;

(2)   steep headwalls that permit rock falls and rock avalanches to feed directly on the glacier surface;

(3)   disconnected icefalls that expose the glacier bed, allowing basal debris to be physically mixed and brought to the surface;

(4)   large low-gradients lower trunks with high ablation rates that permit steeply emerging and decelerating ice to bring basal debris to the surface.

The high precipitation on New Zealand's maritime glaciers precludes condition (1) except in the arid ranges well to the east. The exceptionally high tectonic and geomorphic activity of the Southern Alps provides ample opportunity for conditions (2) and (3). The occurrence of numerous large glaciers with low-gradient tongues fulfils condition (4). Both the Franz Josef and Fox Glaciers have névés on an unusually high, broad plateau minimising prerequisites (2) and (3), while their fast-flowing steep tongues rapidly clear debris. As a consequence, both of these glaciers are exceptionally clean of debris for large New Zealand glaciers (Chinn, 2001). These two glaciers are therefore relatively straight forward to map from satellite imagery as opposed to the large, low-gradient valley glaciers. Failure in detecting glaciers ice in automatic classification methods will at least be as large as the debris cover on the particular glacier. From figure 2.7 this would mean larger the glacier is in New Zealand, the higher is the misclassification in an automatic approach.
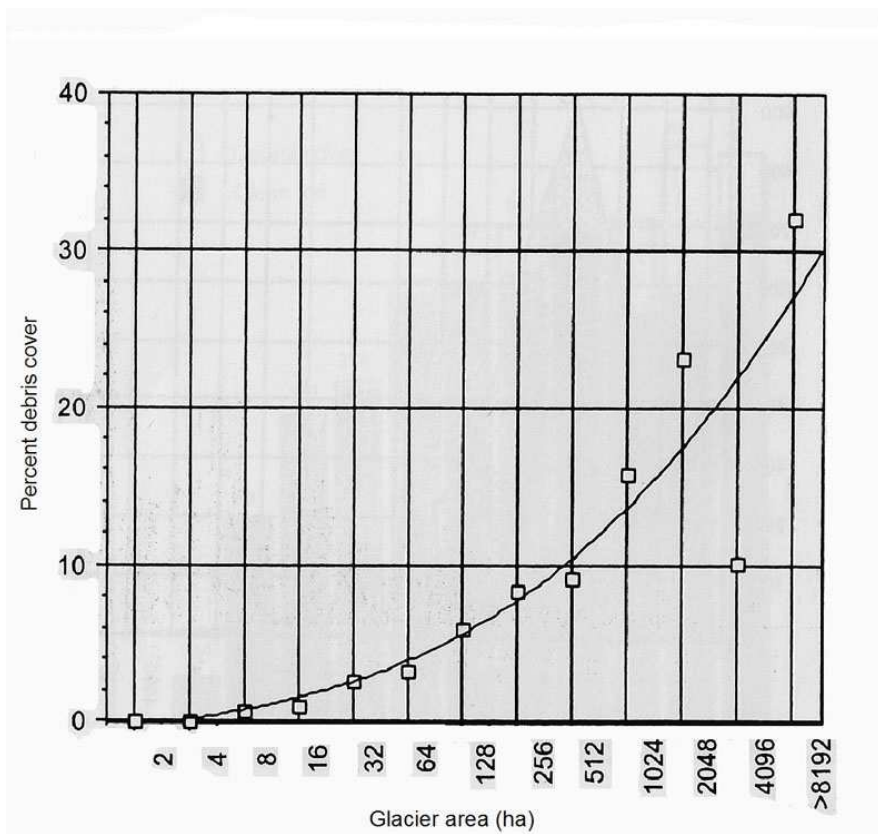
Figure 2.7. *Percent of debris cover versus glacier area for all glaciers. The largest glaciers have very large debris covert and the smaller the glacier, the less covered they are (figure from Chinn, 2001).*

Proglacial lakes

A number of the large debris-covered glaciers have recently entered a period of accelerated retreat by calving into rapidly expanding proglacial lakes. The growth of proglacial lakes involves processes separate from climate forcing, and the rate of retreat of frontal position of calving glaciers is decoupled from the climate signal (Chinn, 1996). When a glacier snout begins to float in a proglacial lake, recession quickens markedly by up to an order of magnitude. As the lake expands, the glacier gradient increases to keep the cliff low, so velocity and discharge both increase. Figure 2.8 shows the different stages from a glacier surface with no water bodies and till the stage where a large proglacial lake has developed. At present many of the large glaciers in New Zealand have reached stage 4.

STAGE 1
Ticker moraine cover furter down glacier

STAGE 2
With rising temperatur the glacier will melt more where the debris cover is thinner, i.e. the surface becomes flatter

STAGE 3
Development of small ponds and lakes with conduits

STAGE 4
All ponds and lakes join to a large terminal lake
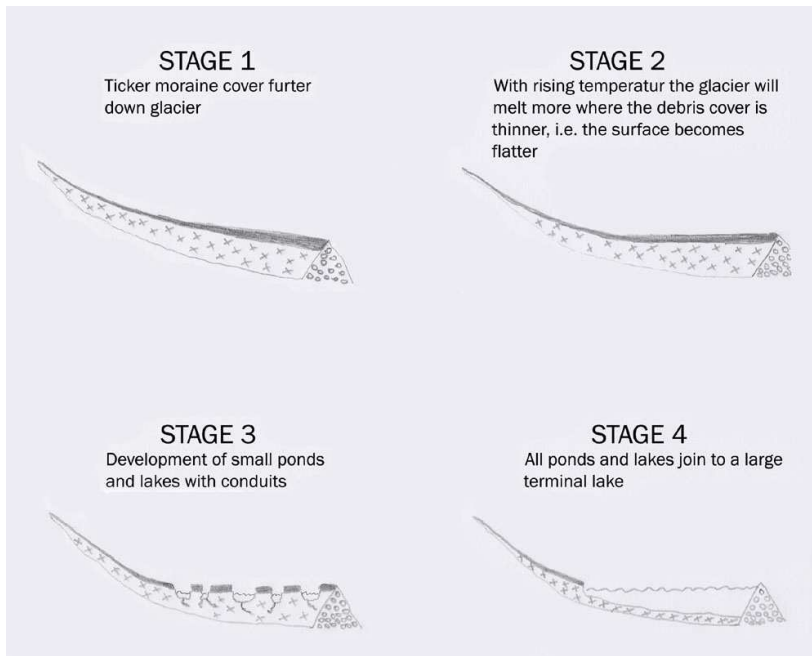
Figure 2.8 *Development of proglacial lake. (Drawings by author after conversation with Doug Benn)*

Surface velocity

Some velocity measurements on glaciers in New Zealand have been done, even though they are relatively rare. Odell (1955 in Fitzharris et al, 1999) reported a five-year average surface velocity at Franz Josef Glacier, calculated from the motion of the wreckage of a small plane, of 1.5-1.8 m d^{-1}. McSaveney and Gage (1968 in Fitzharris et al, 1999) measured surface

velocities of up to 1.9 m d^{-1} during the 1965-67 readvance of the Franz Josef Glacier, and of up to 7.9 m d^{-1} during a rainfall event. For Tasman Glacier, Anderton (1975 in Fitzharris et al, 1999) reported annually averaged surface velocities of up to 0.6 m d^{-1} and Kirkbride (1995 in Fitzharris et al, 1999) reported velocities as measured over various timescales with averages of up to 0.3 m d^{-1}. For smaller glaciers surface velocities might be less than 0.10 m d^{-1}. Surface velocities measured at New Zealand glaciers therefore span two orders of magnitude, and velocities on the steep, active, West Coast glaciers are relatively high when placed in a broader context for non-surging glaciers (Bennett and Glasser, 1996 in Fitzharris et al, 1999). Kääb (2002) reported of ice speeds of up to 250 m year^{-1} for Tasman Glacier, by interpreting repetitive ASTER imagery.

2.1.7 Research on New Zealand glaciers

Fitzharris et al (1999) stated that glacier research in New Zealand had concentrated on only a few key glaciers and been focusing on understanding glacier change. The most touristy and famous glaciers in New Zealand, like Franz Josef, Fox (west of Main Divide) and Tasman (east of Main Divide) are also the most researched glaciers. For these glaciers there is a reasonable history of their behaviour since the middle of the nineteenth century. There have been a reasonable amount of studies investigating the relationship between glacier change and climate systems in New Zealand. Some of these are shortly summarized below:

Hessel (1983) was one of the first to look at the climatic effects on the recession of New Zealand glaciers. He investigated sequences of meteorological parameters observed over extensive periods on the West Coast and compared those with observations of the recession of the Franz Josef Glacier terminus. He was able to establish a statistical significance for relation between glacier retreat and precipitation and between glacier retreat and a pressure gradient term related to the westerly component of the wind. However, he found no significant relationship between glacier retreat and temperature.

Salinger et al (1983) looked at climate relationships for the variation of the Stocking glacier. They established some climatic models to be able to describe the qualitative relationships

between the behaviour of this glacier and climatic variables such as, temperature and precipitation. They found a significant positive regression existed between temperature and glacier retreat in all months of the year, apart from June and July (the winter months), but relationships between precipitation and glacier behaviour were not quite as clear.

Gellatly and Norton (1984) looked at the relationships between glacier behaviour for Stocking and Franz Josef glaciers and climate in the Southern Alps. They concluded that a temperature increase since the 1940s was consistent with atmospheric circulation patterns, particularly the decrease in westerly airflow onto New Zealand since the 1940s, and is associated with a reduction in precipitation in western areas. This temperature increase has been confirmed by a statistically significant, calibrated, and verified reconstruction of annual New Zealand summer temperature from tree-rings. The occurrence of extensive glacier recession throughout the Southern Alps of New Zealand during a period of warming implicated temperature as having an important influence on glacier mass balance and subsequent variations in terminus positions.

Fitzharris et al (1992) also investigated the behaviour of the New Zealand glaciers and the atmospheric circulation changes, but studied the past 130 years. They used reconstructed sea-level patterns back to 1911 and obtained atmospheric circulation indices from pressure differences between appropriate stations extended back to the 1860s. Circulation anomalies for winter and summer were examined. A link between variations in atmospheric circulation patterns in the south-west Pacific and substantial changes in the rates at which New Zealand glaciers were retreating and downwasting was found. The most rapid retreat was associated with higher than normal summer pressures over the New Zealand region, confirmed by a poleward shift of the subtropical high and changes in zonal and meridional airflows.

Later a similar study by Fitzharris et al (1997) looked at atmospheric circulation patterns and glacier balance fluctuations for the glaciers in the Southern Alps. This was done by using the altitudes of the end-of summer snowlines of some 50 index glaciers, well spread over the Southern Alps, and computing mean atmospheric pressure maps for south-west Pacific from long-period meteorological station data. This study also showed a significant relationship between atmospheric circulation and glacier balance changes. The westerlies were further south in the accumulation season for the negative mass balance years compared to the positive years. There was a more dominant anticyclone over Australia for negative mass balance years,

causing a poleward shift in the boundary of the westerlies. The direction of airflow over the Southern Alps was more from the west to north-west for negative mass balance years compared with west to south-west for positive years.

Lamont et al (1999) discussed slopes of glacier in the Southern Alps in relation to atmospheric circulation patterns. They fitted trend surfaces to the ELAs data for each mass balance year, and computed the elevation and slope of each surface. These were compared to atmospheric pressure anomaly maps generated for the southwest Pacific from long-period climate station data. Their results showed that atmospheric circulation patterns exerted a strong control on elevation and slope of the trend surfaces. Steeper sloping trend surfaces across the Southern Alps were associated with anomalous southwest to westerly flow, whereas less steep slopes were associated with anomalous airflow from the south, southeast, and easterly directions.

Hooker and Fitzharris (1999) investigated the correlation between climatic parameters and the retreat and advance of Franz Josef Glacier. Franz Josef Glacier, after a long period of general retreat, showed a major advance beginning about 1982. Atmospheric circulation patterns over the Southwest Pacific and the Southern Oscillation Index (SOI), over the 20-year period that represented advance and retreat phases of Franz Josef glacier were compared. A strong link between atmospheric circulation changes, climate variables and glacier behaviour was found. The retreat phase was characterised by slightly warmer temperatures and markedly lower precipitation in the ablation season, a high pressure anomaly over New Zealand, and a southward shift in the subtropical high pressure zone. In contrast, the advance phase was characterised by anomalous southwest airflow, especially during the ablation season, and higher precipitation.

Chinn et al (2005) discussed the use of the ELA as a practical method of monitoring glacier response to climate in New Zealand's Southern Alps. Over a 28 year period (2005) equilibrium-line altitudes (ELAs) have been measured at some 50 selected glaciers distributed along the glacierized length of New Zealand's Southern Alps. Analysis of the data shows that ELAs are a useful measurement of glacier response to annual climate fluctuations, although there is much variability in the degree of response between glaciers in any given year. The ELA record closely predicts glacier termini responses that follow after appropriate response time delays. The recorded variability in climate response for the Southern Alps suggest no

single glacier is truly representative for detailed studies of glacier-climate relationships, and that a large number of ELA measurements may be as good an indicator of climate as a few mass-balance measurements.

Chinn et al (2005) compared the glaciological and meteorological causes for recent glacier advances in Norway and New Zealand. Both countries experienced glacial advances commencing in the early 1980s and ceasing around 2000, which were more extensive than any other since the end of the Little Ice Age. In common for both countries is that they lie in similar climatic zones dominated by humid maritime westerly wind circulation. Their positive glacier balances are associated with an increase in the strength of westerly atmospheric circulation which brought increased precipitation. In Norway, the changes are also associated with lower ablation season temperatures. In New Zealand,the period of increased mass balance was coincident with a change in the Interdecadal Pacific Oscillation and an associated increase in El Niño/Southern Oscillation events. The Norwegian advances are linked to strongly positive North Atlantic Oscillation events which caused and increase of precipitation in the winter accumulation season. These studies illustrate very well the influence of atmospheric circulation on maritime glaciers.

When making new glacier inventories and to be able to interpret glacier changes as good as possible, a proper understanding of the climatic forcing is necessary. As these studies shows these weather systems influencing on the New Zealand glaciers are complex, but there have been established a reasonable understanding of their forcing.

Other recent studies:

Hochstein et al (1995) discuss the downwasting of the Tasman Glacier and its changes in the terminus region between 1971 and 1993. They could report that gravity surveys in 1971/72 and in 1982 revealed that the average thickness of the glacier was between 150 and 200 m over the large area now occupied by the melt lake. Rapid melting began in the late 60s in a few isolated melt ponds in the centre and in a small elongated lakelet at the eastern lateral moraine. These ponds and lakes grew rapidly in size during the 1970s and coalesced to form a large melt lake by about 1990.

Purdie and Fitzharris (1999) looked at rates for ice loss at the terminus of Tasman glacier. During the 1990s the terminus changed from a regime of slow downwasting under the extensive debris-mantle, to one of calving into the new pro-glacial lake. They wrote that calving at the terminus made the ice cliff retreat at over 30 m year^{-1} up valley.

A similar article on the Hooker glacier was published in 1998 (Hochstein et al). Their studies indicated that between c. 1915 and 1964 downwasting of an axial strip along the terminal section occurred at a rate of c. 0.7 m/yr. Between 1964 and 1986 the rate increased to 1.0 m/yr. Marginal segments of the glacier near the terminus experienced positive buoyancy from 1982 onwards, which promoted rapid melting. Apparent subaqueous melting rates of c. 9 m/yr occurred between 1986 and 1996 over large stretches of the downwasting terminal area. By 1996, a 1.4 km long sector of the glacier had melted down forming a melt lake.

Chinn (1996) investigated the responses of New Zealand glaciers to climate change of the 20th century. By investigating 127 glaciers of the Southern Alps he found that since the end of the Little Ice Age they had on average shortened by 38% and lost 25% in area. The upward shift of glacier mean elevation for the same period was equivalent to a temperature rise of 0.6˚C. He also concluded that extensive debris cover on many glaciers is significant in damping the climate signal, and proglacial lake formation may decouple a glacier from directly responding on the climate. Mean retreat rates for the 100 yr period before 1978 ranged from 7.8 m/a for cirque glaciers to 17.7 m/a for valley glaciers, with a mean for all glaciers of 13.3 m/a. A maximum rate of 66 m/a was found for the Godley Glacier.

2.2 Techniques for glacier inventories

2.2.1 Traditional monitoring

Worldwide collection of information about glacier changes was initiated in 1894 with the foundation of the International Glacier Commission at the 6th International Geological Congress in Zurich, Switzerland. The main motivation was that long-term glacier observations would give insight into processes of climatic change such as the formation of ice ages. Since then, the goals of international glacier monitoring have evolved and multiplied. In 1986 the World Glacier Monitoring Service (WGMS) started to maintain and continue the collection of information on ongoing glacier changes, when the two former ICSI services PSFG (Permanent Service on Fluctuations of Glaciers) and TTS/WGI (Temporal Technical Secretary/World Glacier Inventory) were combined (http://www.geo.unizh.ch/wgms/).

Traditionally glacier inventories have been produced by manually photo-interpreting glacier outlines on aerial photographs and drawn the outlines onto topographic maps. There are many examples of this. For instance the Pamir glacier inventory was published in the 1960s–1970s as a part of the USSR glacier inventory. This inventory was converted into digital format in the 1980s. (Khromova et al, 2006). The first Swiss glacier inventory was made from aerial photographs taken during September 1973. The interpretation of the photos was carried out by stereo-photogrammetry and the glacier boundaries were transferred to topographic maps at a scale of 1:25000 (Paul, 2003). The inventories by Müller et al. (1976) and Maisch (1992) contain an appendix with black and white illustrations of the spatial extent of each larger glacier at a scale of approx. 1:150000, but the maps are available only in printed form and it is very difficult to follow glacier changes since 1973 (Paul, 2003). As part of the modernization of technologies this data were later transformed into GIS-based vector layers by manual digitizing, first for selected part and in full Digital glacier outlines serves a base map for comparisons with former and future (satellite-derived) glacier geometries and help to visualize and measure ongoing glacier changes more efficiently (Paul, 2003).

Glacier inventory data was also compiled for many other parts of the world from aerial photography during the 1970s and 1980s, but digital glacier outlines are not reported (IAHS, 1989 (World glacier inventory – status 1988) in Paul, 2003). This is not correct for New Zealand though, where glacier outlines from 1978 flights reached their final digital form in 1988 (Chinn, 1991).

2.2.2 Glacier monitoring from space

Because of their synoptic view, repetitive coverage and up-to-datedness, satellite imagery is an unprecedented powerful and efficient media by which to study glaciers that are usually located in remote, inaccessible and inhospitable environments. Sensors mounted on air- or space-borne platforms enable to collect data on glaciers at various scales (Gao & Liu, 2001). A large number of glaciological features have been detected and successfully studied using remote sensing and in some cases other associated techniques: For instance mapping and monitoring of glacier boundaries, determination of flow velocity, estimation of mass balance, modelling of snowmelt runoff, etc (Gao & Liu, 2001). There are several remote sensing systems available and two of them are briefly discussed below.

VNIR – space-borne scanning
Space-borne satellite data are recorded repeatedly over a long period. These data make the long-term monitoring of glaciers possible. Compared to aerial photographs, space-borne satellite imagery provides large area coverage. Subsequently, an extensively distributed glacier can be captured by one scene, reducing the number of images and hence processing time. Space-borne scanning can be categorized into earth resources and meteorology by image spatial resolution. Earth resources satellite imagery such as Landsat, SPOT and ASTER has an intermediate spatial resolution on the order of 10 to 79 m.

Microwave remote sensing
Microwave remote sensing, commonly known as radar, falls into two broad categories, imaging and non-imaging. For glaciology Imaging Radar has proved to be useful. Imaging radar includes Shuttle Imaging Radar (SIR), European Space Agency (ESA) ERS-1 and ERS-2, Japanese J-ERS1, Seasat Synthetic Aperture Radar (SAR) and Canadian Radarsat.

As an active remote sensing system, radar imagery is invaluable in studying glaciers over areas that are frequently obstructed by clouds thanks to microwave's ability to penetrate cloud. Operational under all weather conditions, radar sensors can differentiate snow and glacier from other targets at a spatial resolution compatible with the topographic variation in alpine regions (Sidjak and Wheate, 1999).

The introduction of radar interferometry made it possible to generate 3-D surface ice flow patterns by calculating the interference pattern caused by the difference in phase between two passes at two distinct times or positions. (Massonnet and Feigl, 1998; Gao & Liu 2001). Examples of such sensors are LIDAR and SRTM.

2.2.3 Capabilities of satellite sensors and implications for glacier inventory

Several factors must be considered to assess the applicability of a remote sensing system for glacier mapping.

1. The "spatial resolution" of the sensor gives the ground equivalent pixel size, the area covered on the ground by each pixel in the recorded image (this will to some extent vary across the image). It decides the degree of detail that can be detected from the image. For making very accurate maps of small glaciers, fine resolution might under some circumstances be required. Kääb et al (2005) divides spatial resolution into: high resolution (<5 m) and medium resolution (5–100 m). Low (100–1000 m) and very-low resolution (>1000m).

2. The "spatial coverage", gives the ground area or width of the ground track sensed by the sensor. This is roughly related to the spatial resolution of the sensor through technical constraints e.g. concerning detectable level of incoming signal strength (sensor noise-level), or onboard-recording and down-link capacities.

3. The "temporal resolution", is the revisit time of the remote sensing system. This is connected to its spatial coverage, and whether and if so how far the sensor can be rotated in cross-track direction in order to cover areas far off the ground-projected track. The ASTER visible and near infrared (VNIR) instrument can be pointed up to ±24° in both directions allowing for repeat imaging as frequently as every two days

(and better in high latitudes) for urgent priorities, as opposed to 16 days with nadir pointing. However, for ASTER rotation of the sensor is not used very often since this decrease the lifetime of the sensor quite dramatically (Hugh Kieffer, Personal Communication).

4. The "spectral resolution" gives the coverage of the electromagnetic spectrum by a sensor. This is determined by the number and the broadness of bands used by the satellite and it decides what surface parameters that can be recorded, and the dependence of the sensor to weather and illumination conditions (e.g. all-weather and night-time capability of microwave sensors, night time capability of thermal infrared (TIR) sensors).

5. The "radiometric resolution" determines the smallest variation of radiance that can be recorded by a sensor. It describes the sensitivity of the detector, the number of bits used to code the data. E.g SPOT has 8 bits, IKONOS 11 bits and NOAA has 16 bits. ASTER has 8 bits in the VNIR bands.

6. "Stereo, interferometric or ranging capability" of the remote sensing system enables the computation of terrain elevations. ASTER has such capability, having two telescopes for its VNIR subsystem, - one nadir-looking with a three-spectral-band detector, and the other backward-looking with a single-band.

7. The "timing" of data acquisition is of particular importance when remote sensing data are required at a given time of year (e.g. for glacier mapping) or when rapid response is needed (e.g. disaster management). It should ideally be under control of the user, or to coincide with the user needs by chance.

8. The speed of on demand acquisition, access to data archives, simplicity of data formats and size, eventual cost of imagery, etc., are also important factors for choosing satellite system to be used for e.g. glacier mapping (Kääb et al, 2005).

2.2.4 Image preparation

Atmospheric correction

Since the radiation used for remote sensing must pass through the atmosphere, the spectral differences among these covers on the remote sensing media are subject to the attenuation of the atmosphere (Hall *et al*., 1988 in Gao & Liu, 2001). Corrections of these effects would be

important if the user wants to quantify ice and snow properties (e.g. grain size) or compare images taken at different dates. However, for a glacier inventory this would not be of significantly importance. Also, the atmospheric effects vary with height (more aerosols at lower altitude), therefore atmospheric effects are not likely to be very high where temperate glaciers are located.

Geometric corrections

Geometric rectification uses a transfer function to transform every pixel of a raw image, expressed in the image coordinate system (line, column), to a new coordinate system (usually a cartographic system).

Two main methods exist to geo-correct images;

1. Images are transformed using a set of Ground Control Points (GCPs) and polynomial functions. This type of model does not require any knowledge of the acquisition system. GCPs well identifiable in the original image and in the reference map are used to compute transfer equations allowing swapping from the image coordinate system to the map coordinate system.

2. Images are transformed using a mathematical model based on a precise knowledge of the geometric relationship between the sensor and the observed scene. Acquisition system parameters such as sensor attitude and altitude, orbit data, topography are used to compute the mathematical model. GCPs are also required although usually in a more limited number than in a polynomial rectification. Such rectification is called an orthorectification and is highly recommended when the topography of the study site is rugged (e.g. as for the Southern Alps in New Zealand).

In a general Ground Control Points should be clearly identifiable points on the image where latitude, longlitude and altitude are precisely known in a given projection system. GCP collection is the key issue for a good orthorectification. The accuracy of the GCPs will depend on the resolution of the image, the coarser the spatial resolution the harder it will be to choose good GCPs. For ASTER imagery with 15m spatial resolution in VNIR bands, good GCPs are not necessarily easy to choose. Also, GCPs should be:

- well spread over the area
- well distributed in the elevation range

A Digital Elevation Model is a digital representation of the Earth's surface. It is a grid of an area, providing for a given resolution, the relative or absolute (above mean sea level) elevation of every points of the grid. Such DEM can be extracted from stereo imagery using photogrammetric algorithm or made through contour lines from a topographic map.

2.2.5 Spectral properties of ground features – emissivity and reflectance

Whether a glacier can be successfully studied from remotely sensed materials depends on the spectral uniqueness of the targets observed in and around the glaciers, the spectral, spatial and temporal resolutions of the remotely sensed data, as well as the particular feature related to this glacier (Gao & Liu, 2001).

The radiation recorded at a sensor depends on:

- the radiation source,
- the signal transmission through the atmosphere,
- the signal interaction with the terrain surface, which among other things is a function of the reflecting or emitting objects and their neighbours, and
- the sensor characteristics (Kääb, 2005).

The primary radiation sources used in remote sensing are the sun, the earth's surface and the sensor itself. While active sensors (e.g. SAR or LIDAR) emit their own signals, passive sensors register the radiation reflected from the ground, e.g. visible and near infrared (VNIR), or short-wave infrared (SWIR) sensors or the radiation emitted from the ground, e.g. thermal infrared (TIR) or passive microwave sensors (Kääb, 2005).

The total spectral irradiance at the Earth surface is a composite of three components (Bishop et al., 2004 in Kääb, 2005):

1. Direct solar irradiance. During the atmospheric passage, the radiation is modified by *atmospheric scattering* and *absorption* by gases and particles. In mountains, the direct solar irradiance is influenced by the incidence angle of illumination and the vector normal to the surface.

2. Diffuse skylight irradiance. Due to scattering processes the atmosphere produces hemispherical irradiance.

3. Adjacent terrain irradiance. This is a result of interaction with the terrain and the direct solar irradiance and the diffuse skylight irradiance.

At the terrain surface, the incoming radiation is partly reflected (direct, or diffuse = scattered), and partly absorbed, depending on the ground emissivity. The ground reflectance varies, among other things, with the incidence angle of the radiation source and the terrain geometry with respect to the sensor position, and depends on the wavelength and the physical properties of the ground surface material (Kääb, 2005).

Snow

Fresh snow reflects up to 95% of the incoming visible (VIS) and about 50-80% of the near infrared (NIR) radiation. In the VIS spectrum, snow reflectance decreases with dust contamination, and also, but to a lesser extent, with increasing grain size (Kääb 2005). In the NIR, the influence of dust contamination on the reflectance decreases, and the influence of grain size increases. In the short-wave infrared (SWIR), the reflectance of snow is very low with a marked dependency on grain size, but a low dependency on snow contamination. This large reflectance contrast between the VIS and SWIR range signature is exploited for snow classification (König et al., 2001) (figure 2.2.1).

Ice

As a consequence of the reflectance properties of snow, bare glacier ice has a lower reflectance than snow in the VIS spectrum because of the accumulation of optically active contaminants. This effect increases towards dirty glacier ice (Zeng et al., 1983). In the NIR and SWIR, the dependency of reflectance on increasing grain sizes from snow to ice is effective. In addition, the presence of liquid water on the ice surface might lead to reduced reflectivity in the NIR (König et al., 2001; Kääb 2005). For debris-covered ice, the spectral signature of debris may prevail over the ice signature depending on the percentage of the debris-covered surface area. If the ice surface within a pixel is covered with debris by more than several ten percents of surface area it can hardly be separated from pixels of periglacial debris or bedrock using multispectral data (Kääb, 2005) (figure 2.2.1).
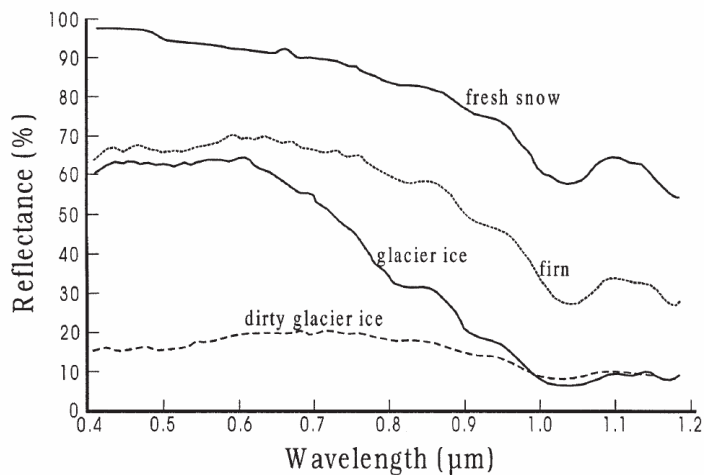
Figure 2.2.1 *Spectral reflectance curves between 0.4 and 1.2 μm for fresh snow, firn, glacier ice and dirty glacier ice (adapted from Zeng et al., 1983). There is a good correlation between snow density and spectral reflectance within this wavelength range. The spectral reflectance gradually decreases from 95% to 60% within visible range while snow is metamorphosed to glacier ice. These curves suggest that some properties can be spectrally discriminated as long as the spectral resolution of the image is sufficiently narrow (not too wide bands).*

Rock

Compared to snow and ice, rock or debris-covered surfaces show a significantly different reflectance in the VNIR and SWIR. This fact usually allows for good spectral discernibility of such surfaces against clean snow and ice. The highly variable reflectance, or emissivity, respectively, of different mineral and rock types in the VNIR, SWIR, and TIR (thermal infrared) forms the base for geology mapping from multispectral and especially hyperspectral imagery (Kääb, 2005).

Water

Reflection of open water in the VIS is highly variable depending among other things on its turbidity. In the NIR and SWIR, water strongly absorbs radiation, nearly independent of its turbidity. The ratio of NIR to SWIR reflection of water is similar to that of snow and ice, which involves the risk of misclassification. Inclusion of the VIS thus facilitates separation into two categories (Paul, 2003; Kääb, 2005). Turbidity and temperature of glacial lakes, an important element in their characterization, can be derived from VIS and thermal infrared (TIR) data (Wessels et al, 2002)

Vegetation

Vegetation mapping usually takes advantage of a strong increase in reflectivity in the NIR. In glaciological research, the existence of vegetation may be interesting by itself since it potentially indicates, for instance, comparably stable surfaces, plant succession or lack of surface abrasion. First-order vegetation mapping may be applied for excluding distinct areas from further analyses or removing misclassifications (Kääb, 2005). E.g. for accurately mapping of debris covered glaciers.

2.2.6 Classification methods and extraction of glacier boundaries

The signature of the ground surface in the spectral domain is used to describe and distinguish surface types and conditions. Classification approaches can be combined or applied sequentially. Instead of using only spectral data, some classification algorithms also permit the inclusion of spectral derivatives (e.g. band ratios instead of the bands themselves, or multitemporal data or non-spectral data e.g. DTMs (Brown et al., 1998; Kääb, 2005).

Kääb (2005) concludes that, classification approaches based on multispectral imagery are well developed and strongly established. Several classification approaches have been tested for glacier purposes, some are described below.

2.2.6.1 Manual delineation

Manual delineation for classification is done by combining human photo-interpretation skills and digitizing. This is useful for complex classification of panchromatic or multispectral

images, where expert knowledge is needed, e.g. for distinguishing rock glaciers, dead ice, debris-covered ice, and periglacial debris. An analyst is able to include experience, knowledge and complex logical rules in the decision process, also relying on non-spectral data or knowledge. Manual delineation is also often needed to complement and correct automatic classifications (Kääb, 2005). Manual delineation is used for simple classifications, but also for accuracy assessments, ground truth acquisition, or completion or correction of other classifications (Williams et al, 2006; Kääb, 2005).

Good results for glacier mapping have been reported from combining several of the above mentioned methods (e.g. Sidjak & Wheate, 1999). Sidjak & Wheate (1999) also combined high resolutions DEMs with thematic maps allowing glacier attributes to be derived. After completing an automatic classification it is a well used approach to correct this classification manually. Such a procedure is, for instance, unavoidable for the mapping of debris-covered ice (Kääb, 2005).

2.2.6.2 Thresholding of band ratios

Spectral bands may be inferred in different algebraic algorithms, among which band ratios R

$$R_{ij} = \frac{DN_i}{DN_j}, or \qquad (2.1)$$

$$R_{ij} = \frac{(DN_i - DN_{\min(i)})}{(DN_j - DN_{\min(j)})}, \qquad (2.2)$$

and normalized differences indices (*NDI*, or modulation ratios) are the most widespread (Kääb, 2005).

$$NDI_{ij} = \frac{R_{ij} - 1}{R_{ij} + 1} = \frac{(DN_i - DN_j)}{(DN_i - DN_j)}, \qquad (2.3)$$

Where *DNi* and *DNj* are digital numbers of two bands *i* and *j* that show high discernibility for the category to be classified with respect to other categories in the image, and *DNmin* are the minimum (i.e. darkest) DNs of an individual band. For band ratios, subtraction of the minimum DN for each band applied reduces the influence of illumination differences due to atmospheric scattering (Kääb, 2005). Similarly, the results of normalized differences might be improved by subtraction of the band specific minimum DNs. For ice and snow, usually bands in the VNIR versus bands in the SWIR are applied, e.g. TM 2, 3 or 4 versus TM 5 or ASTER 3 versus ASTER 4 (Kääb, 2005). The normalized difference snow index (NDSI) for ASTER is defined as *(ASTER1-ASTER4)/(ASTER1+ASTER4)*. Similar indices are defined for water and vegetation and can be used to eliminate misclassification from the above band ratios. Thresholds have to be chosen for final segmentation of the ratio or normalized difference image. Image algebra and segmentation algorithms are especially robust (Paul, 2001; Albert, 2002).

The different spectral properties in TM4 and TM5 have been used for characterization of snow and ice zones. A first attempt was presented by Hall et al. (1987). Later Rott and Markl (1989) suggested that ratio images with TM3 / TM5 revealed better results in shadow zones than TM4 / TM5, whereas the latter showed better performance in mapping glacier areas facing the sun. Jacobs et al (1997) used a segmentation threshold of TM4 / TM5 > 1.0 to delineate the perimeter of the Barnes Icecap. However, they had to apply manual corrections for debris-covered glacier areas.

2.2.6.3 Supervised classification

Supervised classification is an application-driven method. Training areas of the categories to be mapped are operator-selected in order to develop the spectral signatures of these classes. Discernibility analysis is applied to test if the selected categories can be distinguished significantly from one another. Overlapping signatures have to be separated artificially. The spectral signatures are then used to automatically segment the entire imagery (Kääb, 2005). Supervised classification often works accurately for high-mountain terrain with reasonable spectral discernibility. Yet, as for all spectral classifications, it cannot solve problems such as debris-covered ice. Good results with supervised classification may be achieved by including not only spectral bands but also derivatives such as band ratios, principle components or

normalized differences (Sidjak and Wheate, 1999). The choice of training areas is especially crucial for inhomogeneous terrain, as it is often found in alpine environments. In general, the spectral class signatures trained from one scene cannot be applied for other scenes, which reduces the automation capability or requires radiometric adjustments (Kääb, 2005).

2.2.6.4 Unsupervised classification

Unsupervised classification automatically segments images in spectral clusters representing artificial categories. Unsupervised classification is, therefore, a data-driven method. The clusters have then to be assigned to specific thematic classes by the analyst (Kääb, 2005). Unsupervised classification methods tend to be successful for relatively homogeneous terrain with few categories only, e.g. clean-ice glaciers, whereas problems often occur for variable terrain with many classes, e.g. clean ice, dirty ice, debris-covered ice, or clean ice in cast shadow (Paul, 2003). The unsupervised categories have to be assigned to classes of user-interest, which leaves the major classification problems for terrain with low discernibility still to the analyst. In general, unsupervised classifications for glaciological purposes seem suited for initial data exploration rather than for final classifications (Kääb, 2005).

2.2.6.5 Object-oriented technique

Edge detection or feature extraction algorithms are able to detect class boundaries (pattern recognition). The spectral and spatial approaches can be combined to spatial-spectral segmentation, for instance, by applying spectral classification to pixel areas aggregated beforehand, by spatially filtering the classification results, or- more advanced – by applying integrated object-oriented image classifications, for instance by using the software eCognition. This software base its classifiaction on the concept that important semantic information necessary to interpret an image is not represented in single pixels but in meaningful image objects and their mutual relations. (http://www.pcigeomatics.com/products/ ecognition.html).

2.2.7 Use of geographic information system (GIS) for glacier inventories

The use of Geographic Information Systems (GIS) for spatial data handling has intensified strongly during the past decade, mainly due to increased speed and memory of computers (Paul, 2003).

One definition was given by Walsh et al. (1998): "A GIS is capable of data capture, storage, management, retrieval, analysis and display." It integrates spatial and thematic data by means of geocoded data layers and associated information stored in attribute tables. The source of each data layer can be a digitized map of a distinct theme or a classified image (e.g., from a satellite) or a scanned map (e.g., from a field survey), both of a specific theme. While the latter two denote information storage in raster format (on a cell by cell basis) with a constant grid spacing (or sample lag), the former contains only the boundary of a specific entity in vector format (figure 2.2.2). While the vector format has preferences in storing discrete items (their boundaries), the raster format is better for storing continuous fields, such as elevation values of a DEM. GIS can be used for classification and detection of glacier areas, calculating size of glacier areas glacier fluctuations etc.
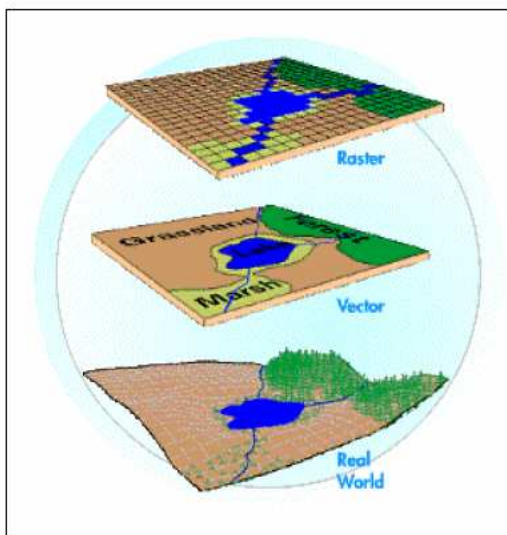
Figure 2.2.2 *Representation of real world objects in the vector and raster domain (from UniAZ, 2002 in Paul, 2003).*

2.2.8 Problems run into when making glacier inventories from satellite imagery

Mapping/extracting glacial debris

Debris at the surface of a glacier in the ablation area is recognized as an important obstacle to glacier mapping (Paul, 2003). Debris effects are seen as a bottleneck for rapid, automated assessment of glaciers from satellite data in some mountain areas. The distribution and particle sizes of materials covering the glaciers are highly variable, ranging from dust to house-sized blocks and from rare occurrence to complete coverage. The larger sized till (stones, rocks) is often arranged to medial moraines, which originate where two glacier basins join. If the fraction of debris cover exceeds a certain limit within a pixel, the spectral signal is dominated by debris and the ice underneath cannot be detected by optical sensors (Paul, 2003).

Traditional statistical multispectral classification algorithms are of limited value in these areas. For example, multispectral data analysis is challenged to discern dirty, shadowed ice from extremely turbid water or debris-covered glacier ice vs. ice-free moraines. Such glaciers can be mapped manually, although the combination of multispectral classifications with DEM derivatives and neighbourhood analysis has revealed promising avenues for semi-automated mapping (Kargel et al, 2005).

Based on the observation that debris-covered glacier tongues are rather flat, transects of slope values are generated for several glaciers for the Swiss Glacier Inventory (Paul, 2003). Slope values below 20˚are indicative of the debris-covered glacier tongue. For other glaciers tested, slope values are at least below 25˚and the selected 24˚ thresholds valid only for this sample, but a good starting point nevertheless. For mapping of debris-covered areas, the slope facet is combined with the glacier map and a map of vegetation-free areas (Paul, 2003).

Larger errors result if the glacier terminus was covered by debris and barely visible with TM or MSS. Rott and Markl 1989 used manual delineation for assessment of snow and glacier areas with TM. They had also shown that interactive cursor tracking of glacier boundary by an expert revealed more accurate results than an automatic algorithm (Paul, 2003).

Paul (2003) refers to some different classification methods that have been used for glacier classification, but most of them have problems classifying debris automatically and some manual correction has to be applied.

Gratton et al. (1990) used a GIS to improve the classification accuracy of Landsat MSS and TM data for mountain glacier mapping. Within the GIS environment they performed automated selection of training areas for a Maximum-Likelihood classification. Although high accuracy was achieved for most classes (snow, clean ice, vegetation, rock, water), regions with debris had to be classified by visual inspection. The DEM was not used to obtain glacier parameters.

An inventory of the entire Southern Patagonian Icefield (SPI) based on TM data from 1986 was performed by Aniya et al. (1996). They used cluster analysis (ISODATA) with TM bands 1, 4 and 5 on Morenoglacier and grouped the 20 clusters into three classes (snow, ice and rock). For the whole SPI a parallelepiped (or Maximum-Likelihood in cases of ambiguity) classification was performed. In case of misclassification (ice in shade, supraglacial till) Li et al. (1998) used a supervised classification for delineation of the Moromaha Icefield in Tibet. They improved their classification by interactive manual correction.

Spectral mixture analysis was applied to TM data for ice / snow discrimination on tropical Andean glaciers by Klein and Isacks (1999). The spectral endmembers that they used also allowed glacier classification, but problems occured for ice in shadow and under debris cover. A detailed evaluation of different glacier mapping algorithms was carried out by Sidjak and Wheate (1999). They applied supervised Maximum-Likelihood classification to different combinations of input bands. These bands were made of principal components (PC) 1-4 or 2-4, partly under a glacier mask derived from PC2 by thresholding, a NDSI, a TM4 / TM5 ratio image or a TM543 composite image. The best classification was revealed with a combination of PC 2-4, TM4/TM5 and the NDSI as the input bands. Even nunataks and medial or ispersed supraglacial debris were correctly mapped (Paul, 2003).

Shadows

Automatic mapping of glaciers is constrained by the strong shadow effects typically found in mountainous regions. Digital classification of satellite data, which is based solely on the spectral properties of glaciers, is unable to map glacier extent in the alpine environment at a satisfactorily accurate level, because of topographic shadow Gao & Liu, 2001). Auxiliary data such as DEM have been incorporated into the mapping to compensate for the effect of topographic shadow in mountainous terrains (Gao & Liu, 2001).

Clouds

Automatic mapping of glaciers by means of remote sensing can be complicated by the presence of clouds, especially in maritime environments where cloud-free imagery is difficult to obtain. Difficulties in accurate discrimination between snow and cloud have handicapped the use of satellite data in operational glacier mapping because both snow and cloud share a similar spectral response, especially in the visible and IR wavelengths (Kääb, 2005).

3. Methods

Summary of the methods

The best available ASTER image covering the Central Southern Alps was chosen in the ASTER gateway service. This image was recorded the 14th of February 2002. The image was orthorectified using a combination of field collected ground control points (GCPs) and height points extracted from the New Zealand topographic data base and a DEM made from contour lines in PCI. The glacier areas in the ASTER image were extracted both manually (by on-screen digitizing) and automatically. Three study areas in the image, all containing field work and different characteristic glacier types were chosen for testing of automatic glacier extraction. For these areas band3 /band4 ratio and the Normalized Difference Snow Index (NDSI) were calculated. For one of the areas a supervised classification was performed. For the band ratio and the NDSI different thresholds were tested and all three methods were compared to the manual digitizing. Confusion matrixes for these results were computed. For validation of the manual digitizing field work was conducted during the late summer of 2005. This consisting of a GPS survey of the boundaries of 9 glaciers for validation and a GCP collection for the orthorectification. The glacier area from the 1978 inventory within the extent of the 2002 ASTER image was calculated and this was compared to the manual digitizing of the image to get the area change in the 24-year period.

3.1 Study area: Central Southern Alps of New Zealand

The Central Southern Alps of New Zealand, are located within these latitudes and longitudes; West – 169.79º, East – 170.75˚, North – 43.36˚, South 44.03˚ (figure 3.1.1). The by far largest glaciers in New Zealand are located within the study area. This is shown in figure 3.1.2 where the largest glaciers in New Zealand over 300 ha (3 km²) are arranged in descending order of area. Of the 8 largest, all except Volta/Therma are found within the study area. The study area is also the most accessible glaciated area of New Zealand, although generally the mountains of New Zealand are very remote as opposed to e.g. the European Alps. One the west side of main divide, roads take you almost to the very terminus of the famous and touristy tropical glaciers Fox and Franz Josef (but to no other of the western glaciers). On the eastern side of the main divide Mt Cook Village is a very good starting point for both climbing and scientific

explorations. Figure 3.1.3 present a plot of intensity of glacierisation as hectar (ha) per km southward along the Divide, together with topographic heights. It clearly shows that the greatest areas of ice-cover logically occur on the highest ranges along the Main Divide, and the area with the very largest glaciation is within the study area.
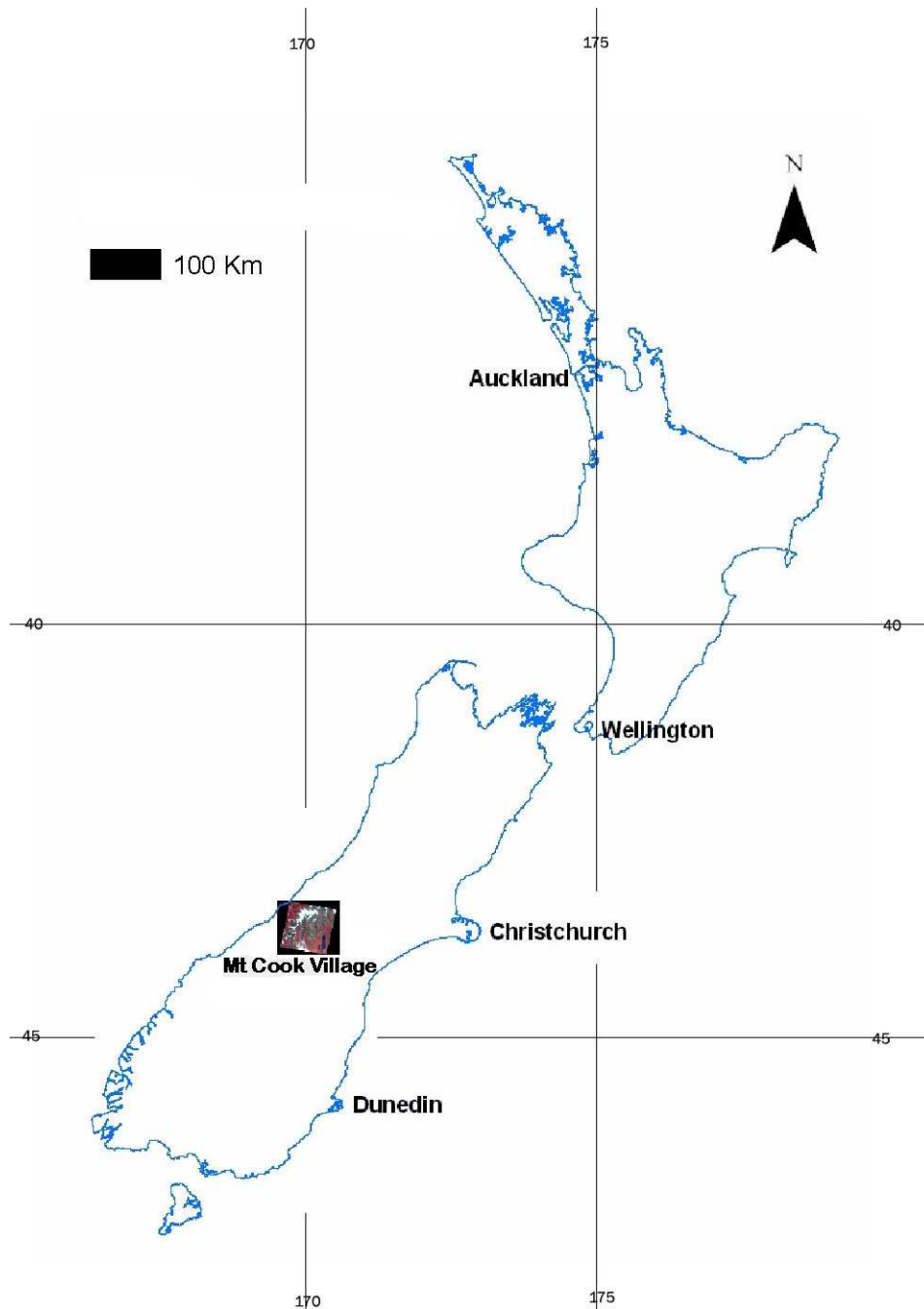
Figure 3.1.1 *Map of New Zealand, showing the location of the study area and the ASTER image used in this research.*
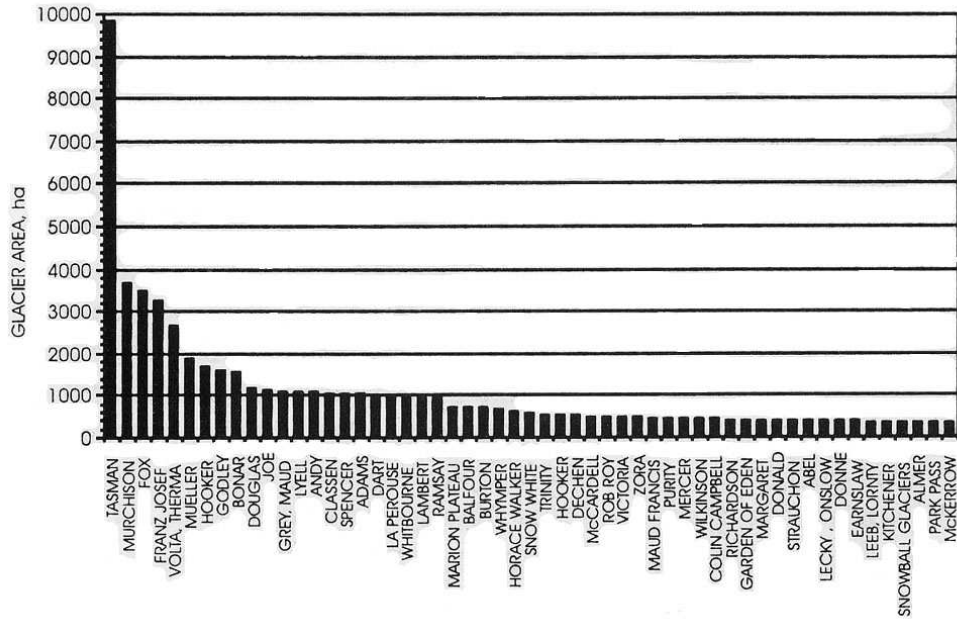
Figure 3.1.2. *The largest glaciers over 300 ha (3km²), arranged in descending order of area (from Chinn, 2001).*
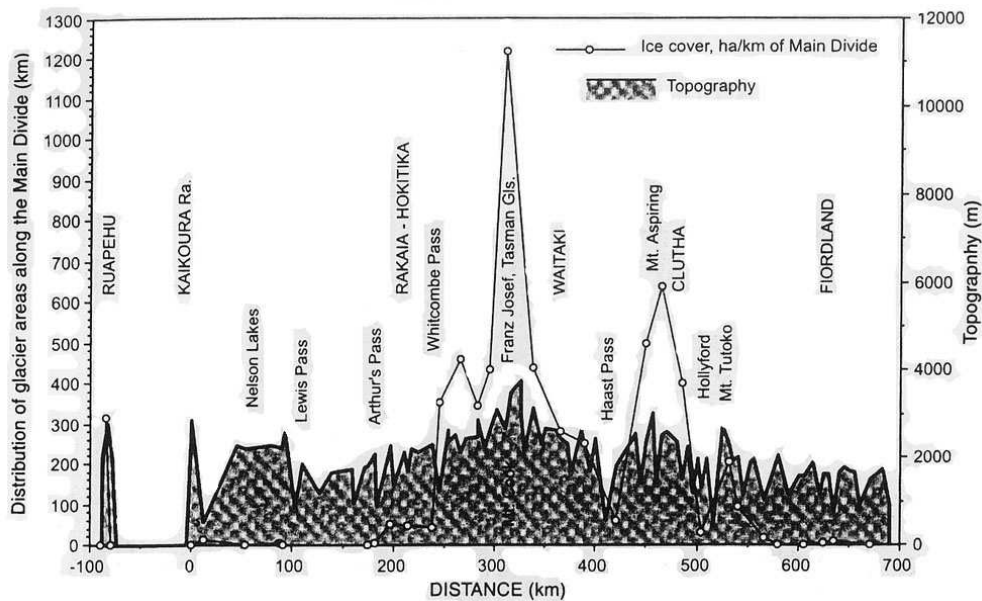
Figure 3.1.3. *Intensity of glacierisation in the South Island of New Zealand along a North – South Gradient expressed as ha per km of distance along the Main Divide. Associated maximum and minimum topographic heights are also plotted in profile. Position of Mt. Ruapehu not to scale. North is left on the figure and south right. The study area is around 300 km along the Main Divide from Kaikoura (from Chinn, 2001).*

3. METHODS

The glaciated areas, within the study area, belong mainly to either Mt Cook or Westland National Parks. The elevation range within the area ranges from sea level at the west coast and up to the summit of Mt Cook at 3754 m a.s.l. Mt Cook Village is situated at approx 700 m a.s.l. Figure 3.1.4 illustrates the height distribution within the study area. Elevations above 3000 m a.s.l. are mainly clustered around the Main Divide of the Southern Alps and elevations between 2-3000 meters are mainly elongated in a south-north direction around the Main Divide and the other largest ranges in the area. Figure 3.1.5 illustrates the enormous vertical distribution in the relatively small, in a world context, mountain ranges of New Zealand. When counting from the Tasman glacier and to the very top of Caroline Face, this face is not far from 3000 vertical meters, making it close to the size of the highest face in the Himalayas (South face of Lhotse which is 3000 vertical meters).
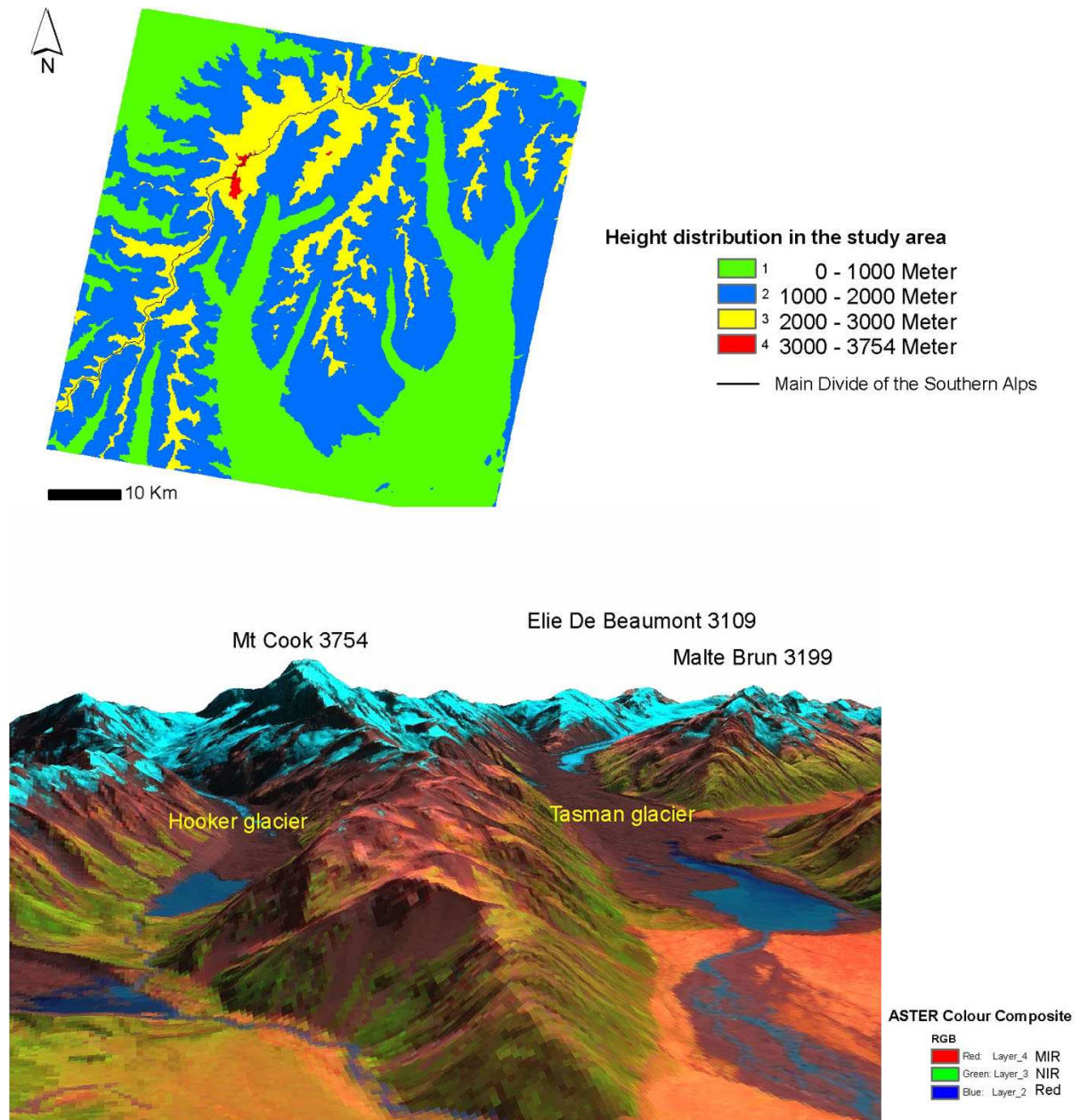
Figure 3.1.4 Top. *Height distribution in the study area. Bottom. The 3D model views the area from Mt Cook Village. From the terminal lake of Tasman Glacier and to the top of Mt Cook there are more than 3000 vertical meters.*

Figure 3.1.5 *Climber on the upper part of the East Ridge/Caroline Face on Mt Cook.*

The steep rise in elevation causes a very steep precipitation gradient. About 10 km west of the main divide is where the peak rainfall occurs (Chinn, 1979). The rainfall reaches near a world record of approximately 12 m a year (figure 3.1.7). One site even had 15 m one year (Chinn, personal communication). From this maximum, precipitation diminishes approximately exponentially to about 1000 mm in the eastern ranges (Chinn, 1979). The high rainfall zone is very narrow and Chinn (1979) found big differences in raingauges less than 250m apart. The enormous precipitation along the main divide creates rapid flowing glaciers with large crevasses (figure 3.1.6).

Figure 3.1.6. *Crossing a large crevasse on Linda glacier, north-east of high peak of Mt Cook.*
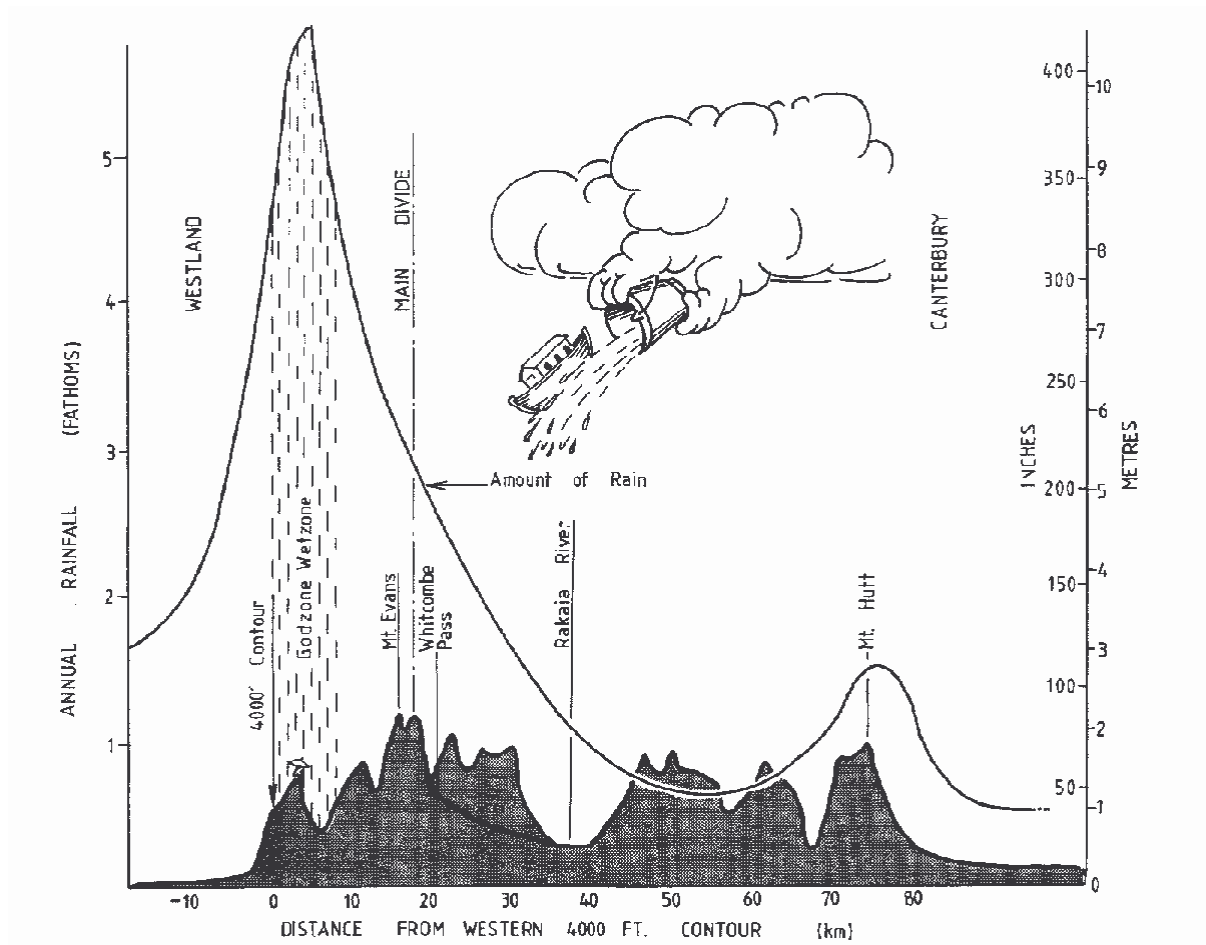
Figure 3.1.7 *Concentration of rainfall in a section across the Southern Alps (from Chinn, 1979).*

Glacier mean elevations rise from 1500 m in the west to colder elevations over 2000 m on eastern glaciers (Chinn, 2001). The easternmost ranges extend into semi-arid climates and here, where there is a low ratio of snowfall to debris supply, many groups of classical rock glaciers, both active and fossil, are found (Chinn, 2001). Although westerly winds prevail (figure 3.1.8), easterly and, more especially, southerly winds are important sources of snow to the east of the main divide (Chinn, 2001).

Within the study area 6 of the approximately 50 Index Glaciers used for the annual snowline monitoring are situated. These are from west to east; Chancellor Dome, Jalf/Baumann, Salisbury Snowfield, Tasman, Langdale, and Ridge (figure 3.1.9).

Figure 3.1.8 *Photograph taken in north-west direction across Lake Tekapo towards the ranges south-west of Mount Cook Village. The photo illustrates a typical north-westerly storm, which are the type of weather which leaves most precipitation to the area. Good hut weather!*
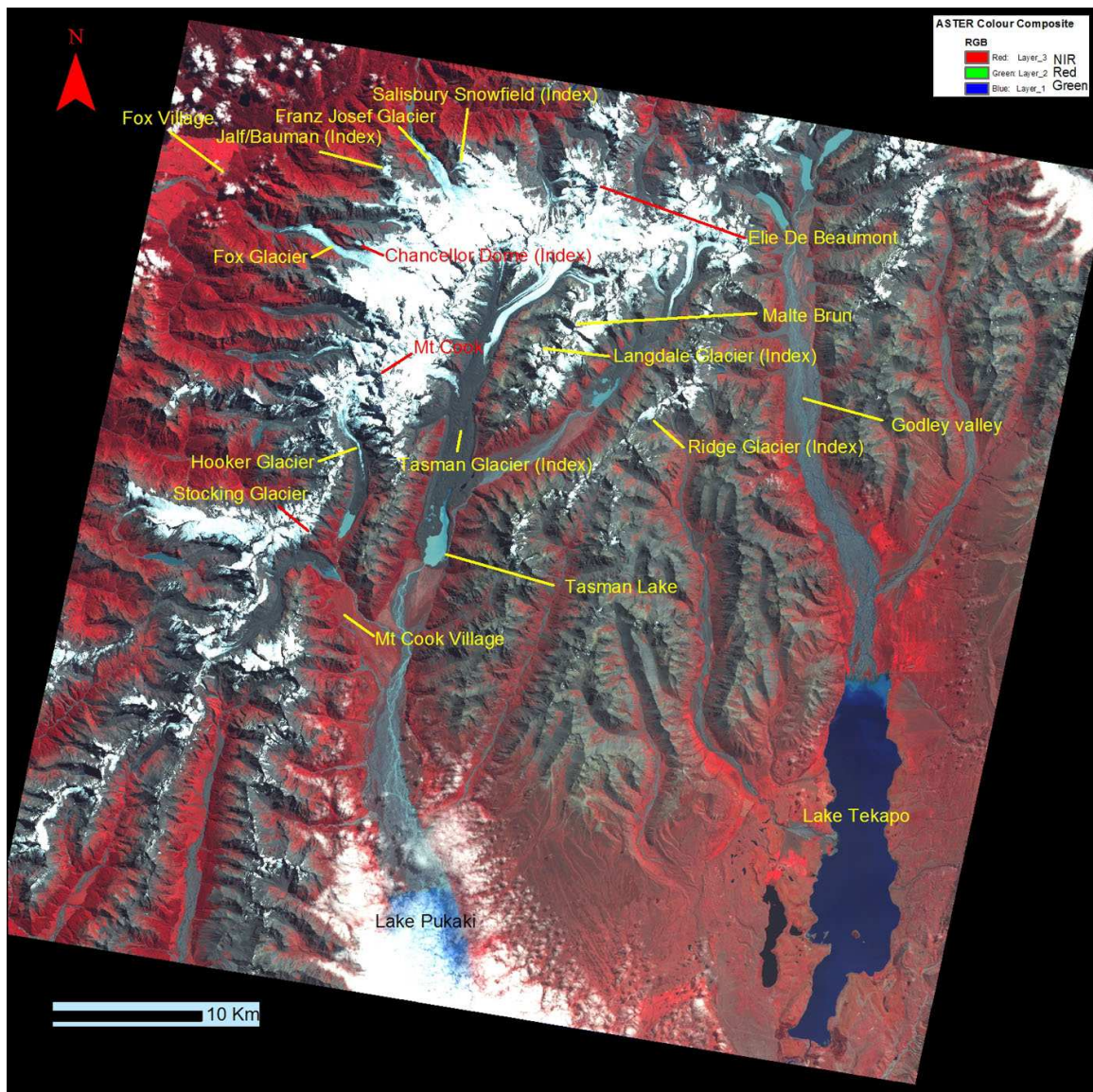
Figure 3.1.9. *The image chosen for the work with the more important geographic places in*

the area. All glaciers labelled (Index) are annually monitored by the NZ snowline survey. All the glaciers with names in this figure have been studied in field for this work.

3.2 Data

Terra spacecraft is the flagship of the *Earth Observing System*, a series of spacecraft that represents the next landmark step in NASA's role to observe Earth from the unique vantage point of space. Focused on key measurements identified by a consensus of U.S. and international scientists, Terra enables new research into the ways Earth's land, oceans, air, ice and life function as a total environmental system. Terra was launched into sun-synchronous Earth orbit on December 18, 1999, and started sending data back to earth in February 2000. Terra carries five scientific instruments: ASTER, CERES, MISR, MODIS, and MOPITT.

3.2.1 The ASTER Instrument on Terra spacecraft

ASTER (Advanced Spaceborne Thermal Emission and Reflection Radiometer) is a cooperative effort between NASA and Japan's Ministry of Economy Trade and Industry (METI), with the collaboration of scientific and industry organizations in both countries. The ASTER instrument provides the next generation in remote sensing imaging capabilities compared with the older Landsat Thematic Mapper, and Japan's JERS-1 OPS scanner (http://asterweb.jpl.nasa.gov/mission.asp). ASTER captures high spatial resolution data in 14 bands, from the visible to the thermal infrared wavelengths; and provides stereo viewing capability for digital elevation model creation. As the "zoom lens" for Terra, ASTER data are used by other Terra (e.g. MODIS) and space-borne instruments for validation and calibration. (http://asterweb.jpl.nasa.gov/mission.asp). The ASTER instrument consists of three separate instrument subsystems. Each subsystem operates in a different spectral region, has its own telescope(s), and was built by a different Japanese company. Figure 3.2.1 illustrates the spectral bands of ASTER. Table 3.2.1 gives the ASTER instrument characteristics. Figure 3.2.2 illustrates the stereo capabilities of the ASTER instrument.

3. METHODS

VNIR (Visible and Near Infrared)

The VNIR subsystem operates in three spectral bands at visible and near infrared (NIR) wavelengths, with a resolution of 15 m. It consists of two telescopes - one nadir-looking with a three-spectral-band detector, and the other backward-looking with a single-band detector. The backward-looking telescope provides a second view of the target area in Band 3B (NIR) for stereo observations. Cross-track pointing to 24 degrees on either side of the track is accomplished by rotating the entire telescope assembly.

SWIR (Shortwave Infrared)

The SWIR subsystem operates in six spectral bands in the medium infrared (MIR) region through a single, nadir-pointing telescope that provides 30 m resolution. Cross-track pointing (± 8.5 degrees) is accomplished by a pointing mirror. Because of the size of the detector/filter combination, the detectors must be widely spaced, causing a parallax error of about 0.5 pixels per 900 m of elevation. This error is correctable if elevation data, such as a DEM, are available.

TIR (Thermal Infrared)

The TIR subsystem operates in five bands in the thermal infrared region using a single, fixed-position, nadir-looking telescope with a resolution of 90 m. Unlike the other instrument subsystems, it has a "whiskbroom" scanning mirror. Each band uses 10 detectors in a staggered array with optical bandpass filters over each detector element. The scanning mirror functions both for scanning and cross-track pointing (± 8.5 degrees).

Kargel et al (2005) writes; "*ASTER has unique attributes and handicaps compared to other remote sensing systems. Other systems lack the stereo, same-orbit imaging capability that ASTER has. ASTER stereo-derived topography lacks sufficient vertical resolution to be useful in ASTER-to-ASTER glacier surface topography change assessment, except in extraordinary circumstances; but it is useful for comparison with reliable topographic map data where the baseline extends over several decades and to assess rapid thinning during glacier surges. ASTER topographic mapping lacks the large layover of synthetic aperture radar, but of course it cannot see through clouds; and ASTER has a higher lateral spatial resolution but lower vertical resolution compared to laser methods. ASTER stereo DEMs (digital elevation models) are being used to generate stable image orthorectifications and to map glacier lake, glacier terminus, and snowline elevations. ASTER's 90-m five band thermal imaging is unparalleled, but has just begun to be exploited for glaciological studies. Six short-wave*

infrared bands (30-m resolution) are well placed spectrally to be used with three visible/near-infrared bands (15-m resolution) for ice and water detection. Other systems duplicate or exceed some of ASTER's specifications, but none duplicate the whole package for glaciological investigations. ASTER imagery has already been used in e.g. Afganisthan and Pakistan, Butan, Antarctic Peninsula, Polar Research, Swiss glacier inventory, New Zealand".
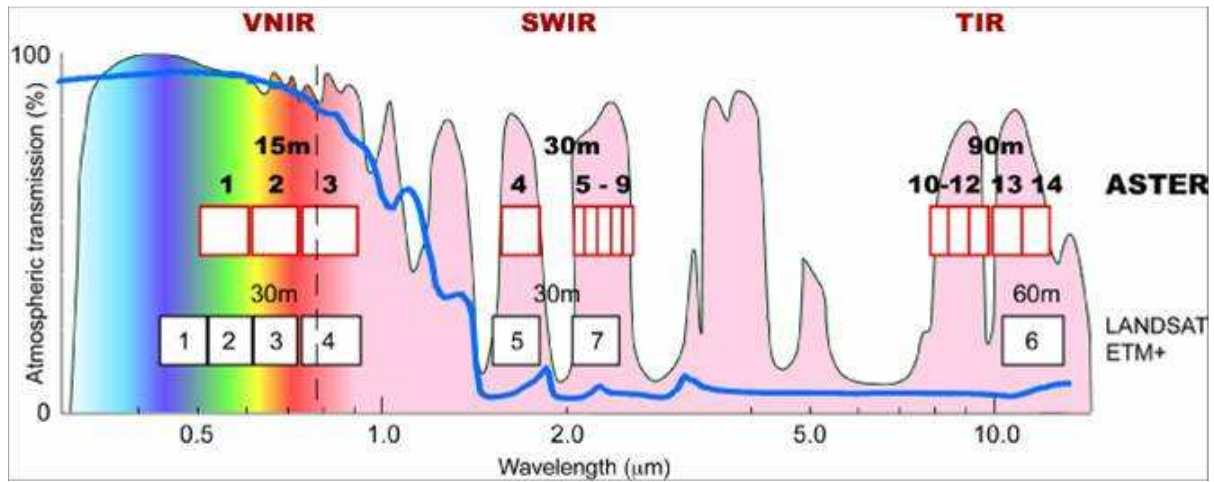
Figure 3.2.1. *ASTER spectral bands compared to Landsat ETM+. The rectangular boxes (red: ASTER, black: Landsat ETM+) indicate the sensor channels. The respective spatial resolution is indicated on top of the boxes. The coloured curve in the background represents the atmospheric transmission in dependency on the wavelength. The vertical dashed line marks the approximate margin of visible light. Abbreviations for sections of the light spectrum: VNIR (visible and near infrared), SWIR (short-wave infrared), and TIR (thermal infrared)* (adapted from Kääb et al, 2002).

Specification		Value	
Launch date		December 1999	
Orbit height		705 km, sun-synchronous	
Orbit inclination		98.3 degrees from the Equator	
Orbit period		98.88 minutes	
Equator crossing		10.30 a.m. (north to south)	
Ground track repeat cycle		16 days (or 233 orbits), *i.e. every 16 days the pattern of orbits repeats itself*	
Image sensors		multi-spectral, SWIR and TIR	
Spectral bands and range (µm)	VNIR	SWIR	TIR
	1: 0.52 – 0.60	4: 1.600 – 1.700	10: 8.125 – 8.475
	2: 0.63 – 0.69	5: 2.145 – 2.185	11: 8.475 – 8.825
	3N: 0.76 – 0.86	6: 2.185 – 2.225	12: 8.925 – 9.275
	3:B 0.76 – 0.86	7: 2.235 – 2.285	13: 10.25 – 10.95
	(backward looking)	8: 2.295 – 2.365	14: 10.95 – 11.65
Ground resolution at nadir (m)	15	30	90
Swath width (km)	60	60	60
Data rate (Mbits/sec)	62	23	4.2
Cross-track pointing (deg.)	±24	±8.55	±8.55
Cross-track pointing (km)	±318	±116	±116
Radiometric resolution/Quantization (bits)	8	8	12

Table 3.2.1 *ASTER instrument characteristics (adapted and modified from Gao & Liu (2001) and from http://asterweb.jpl.nasa.gov/mission.asp)*
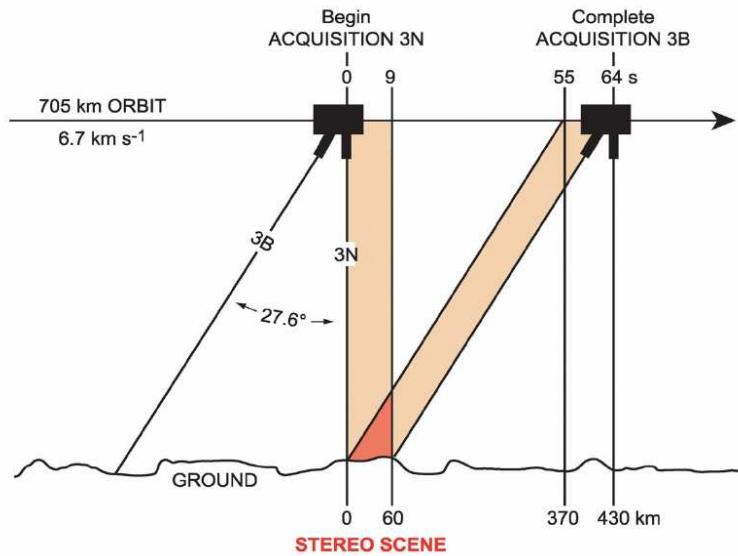
Figure 3.2.2 *ASTER stereo geometry and timing of the nadir-band 3N and the back-looking sensor 3B. An Aster nadir scene of approximately 60 km length, and a correspondent scene looking back by 27.6˚ off-nadir angle and acquired about 60 seconds later, form together a stereo scene (dapted from Kääb et al, 2002).*

3.2.2 Selection of the ASTER image

The ASTER image was selected considering the following criteria: cloud free, end of summer, and year with a negative mass balance. Because of New Zealand's isolated situation in the middle between two large oceans, the Tasman Sea on west and the Pacific Ocean on the east, the weather is unstable with many of fronts moving through. This combined with the ground track repeat cycle (time of revisit) of the Terra spacecraft containing the ASTER instrument (16 days), makes the number of good cloud free images of Central Southern Alps a minimum. In order to best be able to detect the glacier outlines, and at the same time to map the glaciers at their smallest size for the year (at the end of the glacier annual cycle for New Zealand in March/April) without having the image affected by early winter storms (which can occur even early in the summer), make the chances of obtaining usable images for glacier inventory to a minimum. For making glacier inventories from satellite imagery it is also an advantage if this is done in a negative mass balance year were all the seasonal-snow patches in the area are disconnected from the glaciers and cannot be misclassified as glaciers. Considering all these conditions the best ASTER image covering the Central Southern Alps was selected in the Earth Observing System Data Gateway library including images from

2001 to 2005. This image was recorded 14th of February 2002. 2002 was a very suitable year for making glacier inventory in New Zealand since it was the most negative year between 2001 and 2005 as shown in the snowline survey (Chinn et al, 2005). However, this does not mean that the actual extent of the glaciers was much smaller in 2002 compared to the adjacent years, but rather that most of the surrounding snowpatches present in late summers in other years were gone and were not misinterpreted as glaciers.

The chosen satellite image covers and area of 3939 km², or more than 2.6% of South Island's total area of 151215 km².The extent of the image contained in 1978 more than 40% of the total glacier area in New Zealand. If volume had been calculated for the image area that would probably have shown an even higher volume content compared to the total glacier volume in New Zealand, since the glaciers in the Mt Cook area are not only large in extent, but also very thick. Tasman glaciers itself is estimated to contribute to almost 1/3 of the total ice volume in New Zealand (Chinn, 2001). The glaciated areas within the boarders of the image in 2002 were 428 km², covering almost 11% of the image.

3.2.3 Selection of glaciers for field investigation

For validation of the different glacier classification methods used, GPS outlines of selected glaciers were collected in field. One problem with this approach was that the image was from 2002 and the field work was to be collected during the late summer/autumn of 2005. Potential glaciers for field work were thoroughly considered in order to select glaciers representative of the whole glaciated areas of Central Southern Alps. To reduce the negative effects of the time difference between the fieldwork and the image collection we selected 5 of the 6 Index Glaciers of the area since aerial photograph of these glaciers existed both for 2002 and 2005, so eventual changes during these years could be carefully considered. The Index Glaciers were also well spread over the study area, covering both eastern and western glaciers. Four of the six Index Glaciers were at convenient size and location that they were suitable for GPS ground mapping: Jalf/Bauman, Chancellor Dome, Langdale, and Ridge glacier. Salisbury Snowfield is way too large and in addition its terminus is too steep for GPS outlines. As a result of the steepness the terminus is constantly subject to ice calving. The glacier terminus has also pulled back quite a bit between 2002 and 2005 so GPS records of the terminal part would not be useful for validation purposes. The fifth Index Glacier, Tasman glacier, is the

largest glacier in New Zealand. GPS outlines of the whole Tasman was clearly not feasible and is likely not to have been very useful for validation. Also it is catastrophically retreating to the erosion by its huge proglacial lake. However, since this glacier is one of the most studied in New Zealand and is also one of the glaciers which have retreated most during the last decades it was considered interesting to get some records of the terminus of this glacier as well. Thanks to Glacier Explorers bringing tourist in boats on Tasman Lake 7 months a year, outlines of the frontal terminal part were collected fairly easily. This would not be useful for the validation of the classifications of the image, but would give a very good view on how much Tasman glacier lake expanded between 2002 and 2005. In addition to these 5 glaciers, Hooker, Fox and Franz Josef, and Stocking glaciers have been researched. Hooker glacier is similar to Tasman, but is quite a bit smaller and is also close to Mt Cook Village and would not be too time consuming to study. Some good GPS validations for a heavily debris covered glacier would be good to get, since these have the most difficult outlines to interpret. Franz Josef is maybe the most studied glacier in New Zealand and probably the most famous. Outlines for this one was thought to be very interesting. After the fieldwork was done, we learned that the Geographic Department of University of Canterbury annually collects GPS records for the very terminal part of Franz Josef. We obtained these outlines from 2002, collected the 22nd of April. GPS outlines from the same year as the image was very valuable for the validation. GPS data from Fox was also highly useful, though from 2005. Stocking glacier drains eastwards from the main divide toward Mt Cook Village. As a guest at the famous Hermitage Hotel in Mt Cook Village, this is the glacier you would look straight up onto from your hotel room. Thus, Stocking glacier is the glacier in NZ with the longest photographic record. The terminus was likely to have changed between 2002 and 2005 but the eventual change was considered to be interesting to determine from a climatologically point of view. All in all this added up to 9 glaciers (see figure 3.1.9).

3.2.4 Field data collection

3.2.4.1 GCP and CP collection

The purpose of collecting GCPs and CPs was to orthorectify the image. Prior to conducting the field work for GPS data collection, thorough preparation was required to choose

appropriate GCPs. In total, 31 points were collected in the field using a Trimble Pro-XRS GPS instrument. Because of the remoteness of the area this was not an easy task. Most points were collected close to glaciers (e.g. prominent rocks) and at road intersections within the image. The collected points were sort of clustered (both in planimetry and altimetry), some points around 200 m a.s.l. on the westcoast, some more around 700-1100 m a.s.l. around Mt Cook Village, Tekapo Village and around the roads on the eastern side of the main divide, and points around 2000-2300 m a.s.l. collected on the field glaciers (figure 3.2.3). Points were lacking in the ranges between 300 – 700 m a.s.l., 1200 - 2000 m a.s.l., and 2300 – 3754 m a.s.l. In addition the points were not evenly spread in the image, but as good as what's possible using only field collected points in such a relatively remote and steep area. Of the total of 31 field collected points only 22 were finally found to be accurate enough for the orthorectification, due to difficulty of accurately identifying all the points in the ASTER image. GCPs collected from the field were post-processed by using the smart code and carrier processing method with data collected from the 40 Trimble Base Station located at the University of Otago School of Surveying. After postprocessing, the position of the points was visualised in ArcGIS software. The theoretical accuracy of the points after correction was on a sub-metre scale. The points were collected from late February till late April 2005.
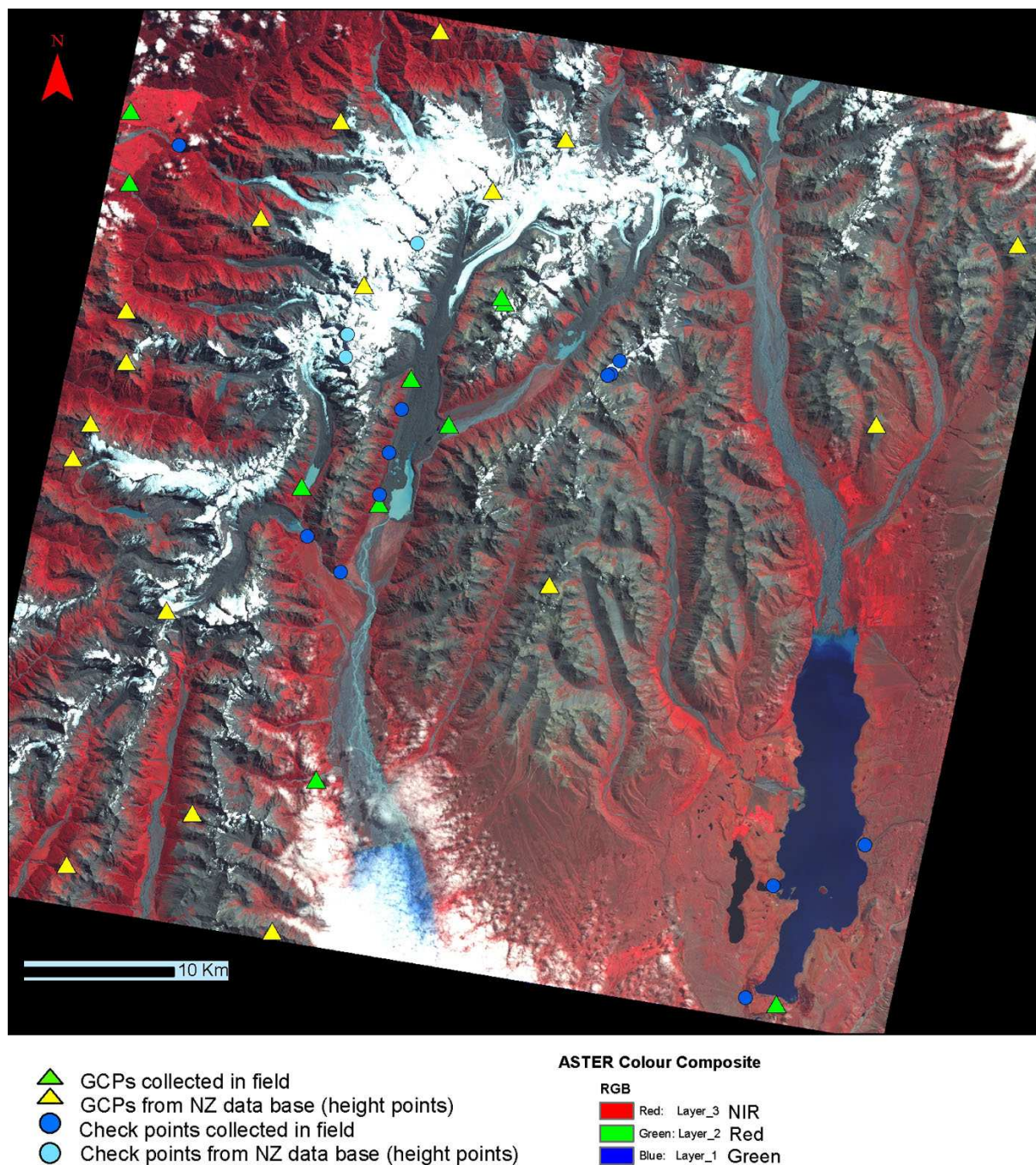
Figure 3.2.3 *Ground Control Points and Check Points from the field and from the New Zealand topographic data base*.

3.2.4.2 GPS recorded glacier outlines

GPS outlines for the individual glaciers were obtained by walking at the boundary between snow and rock (figure 3.2.6). The GPS were set to record a new position every 5 seconds. It had to receive at least 5 satellites at the time to get a position. This threshold was set in order

to get a high accuracy. However, this caused some problems in steep areas with cliffs above, reducing the view of sky. For instance on Ridge Glacier the outline was not closed as a polygon resulting from lack of recorded data from a part of the glacier with high cliffs above. This problem could have been minimized by finding the times during the day when there would be a maximum of satellites viewable from the Mt Cook region, or eventually by setting a lower threshold. However, we preferred to not compromise the quality of the GPS data, and planning GPS work in these areas is difficult in reason of cost (helicopter time) and security issues (weather, availability of climbing partner).

As for the points collected from field the glacier outlines were also post-processed by using the smart code and carrier processing method with base station data collected from the 40 Trimble Base Station located at the University of Otago, School of Surveying.

For some glaciers the GPS positions could not be recorded at the believed exact boundaries. For instance on Tasman Glacier a certain distance to the ice cliffs had to be kept while driving the boat. On Hooker glacier it was not possible to walk at the very end of the ice cliffs, and the same for Fox and Franz Josef and Stocking where there where not always possible walk at the ice boundaries because of the overhanging treat of ice calving. In these cases the average distance to the believed exact boundaries was noted and the positions were later adjusted in ArcGIS. The dates of the GPS recording are shown in table 3.2.1. The obtained glacier outlines from the field work are shown in figure 3.2.4 and 3.2.5.

Field glacier	Date/s of recording
Ridge Glacier	14-16th of March 2005
Jalf/Bauman	21-23st of March 2005
Stocking Glacier	Mainly 5th of April 2005, but also some on the 3rd
Chancellor Dome	9th of April 2005
Fox Glacier	10-11th of April 2005
Franz Josef Glacier	12th of April 2005
Tasman Glacier	19th of April 2005
Hooker Glacier	22nd of April 2005

Table 3.2.2 *Dates when the field work was carried out on the different glaciers*
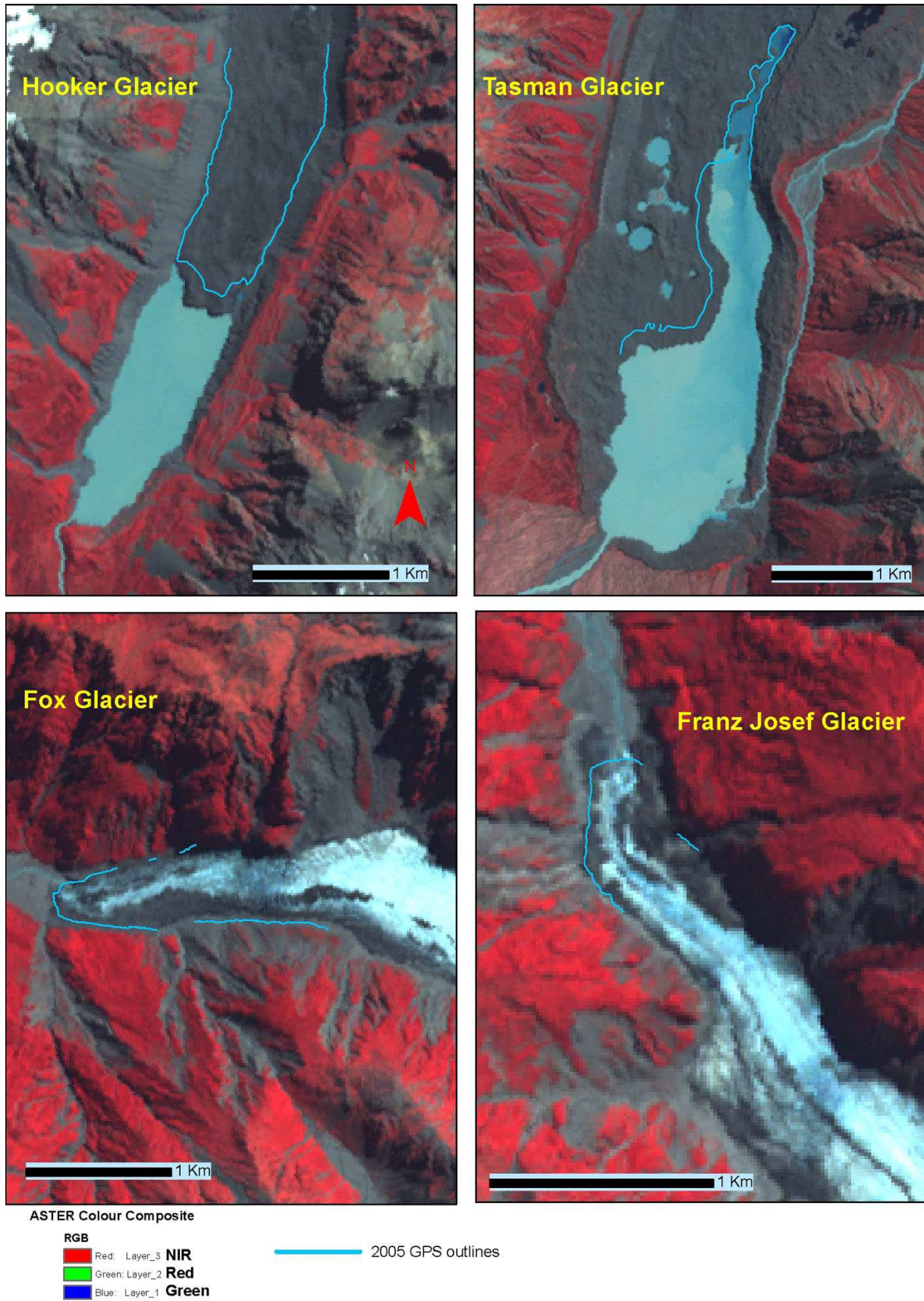
Figure 3.2.4 *Field work on the largest glaciers studied (Tasman, Hooker, Fox and Franz Josef glaciers).*
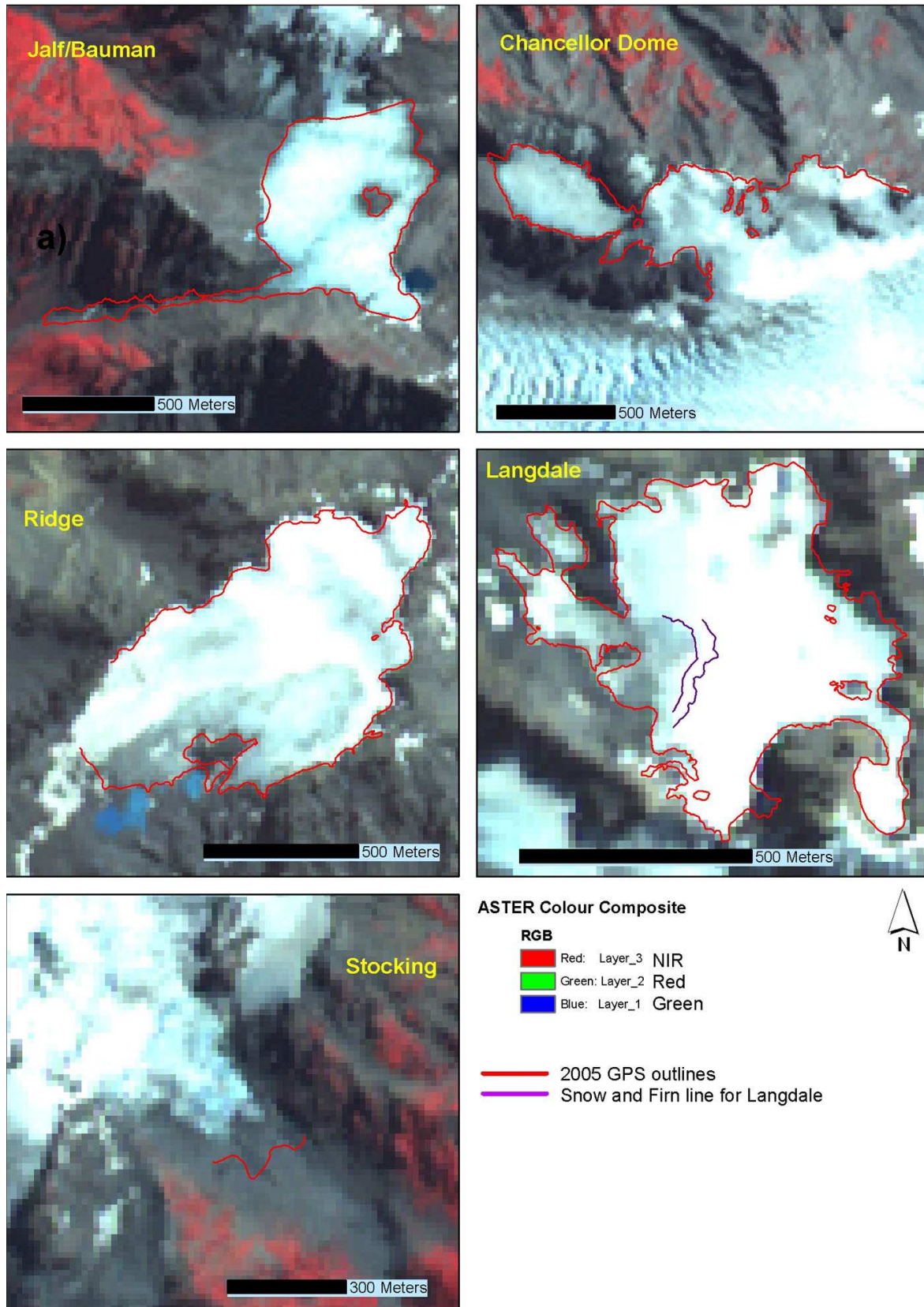
Figure 3.2.5 *Field work on the smallest glaciers studied. Snow and Firn line for Langdale glacier were recorded on request from Trevor Chinn for validation of the annual snowline survey.*

Figure 3.2.6 *Field collection of the glacier outlines. The photograph is from Ridge glacier (photograph, Pete Sinden).*

3.2.5 Oblique aerial photographs

Aerial photographs of the 5 field work Index glaciers, were used to adjust for eventual changes in the glacier outlines between image acquisition (2002) and the in-situ recordings (2005), when validating the manual digitizing of the satellite image.

Chinn and Salinger (2001) writes; *"On the annual snowline flights, a folder of photographs of each glacier is held by the "navigator" seated beside the pilot. These photographs are used to closely duplicate the position from which previous photographs were taken. The photographer operates from the back seat, shooting from both sides of the aircraft. These surveys also provide the opportunity to record geomorphic features and events, other glaciers, and selected glacier termini in addition to the index glaciers. The flights are made mainly between 9000 ft (2700 m) and 10 000 ft (3000 m). An altitude of at least 10 000 ft gives the best angle on the glacier snowlines, but civil aviation regulations do not permit normal flights to remain above this altitude for prolonged periods"*. The timing of these

flights is critical as they should be made at the end of the glacial summer after all significant snowmelt has ceased, but before the first winter snowfall covers and obscures the subtle annual snowline. Figure 3.2.7 shows the annual snowline survey photos for 2002 and 2005 for 4 of the 6 index glaciers in the area.

a) Chancellor Dome, 2002

b) Chancellor Dome, 2005
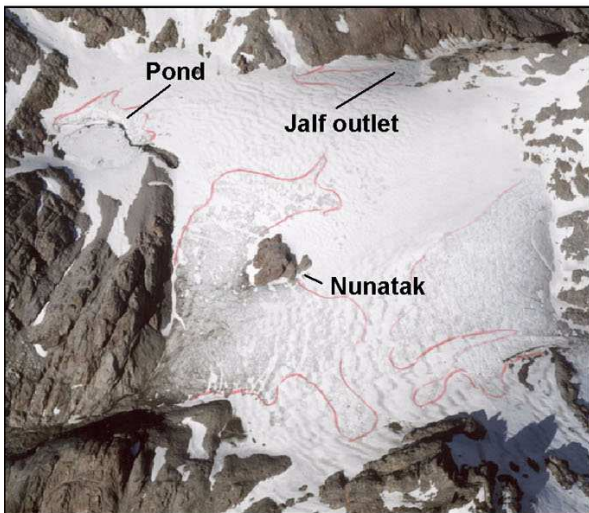
c) Jalf/Baumann, 2001
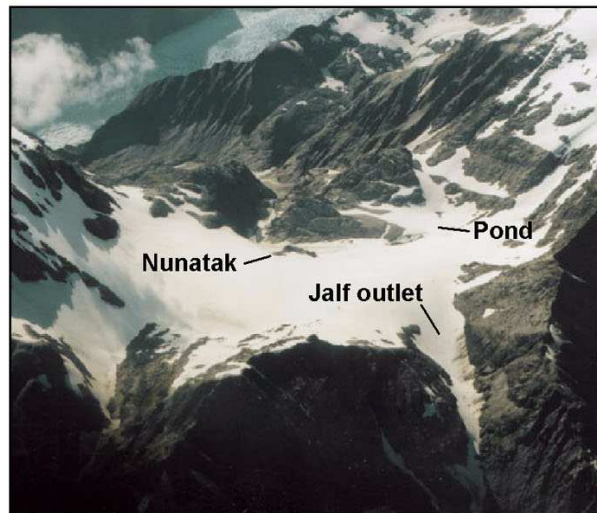
d) Jalf/Baumann, 2005
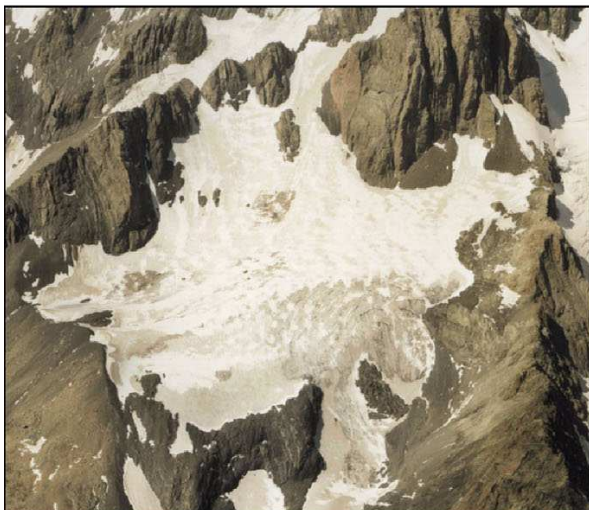
e) Langdale, 2002

f) Langdale, 2005
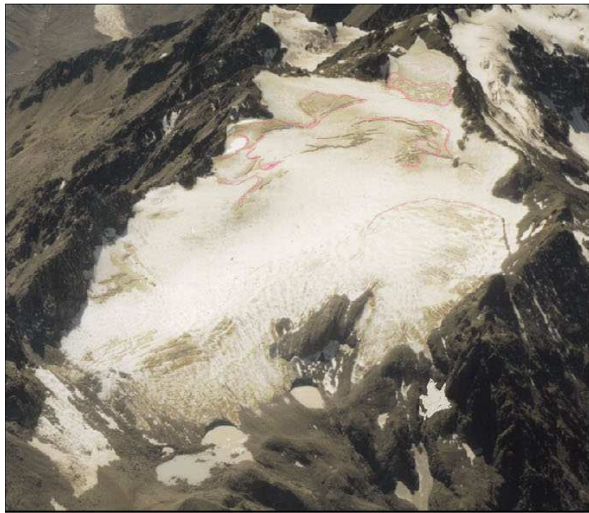
g) Ridge Glacier, 2002

h) Ridge Glacier, 2005

Figure 3.2.7 *Oblique aerial photographs of four of the field studied glaciers taken in 2002 and 2005. Due to bad weather/fog, photograph of Jalf/Bauman from 2002 was not recorded. The red marks in some of the images are the photographer's interpretation of the snowline. All photos are taken in late March (photographs Trevor Chinn).*

3.2.6 Digitized glacier inventory from 1978

Vertical aerial photographs were used for initial identification and mapping of glaciers for the New Zealand glacier inventory. However, the Glaciology Section, Water and Soil Division of the Ministry of Works and Development, found that the majority of the vertical aerial photographs of the New Zealand Alps were taken at times when seasonal snow cover still persisted, obscuring the true outlines of the glaciers. Consequently, a programme of annual aerial flights over the glaciers in New Zealand was inaugurated both to overcome this problem and to monitor the glacier mass balance and other changes. The aerial flights have continued from 1977 with only a few years missed because of weather or other reasons. The 1978 set of oblique aerial photographs gave the best coverage of the early glacier flights, and the inventory has, whenever possible, been mapped for autumn 1978. One exception is the North Island on Mount Ruapehu, where no suitable photographs were available until the first glacier flight to the North Island was made in 1988. Ruapehu has no influence on this study, though. Some 50 index glaciers, well distributed along the Southern Alps were chosen for annual snowline survey, but in addition by varying the flightline each year, this programme has photographed almost every one of the approximately 3150 glaciers in New Zealand, and

amassed an archive of some 10.000 photographs all of which have subsequently been identified, annotated and archived (Chinn, 1991).

3.3 Data preparation

3.3.1 Preparation of the ASTER image

Stacking of layers

In order to be able to view the information in the 4th spectral band (the first of the SWIR sensors) together with the VNIR bands, this band had to be resampled down to 15 m spatial resolution (compared to the original 30). After the resampling the orthorectification could be performed on all the bands. The 4th spectral band was used both for the NDSI and for the band3/band4 ratio. However, this resampling could have been done directly in PCI.

Orthorectification

The image had to be orthorectified to ensure an appropriate mapping accuracy. The field collected points were divided into ground control points (GCPs) and independent check points (CPs). 10 GCPs were used to generate the orthorectification, while 12 CPs were used for the validation. Toutin (2003) noticed that more than 12 GCPs does not increase the accuracy, provided that there is no extrapolation in planimetry nor in elevation. The residual errors for the GCPs and CPs were observed in terms of the Root Mean Square Error (RMSE). For the GCPs RMSE (X and Y) was in meters 3 and 4.5, respectively and for the CPs the RMSE (X and Y) 15.45 and 13.8 meters, respectively. In practical terms these errors are generally less than 1 pixel (15 meters), which is very good. These errors are absolutely within the acceptable limits to produce a reasonably accurate orthorectified image in mountainous areas (Toutin, 2004). The DEM used for the orthorectification was made of contour lines, with a 20 meter interval, from the New Zealand topographic data base using PCI. These contour lines were made from aerial photographs recorded in 1986. The 22 field collected points were points we felt very confident in. All these points had accuracy better than 15 m when overlaying the DEM. The software used for the orthorectification was Geomatica Orthoengine in PCI.

3. METHODS

However, when overlaying rivers, height points, roads, etc from the Land Information New Zealand (LINZ) topographic database this clearly showed that the orthorectification was not good enough. In some areas close to the field collected points it was really good (i.e within 1 pixel and max 2, as suggested by the RMS) but in other areas there were large shifts. For instance Mt Cook was shifted more than 6 Pixels (90 meters). The shift varied highly from area to area, in the western part the orthorectified image was some places shifted up to 6 pixels west of the height points from the database, as for Mt Cook, but in the north-eastern part of the image it was up to 4 pixels (60 meters) in the exact opposite direction. The reason for these shifts is likely to be due to planimetric and altimetric extrapolation due to the relatively clustering of the field collected points (Toutin, 2004) (see figure 3.2.3). It was difficult to get points over the whole height and spatial ranges in the field.

To improve the orthorectification height points from the LINZ database were added as GCPs and CPs. Finally 28 GCPs and 15 check points were used for the orthorectification. Since it is common to have approximately the same amount of CPs and GCPs, the 43 points were first divided into the same amount of GCPs and CPs. However, when visual comparing the orthorectification to the topographic data it was not very accurate compared to when using 28 GCPs and 15 CPs. The ideal situation could then have been to collect more Check point, but since the determination of good points in the image was very time consuming this was not considered to be critical. The RMS error for the final orthorectification was for the GCPs (X and Y) 15.3 and 14.55 meters, respectively, and for the CPs (X and Y) 17.1 and 14.7 meters, respectively, which was also very good. When displaying the orthorectified image in 3D in Arc Scene and overlay rivers and other topographic features, they seemed to match really well.

Atmospheric correction

Spectral radiance from ground features will depend on aerosols in the atmosphere, viewing angle of the satellite etc (Kääb, 2005). When comparing several satellite images of the same area, it would be important to correct for these errors. This could be computed using atmospheric data such as visibility collected from the nearest airport on the days images are recorded, or by normalizing one date according to another (Kääb, 2005). The reflectance values in the image would be improved compared to the real reflection from the ground, however, when working only on one image this would not be critical and was not done for this work.

3.3.2 Preparation of the digitized glacier inventory from 1978

The data from the 1978 inventory was available in MapInfo files. These were exported as MIF (Mapinfo Interchange Format), opened in ArcGIS, and converted to Shape files. All the files were originally in New Zealand Map Grid (NZMG) coordinate system, and were reprojected into New Zealand Transverse Mercator (NZTM). A frame delineating the 2002 image was made and the 1978 outlines were clipped with this frame to get the 1978 glacier area located within the image boundaries. The areas of the polygons were calculated using a Visual Basic Script in ArcGIS.

3.3.3 Choosing 3 study sites in the image for closer inspection

In order to the test automatic classification methods in glacier areas with different characteristics, 3 study sites in the images where chosen. Franz Josef glacier along with Fox glacier are the two largest glaciers on the west-coast. These glaciers represent the wet, warm, maritime end of the glacier response scale. Franz Josef and Fox glaciers have very little supraglacial debris compared to their eastern counterparts. Hooker glacier is heavily debris covered and has a large terminal lake making misclassification with automatic methods more likely. Ridge glacier area, represent the smaller, high elevated glaciers on the eastern side of the divide. Some of these small glaciers have large debris content, others not. All theses three areas contained glacier outlines from field. Automatic methods were tested and compared to the manual digitizing of the satellite image. Choosing optimum thresholds in band rationing will possibly vary according to the characteristics of the specific area. The classification results for these 3 areas where therefore compared to the classification results of the whole area. The 3 study areas are shown in figure (3.3.1).
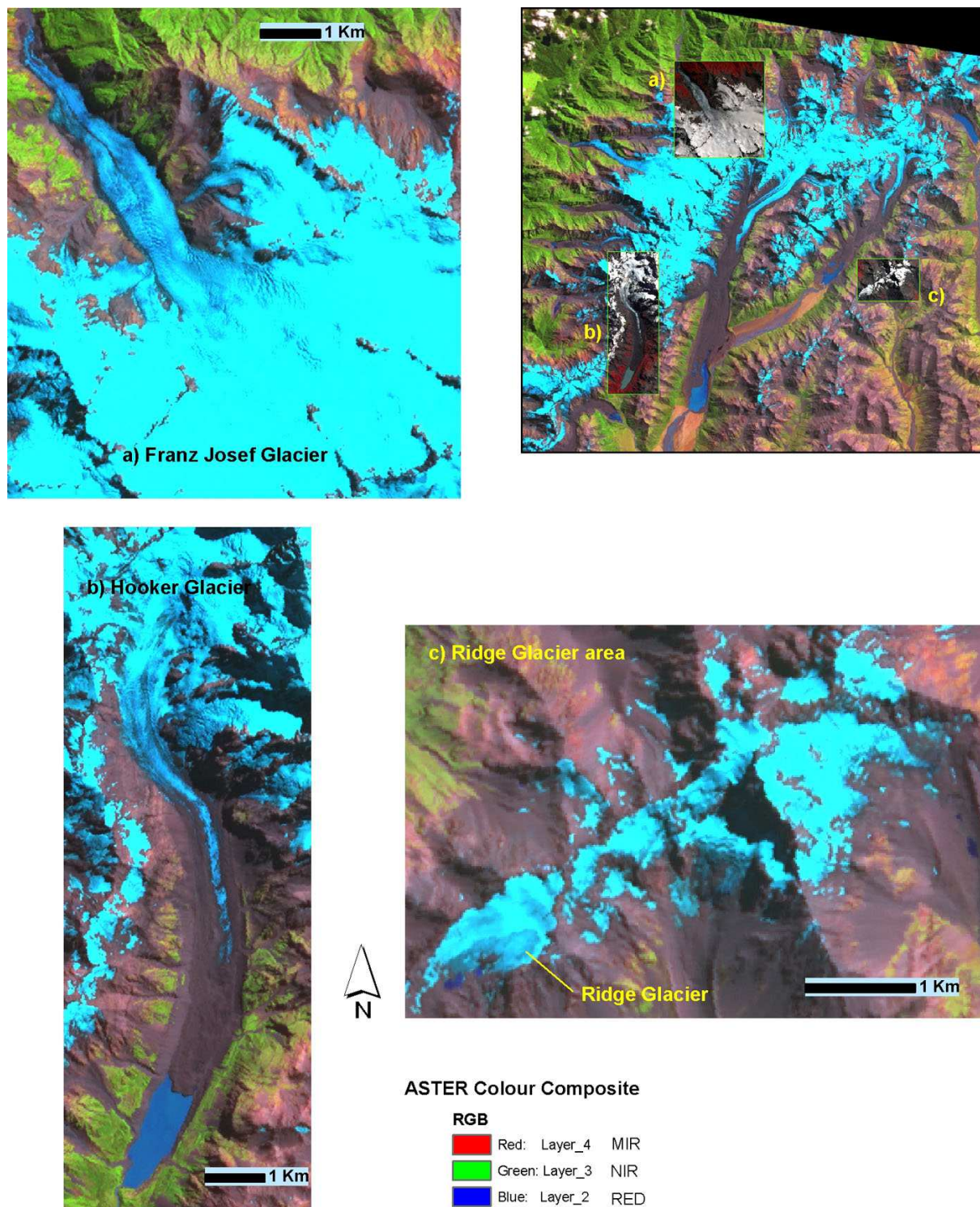
Figure 3.3.1 *The three chosen study sites for closer inspections of automatic classification methods. Franz Josef, Hooker and Ridge glacier area.*

3.4 Extracting land ice area using different classification methods

3.4.1 Image segmentation, band 3/band 4 ratio and NDSI

Band ratios and NDI have proved to be efficient way of glacier extraction (e.g. Paul, 2003). A ratio of TM/4TM5 was found to be the most appropriate method for the New Swiss Glacier Inventory (Paul, 2003). Thus, it was considered interesting to test this method in the New Zealand environment.

The formulas for these segmentations are given in chapter 2.2, and the bands used in these segmentations are shown in figure 3.4.2. When performing the NDSI there was a large misclassification of lakes, especially the turbid glacier lakes with high amounts of suspended material. This problem was overcome by manually removing all the water from the image (figure 3.4.1). Because the VNIR and the SWIR channels are recorded by separate instruments these layers don't overlap perfectly leaving a stripe, especially at the western side of the image, with no information recorded in the one instrument. When thresholding the NDSI this stripe of no information is classified as glacier area. This was removed manually along with the lakes (figure 3.4.1). A manual digitizing of the water and frame area was given values of 0 for lakes and frame and 1 to all other areas. By multiplying this raster with all the NDSI results (a raster of values 1 for glaciers and 0 for all other pixels), the water and frame areas were removed. For the NDSI threshold of 0.3, 0.35, 0.4, 0.45, 0.5, 0.55, 0.6, 0.65, 0.7 were tested both for the three study areas and the whole image. For the band3/band4 ratio, some misclassification occurred to vegetation patches. Clusters of dense vegetation (rainforest) were commonly classified as glaciers. One way reduce this misclassification was to apply a median filter. All the thresholds tested were done with and without a median filter. Thresholds of 1.8, 2.0, 2.2, 2.4, were tested for the study areas and the whole image.
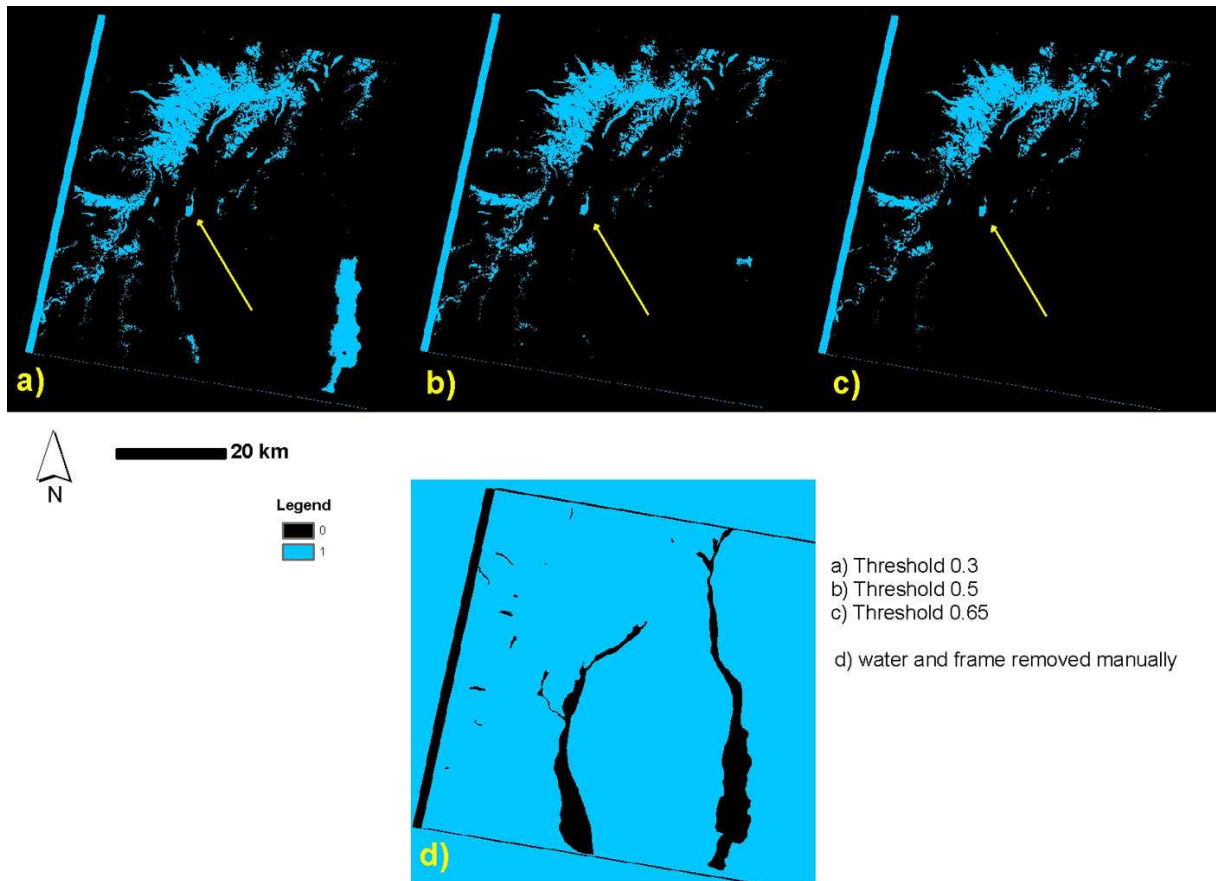
Figure 3.4.1 *a,b,c shows NDSI segmentation of the whole image using different thresholds. Window a) a very low threshold classifies more areas to glaciers than the actual area of glaciers in the image. Even the large Lake Tekapo is classified completely as glacier area. Window c) includes least glacier area using a high threshold. Even so, Tasman Lake is still classified as glacier. Window b) seems to be the optimized threshold. Window d) shows the water and frame areas which were digitized manually and removed from the NDSI results using the raster calculator. The arrow in a), b) and c) point at Tasman Lake.*
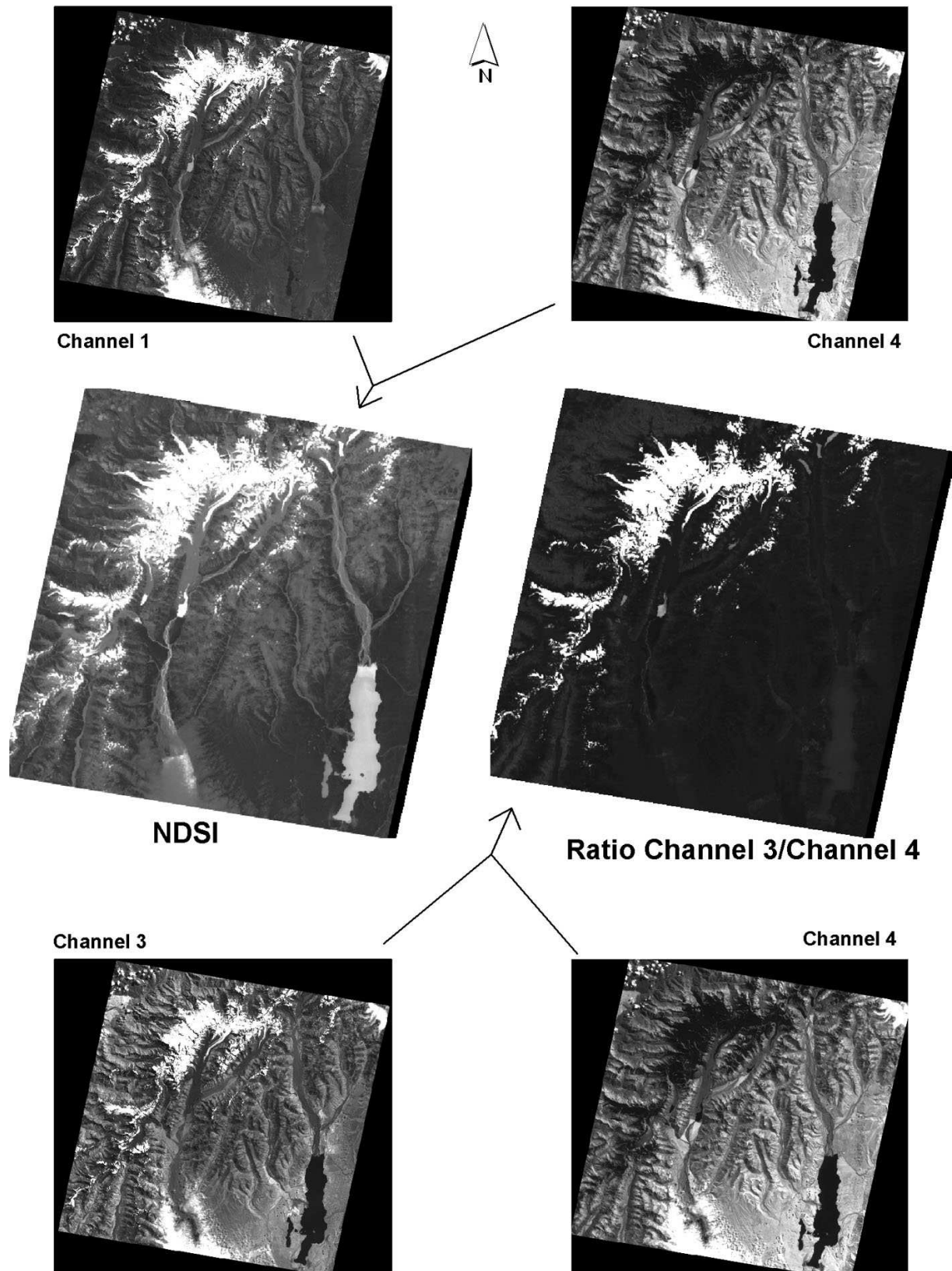
Figure 3.4.2 *The different channels used for performing a NDSI and a band3/band4 ratio. Channel 1 and 4 are used for the NDSI and channel 3 and 4 for the band3/band4 ratio. The two middle figures show the results of these segmentations.*

3.4.2 Supervised classification

This method was only tested for the Franz Josef area. To get a good result this method demands lots of work in selecting the best possible training sites. Misclassification is very likely in areas were lots of the ground features have similar reflectance values. This method is more appropriate when working on a smaller area where the ground features have far from similar spectral signature, or for detailed classification when the majority of the spectral values in an image is masked out, e.g. after having extracted the glacier areas by image segmentation, supervised classification could be appropriate for classifying the different types of snow and ice within these areas.

3.4.3 Manual delineation

As a result of the heavily debris covered glacier tongues of many of the glaciers in the area, in addition to the extreme vertical relief causing a large shadowing effect, it was decided to manual digitize the glacier areas in the image on the whole. This is an extremely time consuming job, thus not making it a suitable method when working on several images. However, when the interpreter has a good knowledge of how the area looks from the ground, and when field work, aerial and ground photograph of the area are present, this is likely to be much more accurate than various automatic classifications. This option was considered to ensure that we would have a good dataset to quantify glacier changes between 1978 and 2002 and as validation for the automatic methods. Another option could have been to use automatic classifications for the whole area and later correct manually for all areas where the algorithms are not able to detect the real glacier boundaries (e.g. debris covered glacier tongues or shadowed areas).

The manual delineation was done as a photo-interpretation of the image displayed in the VNIR channels (near-infrared, red and green). The first SWIR channel (band 4) was not used in this work. In areas of doubt the image was overlaid by contours (from the LINZ database, made from aerial photographs recorded in 1986). In addition printed topographic maps and aerial photographs of the index glaciers were used for the interpretation. The glacier outlines obtained from field were never displayed during this work as to avoid biases in the validation.

The image was mainly digitized on a sub-pixel accuracy, so overall giving more than one point per pixel. The manual delineation was later compared to field work to ensure its accuracy was appropriate. The manual delineation is used for calculating the 2002 glacier areas and for validation of the various automatic classification methods tested.

3.5 Computing 2002 glacier area and the change in glacier area for the 24-year period

As it was considered the most accurate the manual digitizing of the 2002 satellite image was used for calculating the 2002 glacier area. This was done using a visual basic script in ArcGIS. The digitizing of the 2002 image had been done in 3 different shapefiles. One file for the largest glacier areas in the image that were connected (these were originally digitized as lines and later converted to polygons), one file for all the rest of the smaller glacier polygons, and one file for the nunataks. When calculating the areas from the polygons this worked fine, however, later when working in raster all the polygons inside nunataks (small glaciers on nunataks) had to be extracted as a own layer in order to be able to add this glaciers to the 2002 glacier raster after having subtracted the nunataks. The 1978 inventory consisted of glacier polygons, voids (nunataks), and glacier in voids (small glaciers on nunataks). The main divide of the Southern Alps was also digitized to compare changes for both sides of the divide. Figure 3.5.1 illustrates the flow of these calculations. Global change areas were computed in km². In addition maps were produced to analyze how the changes are distributed in space. The 1978 and 2002 outlines were converted to raster files. The glaciers of the 2002 map received a value of 2 and the non glaciers received a value of 0. The glaciers of the 1978 map received a value of 1 and the non glaciers received a value of 0. By summing both raster a new map showing the changes was produced, including 4classes: glaciers in both years (value 3), glaciers only in 2002 (value 2, i.e. advancing glaciers in the time-period, or eventually misclassified glacier area), glaciers only in 1978 (value 1, i.e. retreating glaciers in the period, or eventually misclassified glacier area) and areas not being glaciers in any of the inventories (value 0).

Cartographic model of the 1978 and 2002 glacier area calculation

Original data from the 1978 glacier inventory were in MapInfo format (map) and in New Zealand MapGrid projection

'78POLYGONS.map

'78VOIDS.map

''78GL_IN_VOIDS

Exported to mif format and imported into ArcGis. Then reprojected into New Zealand Transverse Mercator 2000 (NZTM)

'78POLYGONS.shp

'78VOIDS.shp

'78GL_IN_VOIDS.sh

The areas were clipped to fit within the image and in the next step into east and west of the main divide

Substracting the voids from the polygons and adding glaciers in voids gave the glacier area

'78POLYGONS_west of main divide

'78VOIDS_west of main divide

'78GL_IN_VOIDS_west of main divide

Total glacier area in 1978 west of the main divide of the Southern Alps within the extent of the 2002 ASTER image

Total glacier area in 1978 within the extent of the 2002 ASTER

'78POLYGONS_east of main divide

'78VOIDS_east of main divide

'78GL_IN_VOIDS_east of main divide

Total glacier area in 1978 east of the main divide of the Southern Alps within the extent of the 2002 ASTER image

Change in glacier area between 1978 and 2002 west of the main divide of central Southern Alps

Change in glacier area between 1978 and 2002 Within the extent of the 2002 ASTER image, covering approx 50% of the ice in New Zealand

Change in glacier area between 1978 and 2002 east of the main divide of central Southern Alps

2002LARGEPOLYGONS_west of main divide

2002SMALLPOLYGONS_west of main divide

2002NUNATAKS_west of main divide

Total glacier area in 2002 west of the main divide of the Southern Alps within the extent of the ASTER image

2002LARGEPOLYGONS.shp

2002SMALLPOLYGONS.shp

2002NUNATAKS.shp

2002LargePOLYGONS_east of main divide

2002SMALLPOLYGONS_east of main divide

2002NUNATAKS_east of main divide

Total glacier area in 2002 east of the main divide of the Southern Alps within the extent of the ASTER image

Total glacier area in 2002 within the extent of the ASTER image

West of Main Divide

East of Main Divide

Total glacier area within image boundaries

Total change 1978 - 2002 within image boundaries

1978 Polygons

2002 Polygons

Figure 3.5.1 *Flowchart of a carthographic model of the 1978 and 2002 glacier area calculation*

3.6 Comparing individual glacier change from 1978 to 2002

In addition to comparing the actual total area changes in the 24-year period, the most significant changing glaciers are also shown and the reasons behind these changes are later discussed. This includes all the glaciers studied in field in addition to the ones that have changed most.

4. RESULTS: Method assessment

4.1 Methods for assessing the accuracy

In order to validate the manual digitizing of the 2002 satellite image these outlines were visually compared to outlines collected in the field in 2005 and to the oblique aerial photographs from the snow line survey in 2005, in addition to ground photographs from the area. The snowline survey photos were particularly important since the field work was done 3 years after the satellite image was recorded. The results from the annual snowline survey, giving the altitudinal shift in the snowline averaged over all the index glaciers from year to year, was also important information to keep in mind when validating the manual digitizing with the field collected outlines. The accuracy of the manual digitizing is discussed in chapter 5.

After having computed the automatic classifications, these were compared to the manual digitizing first visually, then by computing confusion matrixes for the classification results. This was done by converting the manual digitizing and the automatic classification results to raster formats and given values as described in section 3.5. After taking the sum of these two, the resulting raster with 4 classes showed; pixels of value 3; areas classified to glaciers in both the manual digitizing and the automatic method, values of 2; areas only classified as glaciers in the digitizing (e.g. areas with debris ,shaded areas or wrong human interpretation), values of 1; areas only classifies as glaciers in the automatic method (e.g. turbid water in the NDSI, vegetation patches in the band3/band4 ratio) and values of 0; all areas not classified as glaciers in any of the methods. Confusion matrixes were built for the three validation areas and the whole image, and for all the thresholds tested in order to see how much area dependent the thresholds and the different classification methods tested were. The results from this are displayed in tables, given in percent of the total amount of pixels within the different areas. In order to easier be able to compare the areas, producer's, user's and overall accuracy were calculated. For simplicity this was only done for the threshold that was though to be the optimum (2.0 for Band3/Band4 ratio and 0.5 for NDSI). Producer's accuracy gives an indication on the probability of a reference pixel (glacier in the manual digitizing) being

correctly classified. This is calculated by dividing the total number of pixels in the glacier or glacier free areas classified automatically, by the total number of pixels in these classes as indicated in the reference data (the digitizing). User's accuracy is indicative of the probability that a pixel classified automatically on the image represents that category on the ground. This is calculated by taking the total number of correct pixels in a category (glaciers in the manual digitizing) and divide it on the total number of pixels that were classified in that category. Overall accuracy is perhaps the simplest descriptive statistic (Congalton, 1999) and is computed by dividing the total correct (here with only two classes; glaciers and non-glaciers as given in the digitizing) by the total number of pixels in the error matrix (Congalton, 1999).

4.2 Comparison of manual digitizing with GPS collected glacier outlines

When overlaying the manual digitizing with the GPS collected glacier outlines one could see that the termini of the larger glaciers had changed too much between the time of image acquisition and when field work was conducted, so this comparison could not really be used for validation purposes. However, the lateral margins of these glaciers were believed to be useful for validation. For the smaller glaciers there seems to be a good correlation between the manual digitizing and the field work (except from Stocking glacier), in spite of the three year period between the two data acquisitions, indicating that the manual digitizing is fairly accurate for these small glaciers, and that they have changed little during the 3 years (figure 4.2.1). The correlation is particularly good for Ridge glacier, and for the major parts of Jalf/Bauman, Langdale and Chancellor Dome. Of these glaciers Ridge was probably the most straightforward to map in field, with obvious boundaries except for a few places (see figure 3.2.6), whereas Landgdale and Jalf had more complex boundaries in addition to more seasonal snow around the margins making the field interpretation more difficult. The essential part of Chancellor Dome was also fairly easy to interpret. The overall agreement between the field collected outlines and the manual digitizing is between 1 pixel and rarely more than 2. For the margins of Hooker glacier the agreement between the field outlines and digitizing is not always as good as one could expect (figure 4.2.2). These lateral boundaries of Hooker are

not expected to have changed noticeably between 2002 and 2005 except for a small lowering of the surface elevation. This might indicate that the manual digitizing of debris covered glacier tongues in a valley bottom might not be as straight forward as one would expect. The outlines of Franz Josef terminus from April 2002, recorded by the geography department of University of Canterbury, agreed very well with the manual digitizing. The GPS outlines for Fox and Franz Josef from 2005 indicates a small retreat and a surface lowering since 2002 for these two, in particular for Franz Josef (figure 4.2.3). In figure 4.2.3 there is information from 4 different times. The elevation model is made from contour lines from aerial photographs recorded in 1986, the ASTER image recorded 14th of February 2002 draped over the 3D model, the frontal position of Franz Josef recorded 22nd of April 2002 and the field work from April, 2005. These two glaciers commenced in readvances in 1983/84 in response to positive mass balance. This can be seen in the figure since the surface of the glaciers in the 3D model does not fit the image, nor the outlines.
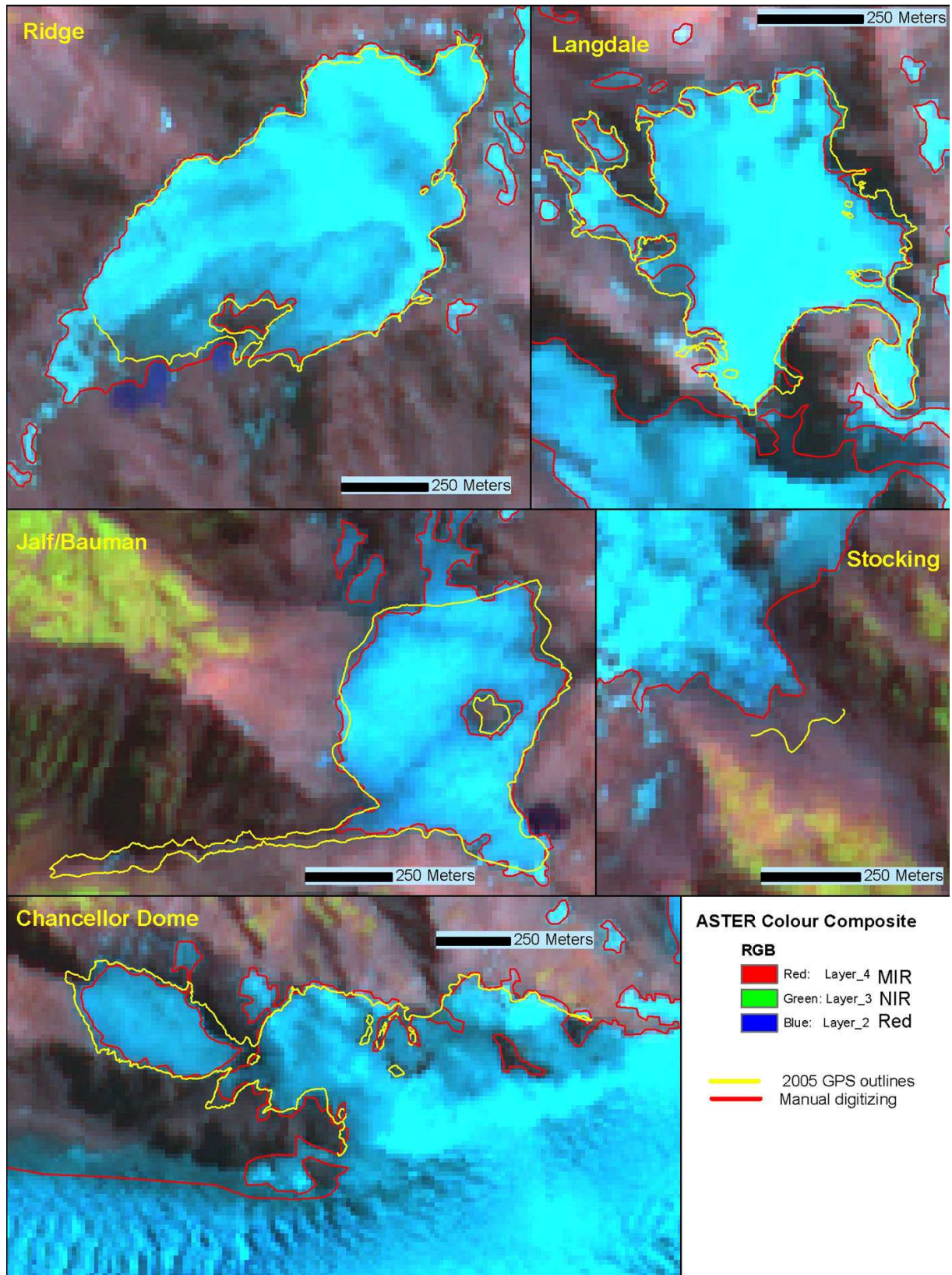
Figure 4.2.1 *Comparison of the 2005 GPS glacier outlines and the manual digitizing of the image for the 5 smallest glaciers studied in field.*
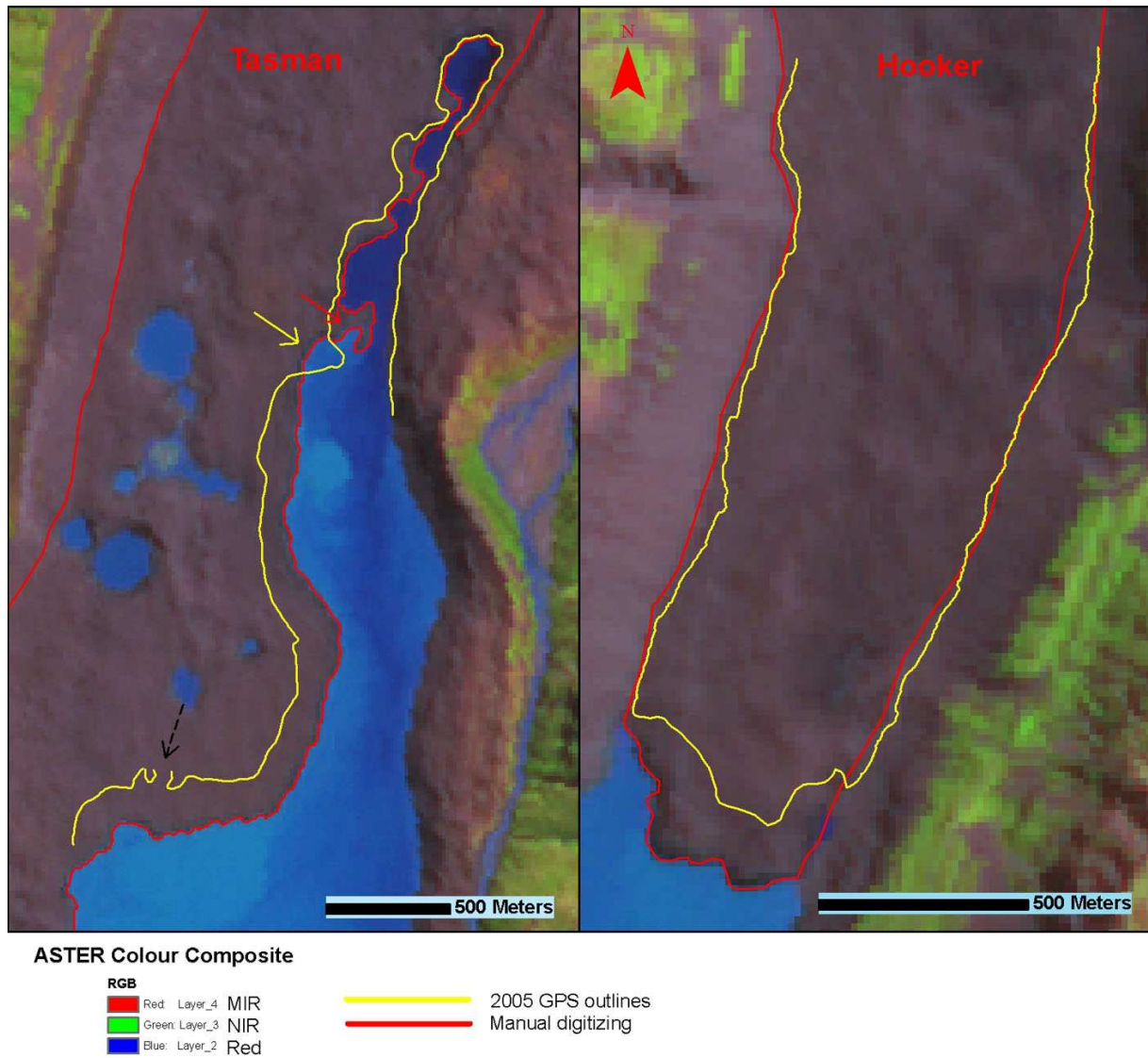
Figure 4.2.2 *Comparison of fieldwork and manual digitizing for Tasman and Hooker glaciers. The two arrows on Tasman illustrate ice movements during the 3 years between the image acquisition and field work. The dotted black arrow on Tasman shows how much the pond on the image had enlarged / and the glacier moved downvalley during the 3 year period. The part with no data in the GPS line (indicated by the arrow) is where this pond was located at the time of the field work (i.e. no longer a pond, but part of the big lake).*

Figure 4.2.3 *GPS recorded outlines for Fox and Franz Josef glaciers compared to the manual digitizing. A vertical offset of 37 meters had to be applied to the shapefiles to make them*

appear as a whole on top of the 3D model. This must be kept in mind when interpreting the lines, especially on the upper left and lower right window where it looks like the glacier in the image is further downvalley than the lines, which is not the case.

4.3 Comparison of the different classification methods used with manual digitizing

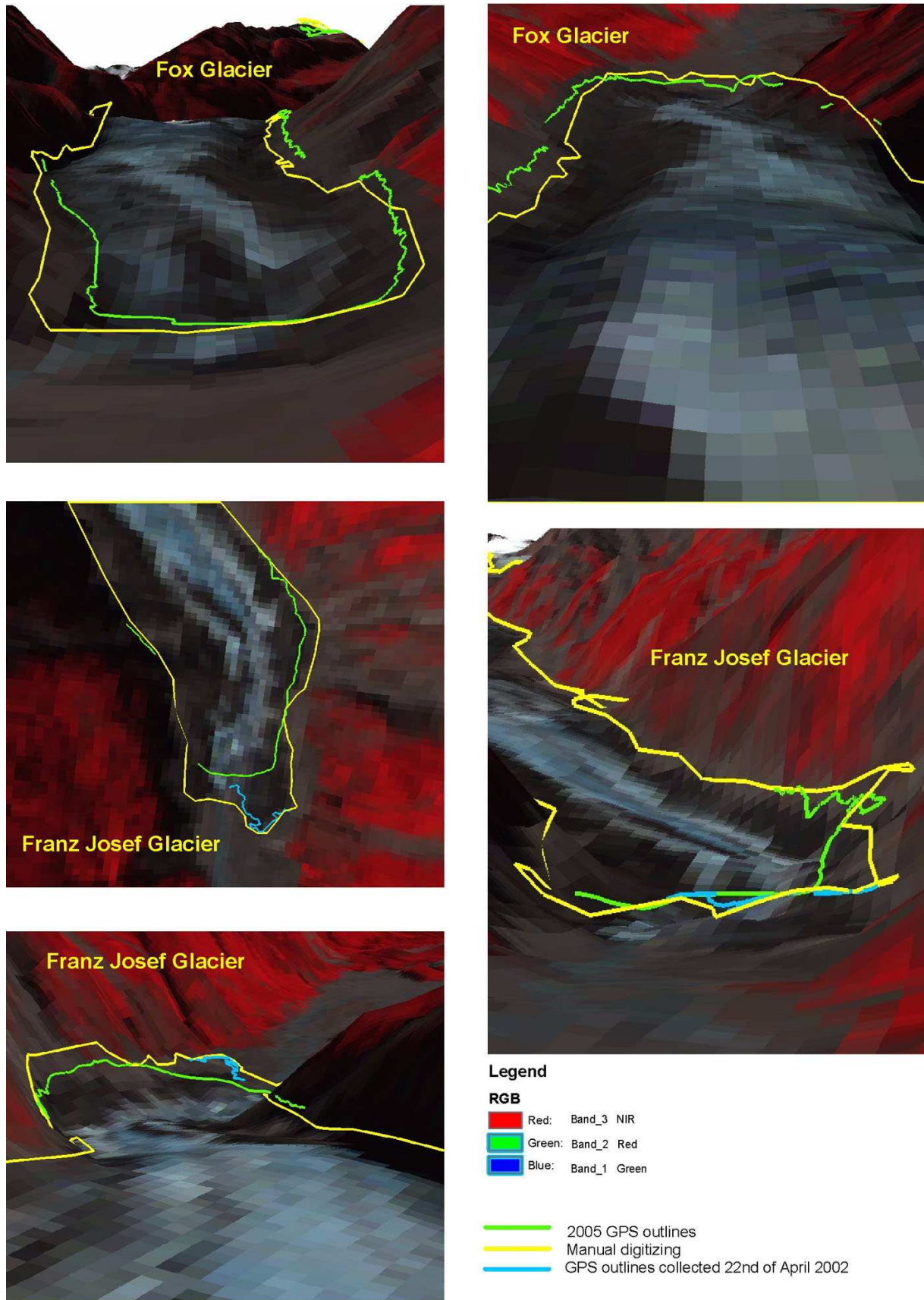The ideal situation would have been that the results from the manual digitizing and the automatic classifications were overlapping perfectly. However, a perfect match would never occur, so the aim is to get to results as close as possible. When testing thresholds for the band-ratios, this is based on an assumption that the manual digitizing is perfect. Whereas in reality, there would be areas where the manual digitizing could be improved. The digitizing is based on a human interpreter and his or her local knowledge and the interpretation will always be subjective. The accuracy of the manual digitizing is discussed more thoroughly in the discussion chapter. The results from the testing of the best threshold for band3/band4 ratio and the NDSI are displayed in confusion matrixes (described in section 4.1) and the producer's, user's and overall accuracy are given for one of the threshold for easier comparison between the areas (see section 4.1). The purpose of the confusion matrixes is to find the closest possible match between the ratio and the validation (the manual digitizing). The optimum threshold for the rationing would be one that includes as much as possible of the glacier area without including much of the areas that are outside glaciers. Large debris areas over ice will not be classified as glaciers no matter how low the threshold is set, so the area classified as glaciers would always be less in the ratios for the study areas with a high amount of debris in comparison with the manual digitizing.

4.3.1 Ratio band3/band4

The band3/band4 ratio was tested with and without a 3*3 median filter. The purpose of applying median filter was to remove individual pixels which were classified as glaciers outside the glacier boundaries. This was commonly pixels representing dense vegetation (rainforest, native shrub or forest) and this misclassification increased with a decreasing threshold. However, applying the median filter could also cause the complete opposite effect - making individual ice pixels surrounded by debris or ice pixels along the glacier boundaries being converted to non-glacier.

Threshold	value 3	value 0	value 2	value 1

FRANZ JOSEF

Threshold	value 3	value 0	value 2	value 1
1.8	62,34	31,92	1,57	4,17
1.8 with median filter	62,36	32,31	1,55	3,78
2.0	62,04	34,06	1,87	2,03
2.0 with median filter	62,07	34,29	1,84	1,81
2.2	61,80	34,70	2,11	1,39
2.2 with median filter	61,84	34,69	2,07	1,40
2.4	61,51	35,07	2,40	1,02
2.4 with median filter	61,55	34,98	2,35	1,10

RIDGE

Threshold	value 3	value 0	value 2	value 1
1.8	17,47	75,52	4,37	2,38
1.8 with median filter	17,63	75,74	4,47	2,15
2.0	17,09	76,08	5,01	1,81
2.0 with median filter	16,96	76,27	5,14	1,62
2.2	16,64	76,40	5,47	1,49
2.2 with median filter	16,51	76,61	5,59	1,29
2.4	16,12	76,70	5,99	1,19
2.4 with median filter	15,97	76,85	6,13	1,04

Hooker

Threshold	value 3	value 0	value 2	value 1
1.8	32,86	55,26	7,91	3,97
1.8 with median filter	32,92	55,32	7,86	3,91
2.0	31,97	56,49	8,80	2,74
2.0 with median filter	32,14	56,59	8,59	2,68
2.2	31,25	57,04	9,51	2,19
2.2 with median filter	31,42	57,10	9,31	2,16
2.4	30,23	57,53	10,54	1,71
2.4 with median filter	30,31	57,55	10,45	1,68

Entire Image

Threshold	value 3	value 0	value 2	value 1
1.8	8,49	87,15	2,13	2,05
1.8 with median filter	8,47	87,73	2,33	1,58
2.0	8,32	88,39	2,48	0,81
2.0 with median filter	8,31	88,70	2,50	0,60
2.2	8,20	88,70	2,60	0,50
2.2 wtih median filter	8,18	88,88	2,62	0,43
2.4	8,06	88,85	2,74	0,35
2.4 with median filter	8,03	88,98	2,77	0,33

Table 4.3.1 *Confusion matrix for the 3 study areas and the entire image. Values are given in percent of total number of pixels within the areas, 1st column (value 3) shows pixels classified as glaciers both in the manual digitizing and in the ratio, 2nd column (value 0) shows area not*

classified as glaciers in none of the methods, and the two last columns shows area classified as glaciers in only one of the two approaches (value 2 manual and value 1 automatic).

	Classes	Prod. acc (%)	User. acc (%)	Overall acc (%)
				99,36
FRANZ filter	Glaciers	97,12	97,17	
	No-glacier	94,99	94,91	
				96,10
FRANZ	Glaciers	97,07	96,83	
	No-glacier	94,38	94,8	
				93,23
RIDGE filter	Glaciers	76,74	91,28	
	No-glacier	97,92	93,69	
				93,17
RIDGE	Glaciers	77,33	90,42	
	No-glacier	97,67	93,82	
				88,73
HOOKER filter	Glaciers	78,91	92,3	
	No-glacier	95,48	86,82	
				88,46
HOOKER	Glaciers	78,41	92,11	
	No-glacier	95,37	86,52	
				97,01
Entire image filter	Glaciers	76,87	93,27	
	No-glacier	99,33	97,26	
				96,71
Entire image	Glaciers	77,03	91,13	
	No-glacier	99,09	97,27	

Table 4.3.2 *Producer's, User's and overall accuracy for the 2 classes (glacier areas and non-glacier areas) for the 3 study areas and the entire image, with and without 3*3 median filter. For these results the threshold is set at 2.0.*

From table 4.3.1 we see that the glacier area contained within each study area vary largely. Franz Josef area has more than 60 % glacier cover, whereas ridge has about 30 % and Hooker about 40%. The whole image has about 10 % glacier cover. We also see that for Franz Josef the agreement between the results from the digitizing and the band ratio is very good, whereas the other areas show a much larger variance. This is mainly due to the small amount of debris

on Franz Josef glacier. For the entire area more than 20 % of the glacier area defined in the digitizing is not detected by the band ratio (table 4.3.1). In table 4.3.2 we see that overall accuracy is by far best for Franz Josef, and this area is also the only one where we see a relatively large difference in the accuracy when applying the median filter. However, this is only true for the two lowest threshold, something which tells us that the amount of noise is increasing with decreasing thresholds, but noise is not really a problem when the threshold is set high. For the other areas the median filter has hardly any effect. The effect of the median filter for Franz Josef are visually illustrated in figure 4.3.1.

In the confusion matrixes (table 4.3.1) the ideal threshold for the rationing would be where the number of pixels in the 3rd column (value 2/glacier area only in the manual digitizing) is low at the same as the number of pixels in the 4th column (value 1/glacier area only in the ratio) is low. Mathematically speaking this would mean that the best threshold is the on the row where the sum of the cells in the 3rd and the 4th column is lowest. However, the real situation is a bit more complex. The lowest sum could be where value in one of the column is very low whereas the value in the other column is quite high. E.g. a very low threshold could make the number of pixels classified as glacier only in the digitizing very small, something which is desired, but at the same time include a high number of pixels that are certainly not glacier area. One could argue that it is better to use a too low threshold than a too high because it would be easier to remove (automatic, with filtering, or manually), pixels that certainly lie outside glacier areas as long as the main portion of the true glacier area is detected as glacier. This is easier than to having to enlarge the glacier boundaries because the threshold includes too little. However, the ideal situation is certainly to find a threshold where a minimum adjusting is needed. For the New Zealand situation, with a high debris cover of many of its glaciers, manual correction would be needed to smaller or larger extent depending of the accuracy needed for the results. Major changes in glacier areas would be detected even though the threshold used is not the optimum. The optimum threshold would depend on the characteristic of the area and could change quite a bit from area to area, so compromises will have to be made when working on a large heterogeneous area.

One important thing to underline is that the optimum threshold for glaciological purposes is highly subjective, depending on what information the interpreter is interested in. *It can not alone be given as a function of statistics.* If the interpreter wants to have a good overlap in shaded areas, one specific threshold might be best here, and if the interpreter are interested in

the terminal areas of the glaciers, the best threshold here might be quite different. Thus, first the purpose of the classification has to be defined.

However, table 4.3.1 suggests that the ideal threshold probably lays around 2.0, which is also confirmed by visual inspection of the classified image.
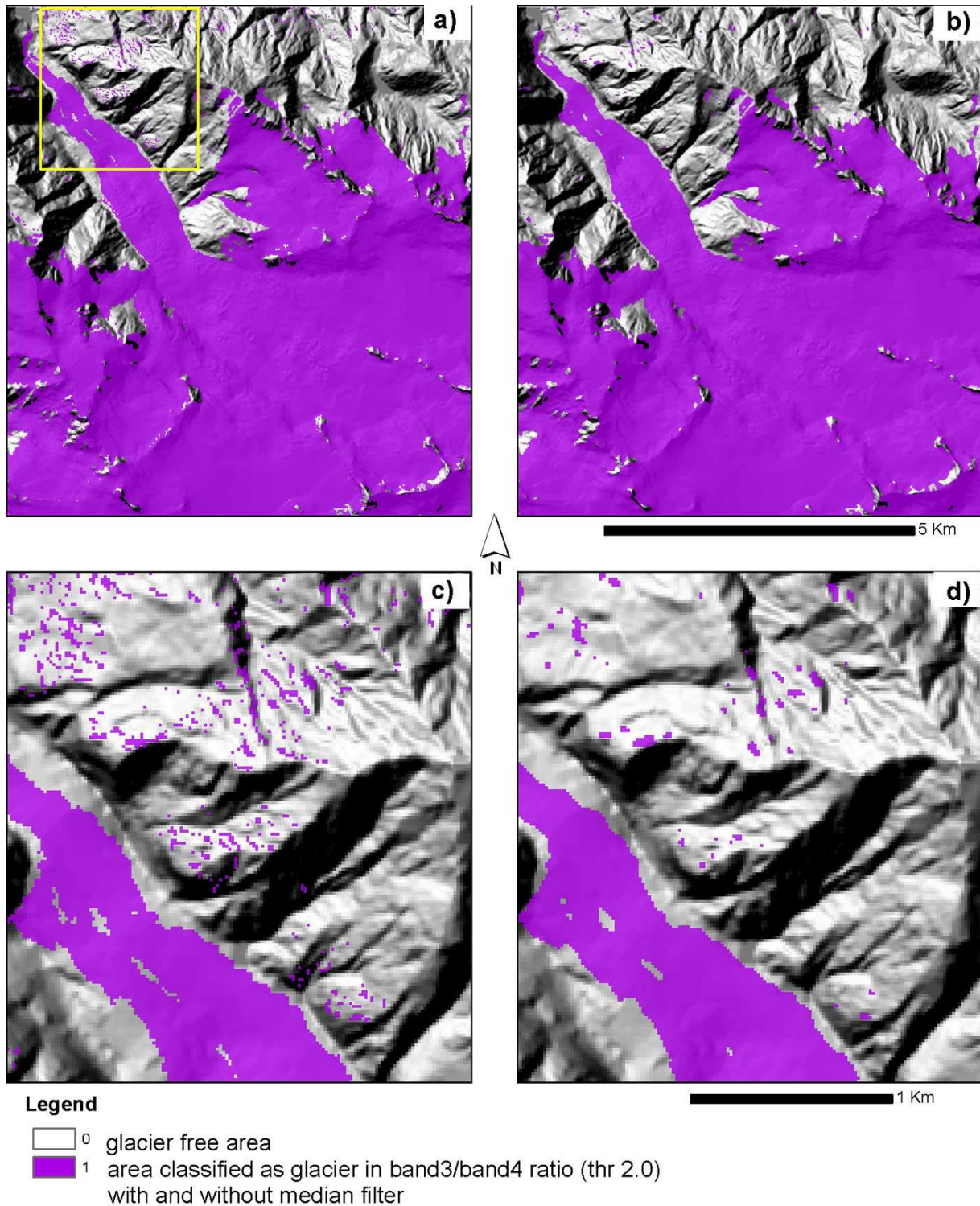
Figure 4.3.1 *The effect of applying 3*3 median filter to Franz Josef area. Figure shows area classified as glacier in band3/band4 ratio using threshold 2.0. Left windows show the result before applying the filter and the right windows show the effect of the filter.*

4.3.2 NDSI (Normalized Differential Snow Index)

Threshold	value 3	value 0	value 2	value 1
FRANZ JOSEF				
0.3	62,38	34,05	1,53	2,04
0.35	62,14	34,45	1,77	1,65
0.4	61,86	34,80	2,05	1,30
0.45	61,49	35,75	2,42	0,94
0.5	60,99	35,43	2,92	0,66
0.55	60,43	35,63	3,48	0,46
0.6	59,74	35,81	4,17	0,28
0.65	58,71	35,96	5,20	0,13
RIDGE				
0.3	17,55	75,62	4,55	2,27
0.35	16,85	76,15	5,26	1,74
0.4	16,10	76,53	6,01	1,36
0.45	15,25	76,92	6,85	0,97
0.5	14,34	77,25	7,77	0,64
0.55	13,45	77,45	8,66	0,44
0.6	12,38	77,64	9,73	0,25
0.65	10,59	77,77	11,51	0,12
HOOKER				
0.3	33,34	54,75	7,42	4,49
0.35	32,85	55,68	7,92	3,55
0.4	32,28	56,56	8,49	2,67
0.45	31,37	57,38	9,39	1,86
0.5	29,86	58,05	10,90	1,18
0.55	27,98	58,48	12,78	0,75
0.6	25,90	58,79	14,87	0,44
0.65	23,40	59,03	17,37	0,21
Entire Image				
0.3	8,50	88,47	2,29	0,74
0.35	8,35	88,65	2,44	0,55
0.4	8,19	88,80	2,60	0,41
0.45	7,99	88,92	2,80	0,29
0.5	7,73	89,01	3,06	0,19
0.55	7,46	89,08	3,33	0,13
0.6	7,20	89,13	3,67	0,08
0.65	6,64	89,17	4,15	0,04

Table 4.3.3 *Confusion matrix for NDSI for the 3 study areas and the entire image. Explaination as for table 4.3.1.*

	Classes	Prod. acc (%)	User. acc (%)	Overall acc (%)
				96,42
FRANZ JOSEF	Glaciers	95,43	98,93	
	No-glacier	98,17	92,39	
				91,59
RIDGE	Glaciers	64,86	95,73	
	No-glacier	99,17	90,86	
				87,91
HOOKER	Glaciers	73,26	96,20	
	No-glacier	98,00	84,19	
				96,74
Entire image	Glaciers	71,64	97,60	
	No-glacier	99,79	96,68	

Table 4.3.4 *Producer's, User's and overall accuracy for the 2 classes (glacier areas and non-glacier areas) for the 3 study areas and the entire image. For these results the threshold is set at 0.5.*

The quality of the NDSI for the individual areas is, as for the band3/band4 ratio highest for Franz Josef (with least debris cover) and worst for Hooker (with most debris cover). The results displayed in table 4.3.3 and 4.3.4 seem nearly as good as the results of the ban3/band4 ratio. However, before comparing the NDSI to the manual digitizing all the water in the NDSI was removed by applying a water-mask (figure 3.4.1). The confusion between water and glacier ice was very high, even for non-turbid water, so the results presented in table 4.3.3. and 4.3.4 would have been far from this good if water was not removed from the classified result. Turbid water, like the Tasman Lake, was still classified as glacier area even with the highest threshold tested. However, these results show that in areas with little water, or if the water later is removed from the NDSI, this method will give very similar results to the band3/band4 ratio. From table 4.3.3 it looks like the optimum threshold would be around 0.5, which was also confirmed by visual inspection. For this threshold the values in 3rd and 4th column are resonable low, not including too much area not excluding too much (if we ignore the debris detection problem). Figure 4.3.2 shows NDSI performed on Hooker glacier with the highest, lowest and believed optimum threshold. This figure illustrates well how much the classified area changes when applying different thresholds to the NDSI, and underlines the importance of finding the best threshold before glacier area is calculated. However, even with

the lowest threshold, the debris is (naturally) left out from the classification. Figure 4.3.3 shows a comparison of the band3/band4 ratio and the NDSI for Ridge glacier area with the thresholds giving the best results. This area has, as mentioned earlier, a relatively high debris cover on some of its glaciers, thus leaving large areas unclassified. The band3/band4 ratio includes most areas of the two, even some areas not interpreted to be glacier area in the digitizing. By closer inspection these areas are either bright rock or very dirty ice, but this area is on a small hill, where there is not likely to be a glacier.

Legend
- 0 glacier free area
- 1 area classified as glaciers only in NDSI
- 2 area classified as glaciers only in manual digitizing
- 3 area classified as glaciers in both approaches
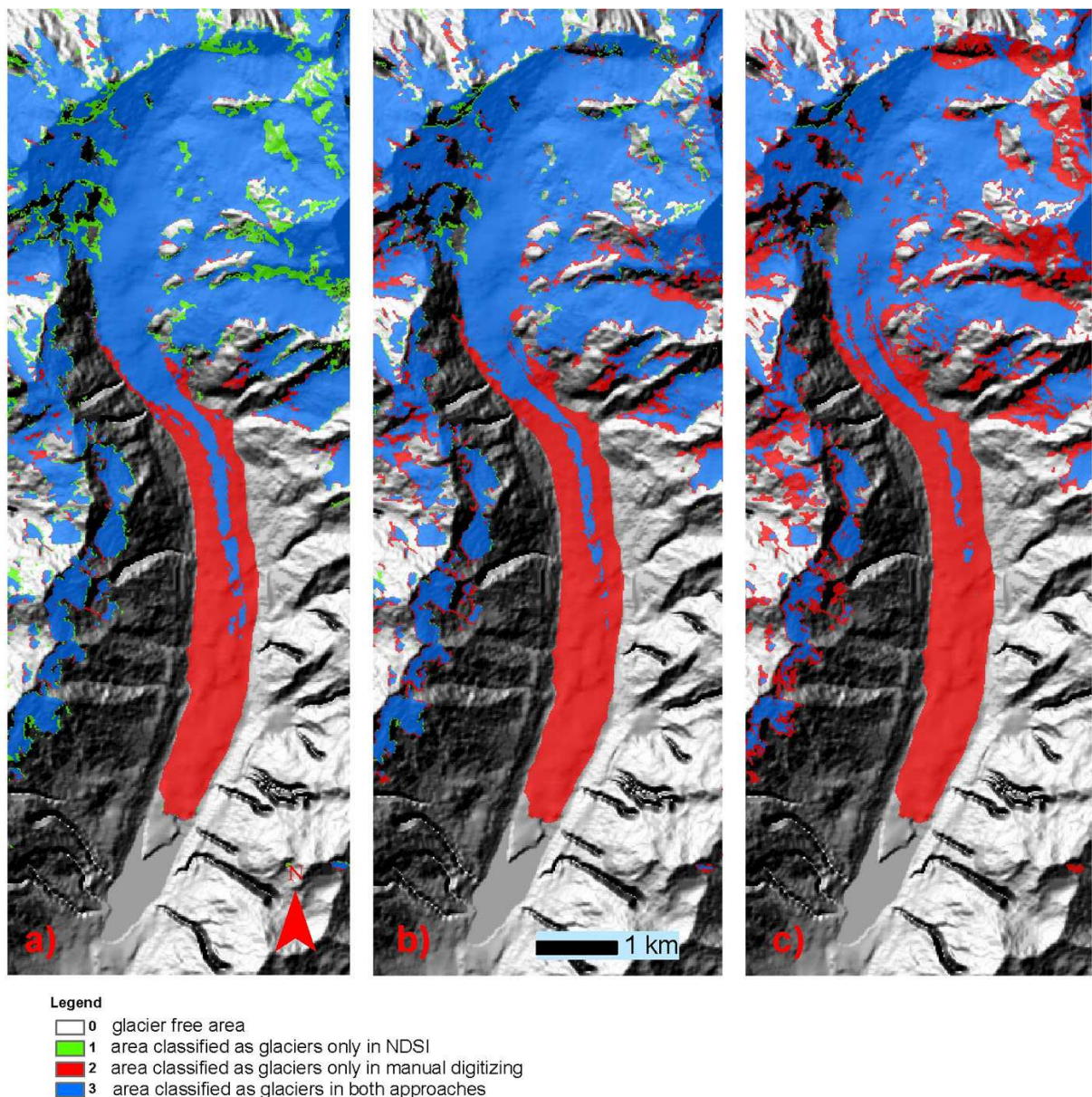
Figure 4.3.2 *NDSI of Hooker glacier with 3 different thresholds a) 0.3, b) 0.5, and c) 0.65. A water mask was applied, if not the Hooker lake would have showed up as blue in all the images. The teminus position in 1986 is indicated in the hillshade (date of DEM).*
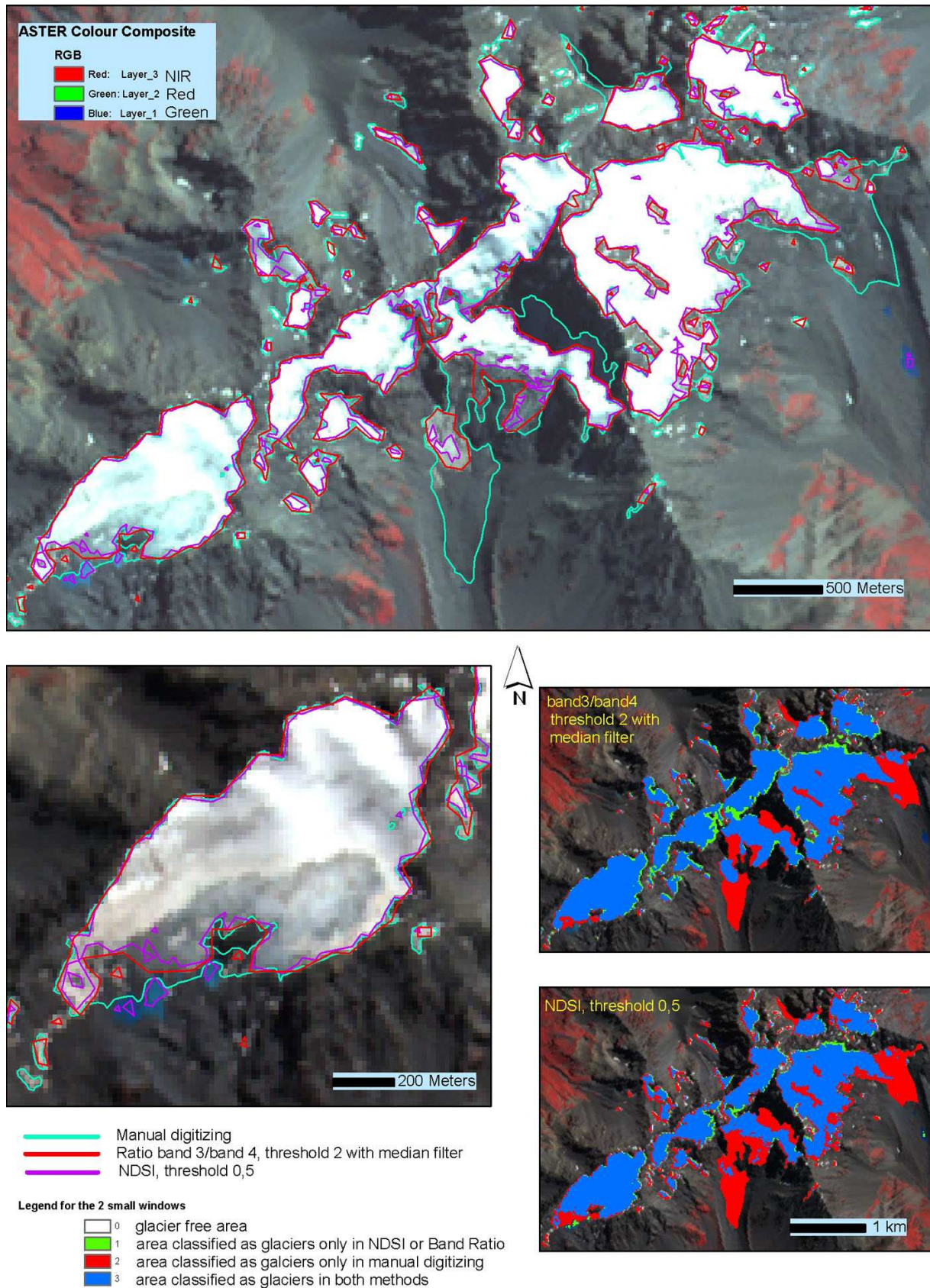
Figure 4.3.3 Top. *Band3/band4 ratio (threshold 2.0), NDSI (threshold 0.5) and digitizing displayed in vector for the Ridge glacier area. Bottom left is zoomed in on Ridge glacier. The*

two smallest windows at bottom right show the performance of the NDSI and the band ratio classifications in comparison with the manual digitizing.

4.3.3 Supervised classification

Supervised classification was only performed for Franz Josef area. 7 classes were chosen (figure 4.3.4), and these were later merged into glacier and non-glacier. The result of the classification is given in table 4.3.5 and is displayed in figures in figure 4.3.4.

value 3	value 0	value 2	value 1
58,16	33,48	5,87	2,49

Table 4.3.5 *Confusion matrix for the supervised classification. Values are given in %, where value 3 is area classified as glacier both in the supervised classification and the digitizing., value 0 are not classified as glacier in any of the approaches, whereas value 2 represent areas classified as glacier in the digitizing but not detected in the supervised classification and value 1 represent areas detected as glacier in the supervised classification but not in the digitizing.*

Classes	Prod. acc (%)	User. acc (%)	Overall acc (%)
			91,64
Glaciers	90,83	95,89	
No-glacier	93,08	85,08	

Table 4.3.6 *Producer's, User's and overall accuracy for the 2 classes (glacier areas and non-glacier areas.)*
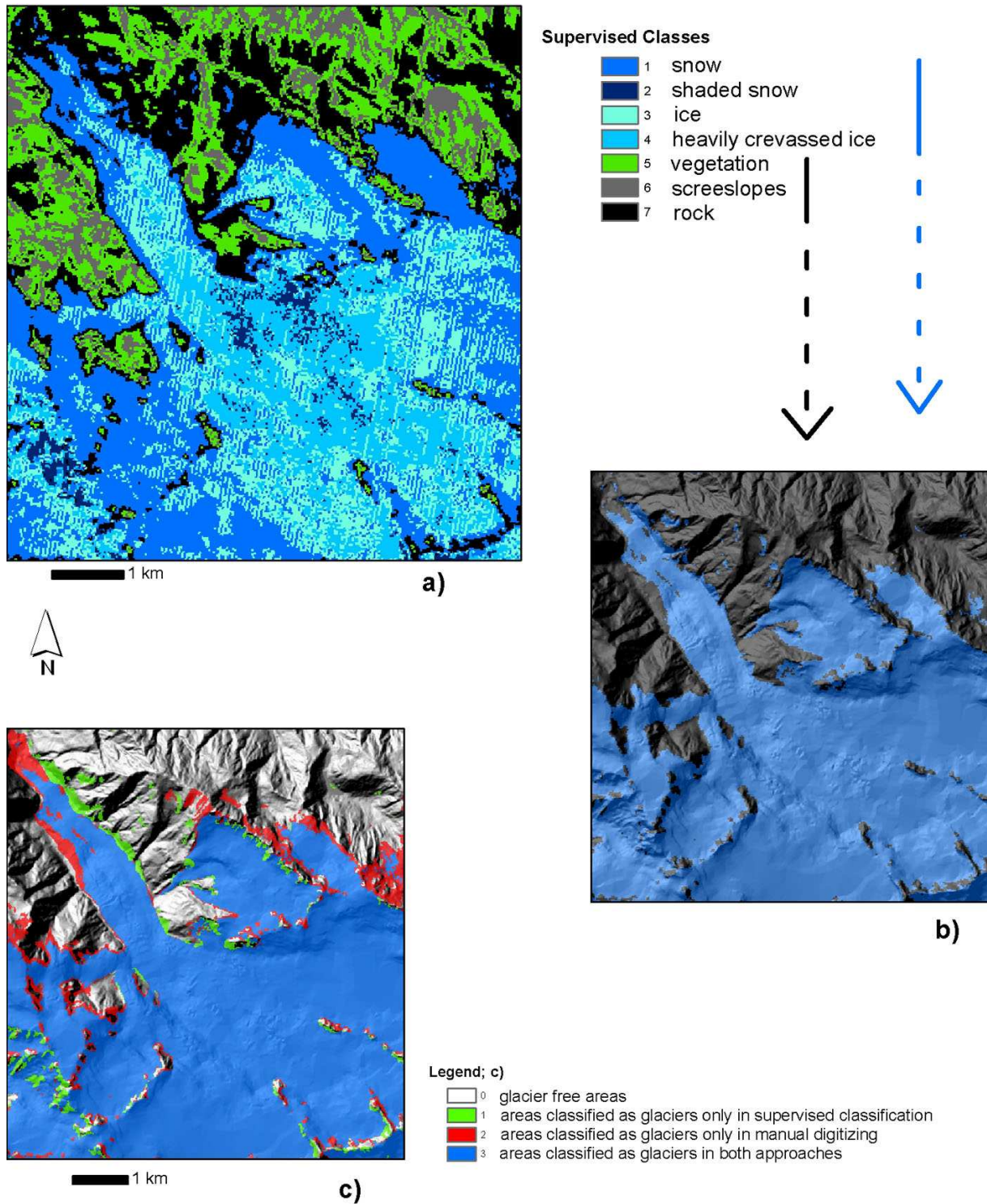
Figure 4.3.4 *Supervised classification of Franz Josef glacier a)Top left shows the area classified into 7 classes. (b) Right window shows this classification merged into 2 classes: glacier and non-glacier area. c) Bottom window shows a comparison of the supervised classification with the manual digitizing.*

The initial test of supervised classification did not give very promising results. Compared with the best thresholds in the band3/band4 ratio and the NDSI the supervised classification both excluded more area classified as glacier in the digitizing and included more area not classified as glacier in the two other methods. The overall accuracy of the supervised classification was 91.6% (table 4.3.6), whereas it for the band3/band4 ratio with threshold 2 and median filter and for the NDSI it was 99.3% and 96.4%, respectively (table 4.3.2 and 4.3.4). In the supervised classified result (figure 4.3.4 a)) most of the accumulation basin has been classified as ice. In reality, this area consists of saturated snow, not ice as the results suggests. This saturated snow had a spectral signature very similar to glacier ice and was therefore hard to discriminate.

5. RESULTS: Change in glacier area from 1978 to 2002

5.1 Glacier outlines from 2002

The image frame was 3933 km², a little larger than the minimum size of an ASTER image (60 km * 60 km = 3600 km²). Of the 3933 km², 2989 km² were located to the east of the main divide, whereas 952 km² were located to the west. When calculating the areas of the manual digitized glacier outlines from the ASTER image, they totalled 428 km² (almost 11% of the image frame), of these 242 km² were on the eastern side of the divide (8% of the frame east of the divide) and 186 km² (19.5% of the frame west of the divide).

5.2 Glacier area within the extent of the ASTER image in 1978 and 2002

When calculating the 1978 glaciated area from the dataset provided by Trevor Chinn, this gave a total number of 3137 glaciers after removing polygons smaller than 1 ha (0,01 km²). The number of discrete glaciers given in literature is 3149 (e.g. Chinn, 1999), 3144 (e.g. Chinn, 2001) and 3153 (Chinn, 1991). The agreement of this study to this is good since there are a few "late" glacier additions and deletions that are not in every inventory copy. The one used here should be the original 1978 version. (Trevor Chinn, personal communication). The glacier area calculated from the 1978 polygons is 1239 km². This is quite larger than the area given in literature, 1158 km² (e.g. Chinn, 2001, 2005). The original inventory was specifically for the glacier sizes as they were in 1978, and these areas were copied to the topographic map series currently in use. Unfortunately the original polygons were lost to a complex computer upgrading process, and some of the surviving glacier polygons on the NZMS 260 series maps were unsystematically altered by the cartographers. So some differences in glacier numbers and areas will persist, depending on the data source. In particular, the topographic map outlines have the recently developed (after 1978) proglacial lakes removed from the glacier polygons.

The 1978 glacier polygons were clipped to fit the ASTER image frame. Within this frame we calculated a total of 513 km² of glaciers, which account for about 41% of the total glaciated areas in New Zealand (when 1239 km² is used). Of these, 296 km² were located east of the divide (10% of the image frame east of the divide) and 217 km² west of the divide (22.8% of the image frame west of the divide). Table 5.2.1 illustrates this in figures along with change in glacier area from 1978 to 2002. Figure 5.2.1 illustrates the changes in the main glaciated parts of the image. When interpreting this figure one have to keep in mind that both for the 1978 and 2002 digitizing there will be some misclassification, thus some of the red areas could also be misinterpretation of the satellite image, as well as some parts of the green areas could have been interpreted wrong from the 1978 data. The area inside the small frame is one such area. Some of the red areas close to the summits (e.g. around Mt Cook) in the area might also be such a misinterpretation. If so, this is because the mountain faces is covered with snow in the satellite image and therefore not is removed as rocks or nunataks even though they can't really be called part of the glaciers below. This is discussed more thoroughly in the discussion chapter.

area	1978 in km²	2002 in km²	reduction in %
in total	513	428	16.6
east of main divide	296	242	18.3
west of main divide	217	186	14.3

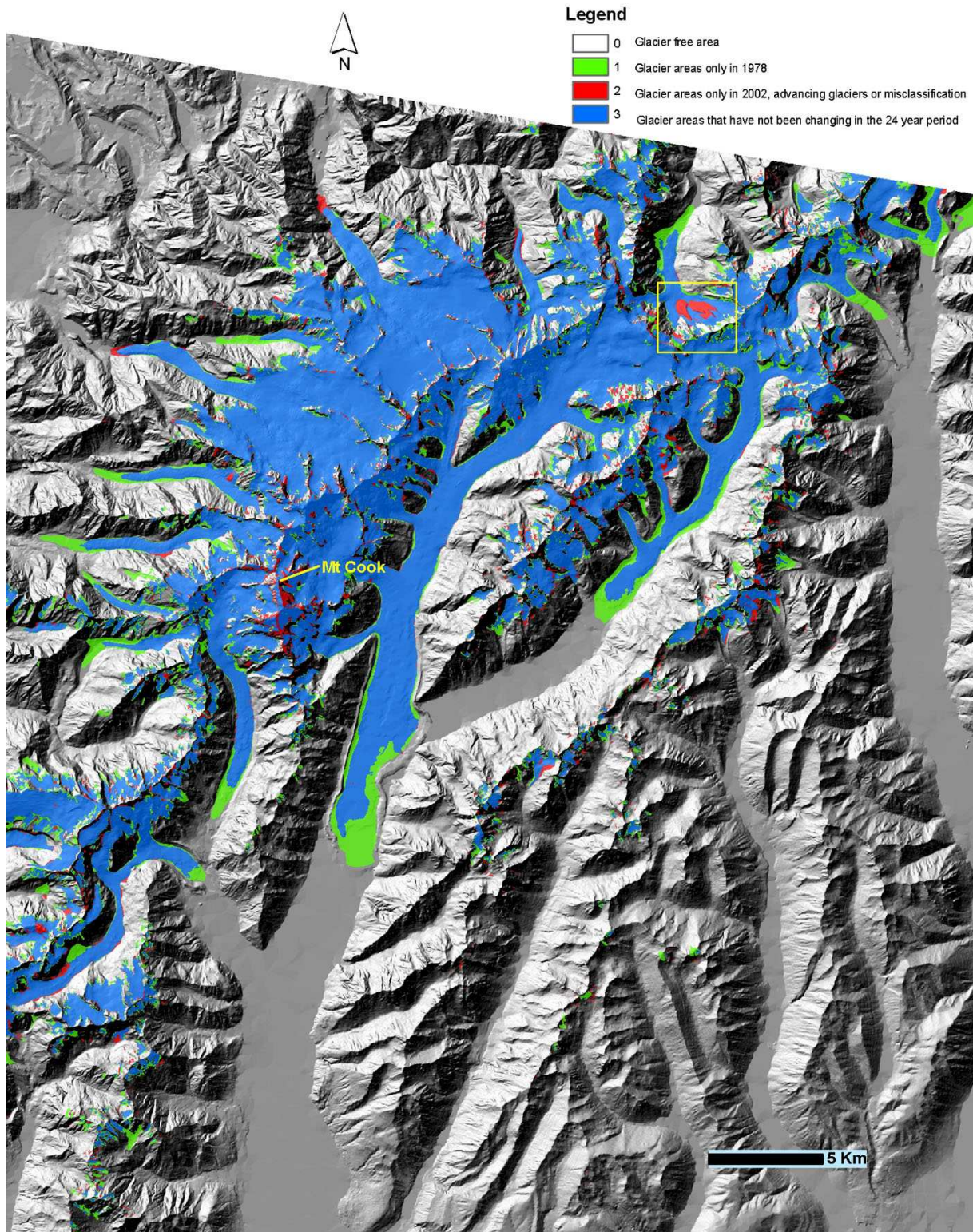Table 5.2.1 *Reduction of glacier area between 1978 and 2002 in km² and percent*

Figure 5.2.1 *The main glaciated area covered by the 2002 satellite image, showing the glacier boundaries for 1978 and 2002. All green areas show where the glaciers have retreated from during in the time period. Most of the green areas are currently lake water. The red areas shows advance. The yellow frame is discussed further in the discussion chapter.*

5.3 Area changes west of the Main Divide, versus changes on the east

In general the glacier retreat has been smaller on the western side of the main divide in the time period compared to the eastern side. The two main reasons for this is, 1; that the two largest glaciers on the west (Fox and Franz Josef glacier) have advanced in the time period, and 2; development of the glacier lakes on the large eastern glaciers, especially on Tasman glacier. The enormous loss of ice mass due to recent growth of these lakes contributes to such a large area, so that the large retreat on most of the other valley glaciers on the western side of the divide is erased from the broad picture. If the glaciers with terminal lakes were subtracted from the eastern glaciers, the difference in retreat east and west of the main divide would be much less and maybe favour the western side. The retreat and advance of the largest western and eastern glaciers is illustrated in figure 5.3.1 and 5.3.2.
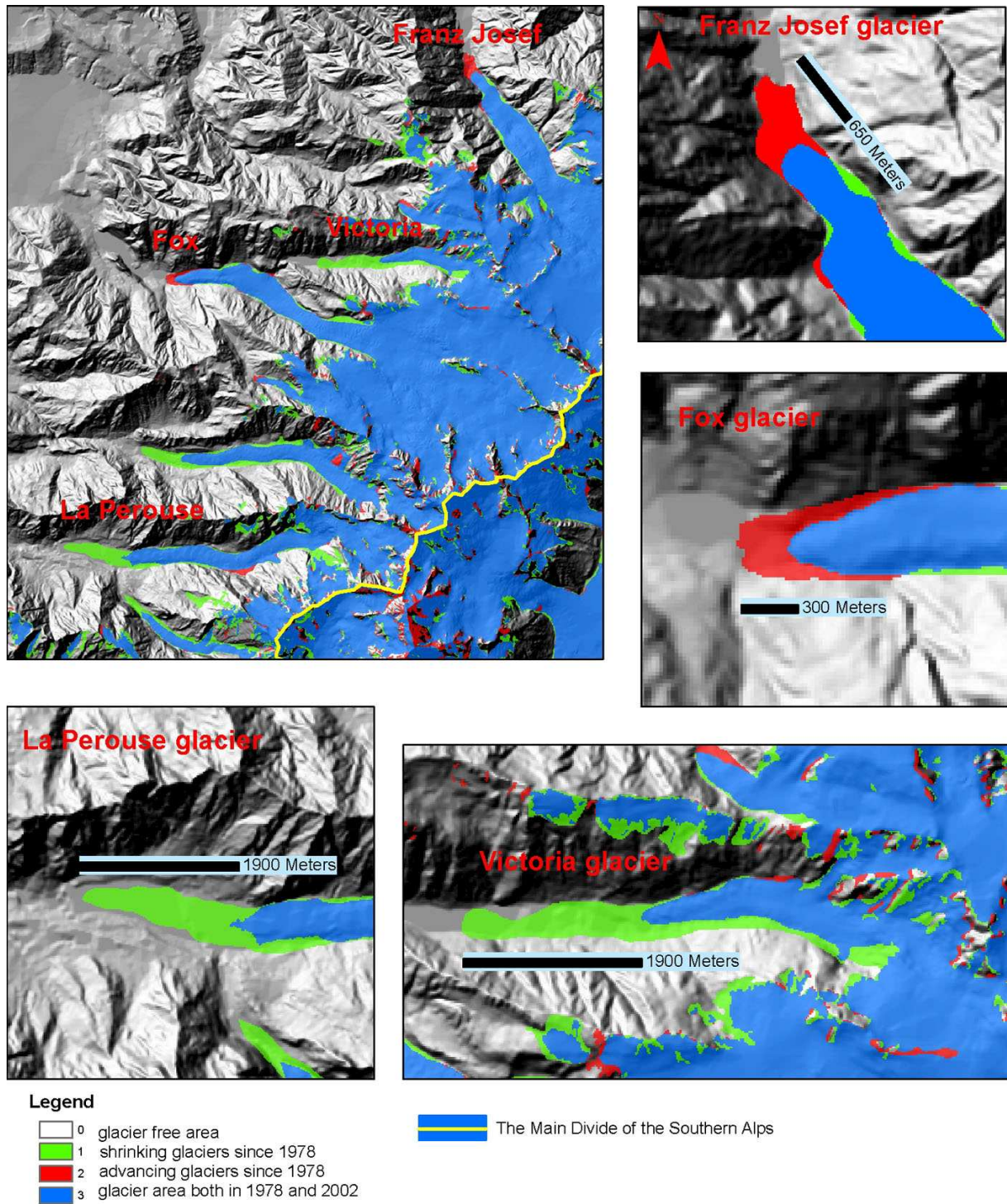
Figure 5.3.1 *Area changes on the western glaciers in the study area from 1978 to 2002. Both Fox and Franz Josef glacier advanced several hundred meters whereas the valley debris-covered glaciers retreated dramatically.*
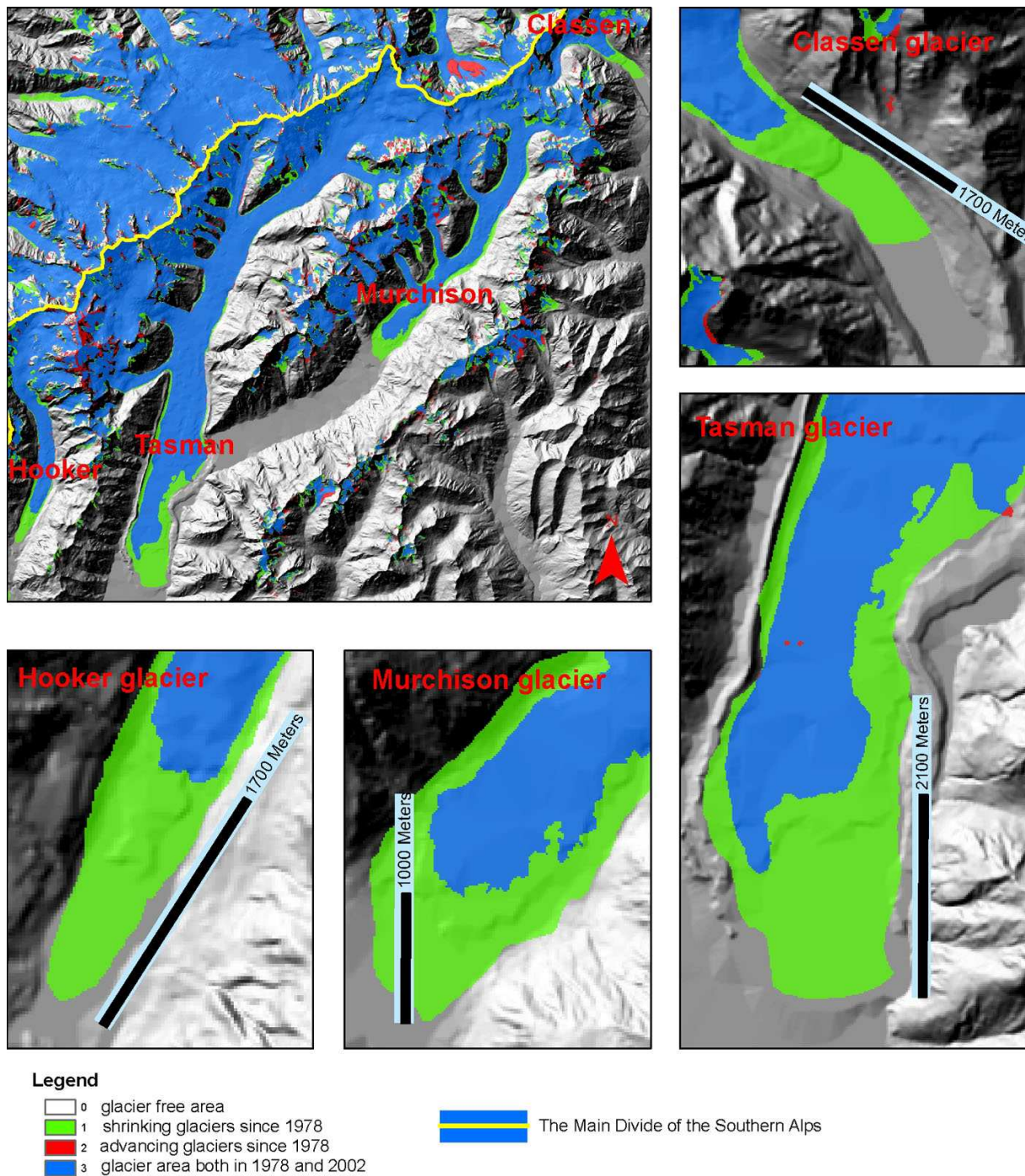
Figure 5.3.2 *Area changes for the eastern glaciers in the study area between 1978 and 2002, showing the enormous retreat in glacier area due to the rapid expansion of proglacial lakes with glacier calving.*

5.4 Changes on the smaller glaciers studied in field for the 24-year period

The smaller glaciers in the area are very important to look closely at before drawing any conclusions on the glacier change in New Zealand during the last decades. This is because they have a short response time, as opposed to the heavy debris-covered valley glaciers. The heavy low-gradient debris-covered valley glaciers have a very long response time and have just recently started to retreat from the terminus position obtained during the little ice age. Thus, their area extent in 1978 did not represent the climate at that time, nor does their extent today represent the present climate. Their fast retreat today as a result of lake calving is not directly linked to the present climate. The smaller, high elevated glacier shows only small retreats compared to the large valley glaciers. Figure 5.4.1 illustrates the 1978 and 2002 glacier outlines for the 5 smallest glaciers studied in field. By looking at these glaciers it's hard to see that the glacier areas have changed much. Some show a small retreats, some are approximately at the same size, whereas some glaciers even seem to have increased at certain parts of the glaciers, which is consistent with the trend to positive mass balances over the past two decades (Chinn, et al 2005).
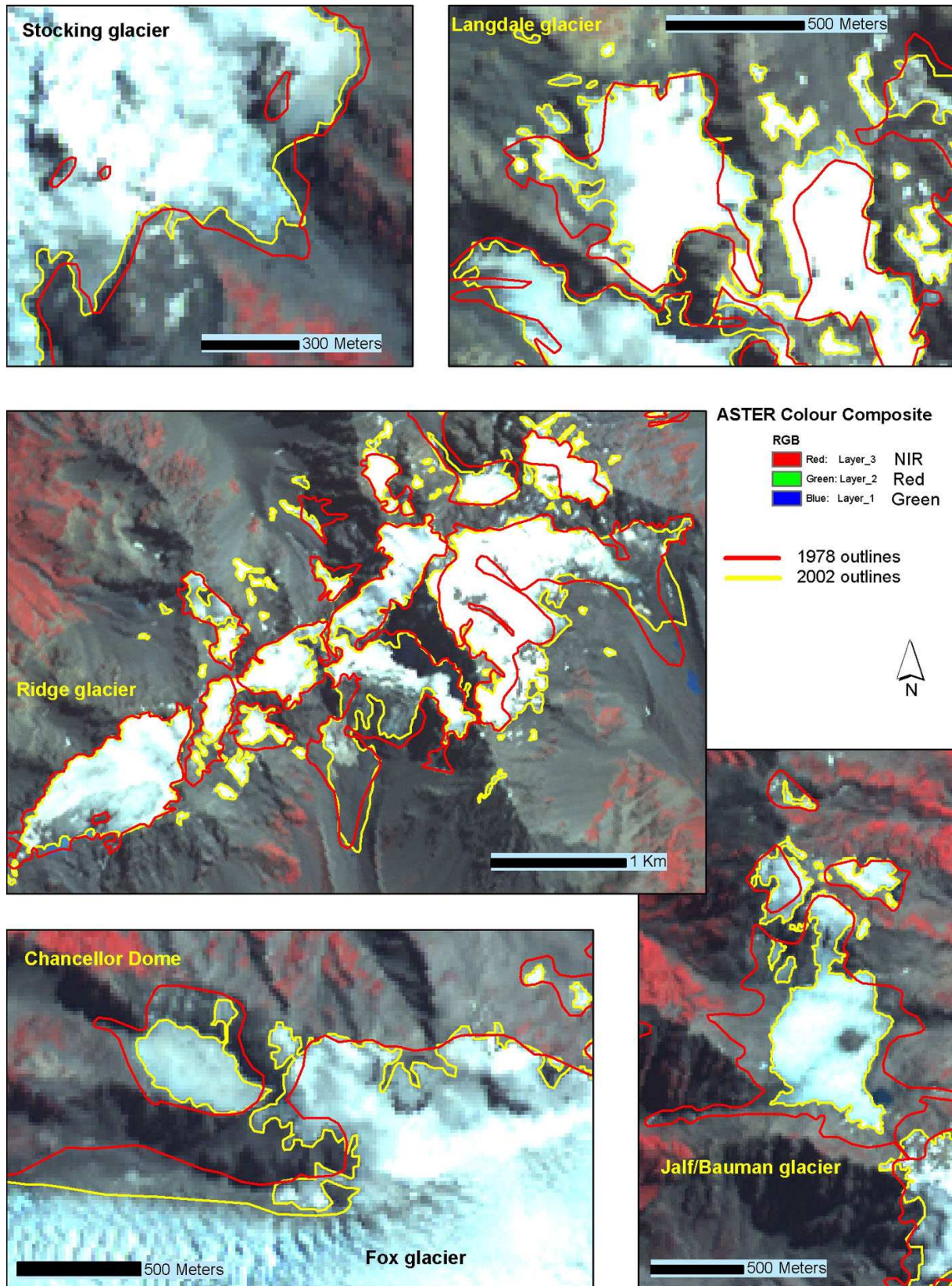
Figure 5.4.1 *Comparison of the 1978 and 2002 glacier outlines for the smallest glaciers studied in the field.*

6. DISCUSSION

6.1 Accuracy of the conducted work

6.1.1 Accuracy of the 1978 glacier inventory

Due to early timing allowing too much seasonal snow around the glacier's true boundaries and some cloud cover, there was a lack of good nadir aerial photographs of the glaciers in New Zealand for making the glacier inventory (Chinn, personal communication). As a result of this, a programme of oblique aerial photography was added to cover all of the New Zealand glaciers to obtain an accurate dataset for the inventory, and the snowline survey programme has continued from this work.

Drawing glacier outlines from oblique photographs is a very time consuming job in itself, and the accuracy would certainly be questionable and depend on the local knowledge to the interpreter in addition to good cartographic information available for the area. The cartographic base for the inventory was a reasonably accurate 1:63360 scale set of contoured maps made from the aerial photographs discussed above. Even so, there are reasons to believe that this would not be as accurate as if the photographs were all taken nadir and were orthoprojected. Figure 5.4.1 shows a comparison of the 1978 outlines drawn from aerial photographs and the manual digitizing of the 2002 satellite image for some of the glaciers studied in field. For these glaciers it looks like more details are included in the digitizing of the satellite image compared to the 1978 interpretation, even though it's done on a dataset with lower spatial resolution. This could mean that the glacier outlines for some reasons were smoother in 1978, but more likely that the 1978 mapping were done more roughly, probably because part of the photographs were oblique, but mostly because details were impossible to transfer to the topographic maps. Whatever the explanation, it must be remembered that the 1978 digitizing was done on basemaps at a scale of 1:63360 (imperial 1 inch to 1 mile) where 1mm is less than 50m, a distance that includes 3 pixels. However, for the 1978 inventory in its

whole, smoothing the glacier boundaries would probably not change the total area too much as long as this generalisation was done in both directions (including extra glacier areas in some places and excluding in others). This would be speculations though.

Despite the high spatial resolution of aerial photographs as opposed to the ASTER satellite imagery, seasonal snow and debris cover would still cause some problems to the human interpreter (Chinn, personal communication). This problem may partly be solved either by field work, which in most cases are very time consuming and expensive, or by studying existing sources of information for these areas. This could for instance be former inventories, and additional aerial photographs, if they exist (the more aerial photographs available taken during the late summer from low altitude, the better), or from ground photographs taken by climbers or explorers. However, this would be a time consuming study, and in areas where the outcome probably would only change to a very small extent (e.g areas where the main debris areas are detected, but not accurately delineated), this is not likely to be undertaken. In general the detection of glacier debris would be easier from aerial photographs compared to satellite imagery, and especially as long as no DEM exist or can be computed from the imagery. Paul (2003) writes that inexact digitizing can have various sources among others; generalization of fine details, which could be the case for in New Zealand, and inaccurate geocoding of the maps. He compared the digitizing by two different persons of an area of about 100 glacier polygons and found an average relative difference on 2.5%. However all this was done when digitizing glacier outlines from old topographic maps and not for making glacier maps as in New Zealand.

6.1.2 Accuracy of the photo interpretation and manual digitizing of the multispectral satellite image

The accuracy of satellite image digitizing will firstly depend on the quality of the orthorectification. For the GCPs in the final orhorectification the RMSE (X and Y) was 15,30 and 14,55 meters respectively, and for the CPs, the RMSE (X and Y) was 17,10 and 14,7 meters, respectively. In practical terms, these results are not much more than a pixel (15 meters). The DEM error was also low, with a difference of less than 15 meters between the GCPs and CPs altitudes in comparison with the altitudes given in the DEM. These results were also confirmed by visual inspection of the orthorectification overlaid by rivers and other

information in the New Zealand topographic database. This mean the orthorectification should not significantly influence the accuracy of the digitizing in this case.

The interpretation of the satellite image was done using the first three channels of ASTER (Green, Red and Near Infrared). This is the closest way of displaying the image to the way humans sense the environment, thus familiar to the human eye. This would also mean easier comparison to photographs from the field. Since the 4 first bands of ASTER were used in this study the other option would have been to display the image in an MIR, NIR, Red composition. A comparison of these two for a particular part of Fox glacier is shown in figure 6.1.1. This figure illustrates that in some occasions displaying the image in a MIR, NIR red colour composition might make the interpreter include more area as glaciers as opposed to when the image is displaying in NIR, Red, Green colour composition. The particular area pointed out in the figure consists of thin, sloping snow and ice patches down towards Fox Glacier. Today this avalanche gulley could not be interpreted as glacier, even though it probably has been part of Fox glacier in earlier times. Thus, interpreting from a NIR, Red Green colour composition is not likely to lead to an inclusion of larger glacier areas than the true glacier boundaries (e.g. inclusion of dead ice).
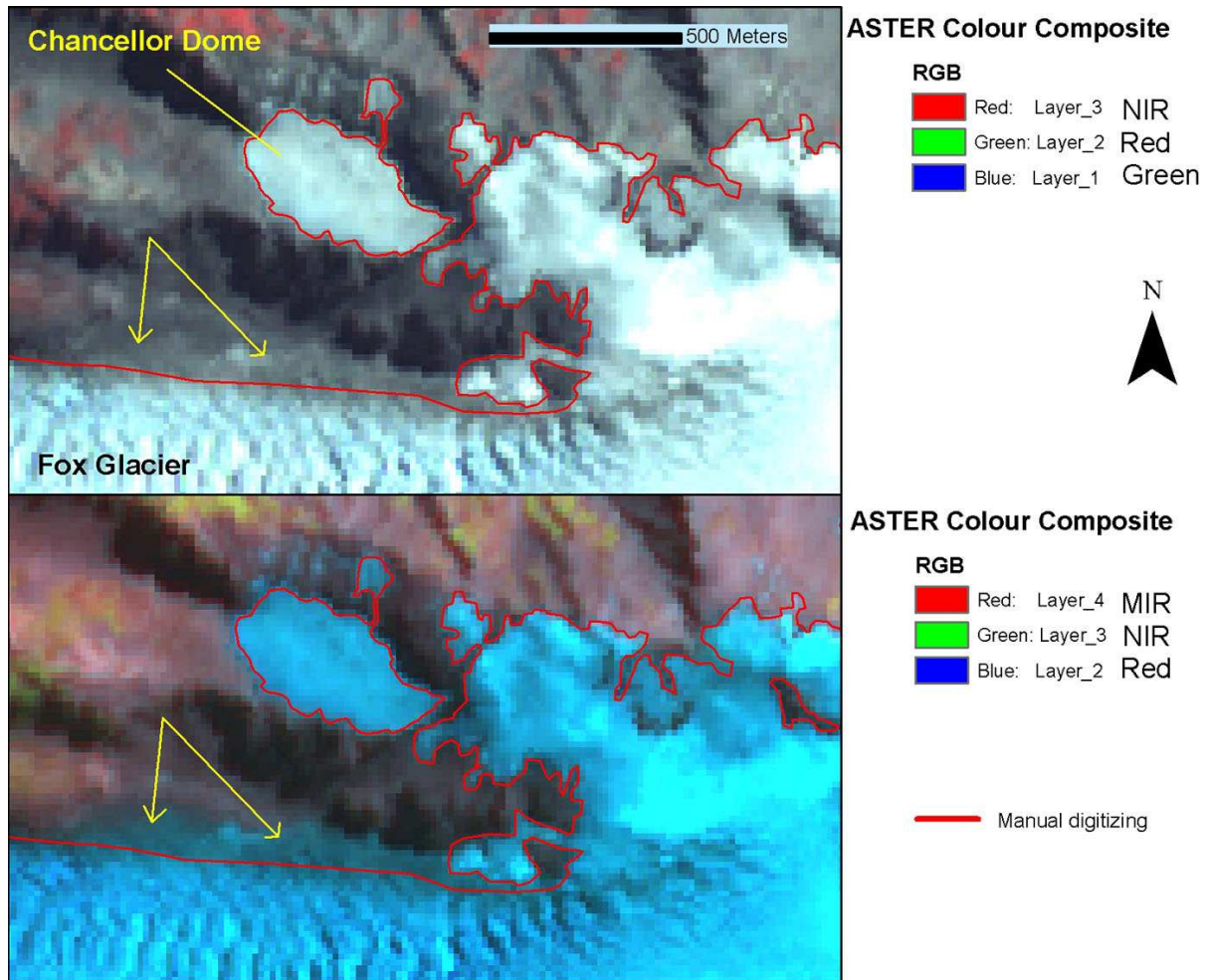
Figure 6.1.1 Chancellor Dome and part of Fox glacier's lateral margin displayed in NIR, Red Green and MIR, NIR, Red colour composite, respectively. The arrows point at an area that would most likely been interpreted differently in the two different colour composites.

All pixels containing snow show up as bright white pixels in the image. Whether this snow is part of a glacier or belongs to an occasional snow patch is impossible to determine from the spectral signature itself. Here the interpretation is subjective, depending on what the interpreter sees as glacier or not. It is this problem that promoted the New Zealand Inventory to include a minimum size of a glacier over a two-decade period into the definition of glacier size. In positive mass balance years, with ample snow and cold ablation season, many snow patches would survive the summer and would be interpreted as snow on a satellite image if automatic extraction was chosen. If these areas were separated from the glacier, they could easily be removed by setting a minimum size for glacier polygons (e.g. 1 ha/0.01 km²). However, if these snow patches are connected to the glaciers, this will cause a larger area to

6. DISCUSSION

be classified as glaciers compared to the true glacier area. This is why it is more appropriate to select an image from a negative mass balance year.

The main problem for the photo interpretation of the satellite image was to identify the debris cover. Even though contour lines were overlain on the satellite image to get information about the slope gradient, and comparisons were made with older topographic maps to see what had been mapped as debris earlier on, the interpretation turned out to be quite difficult. One such area was Whymper Glacier. Here, a large area within the outer boundaries of the glacier was finally considered to be coherent debris cover. Later, when comparing the 1978 and 2002 raster glacier maps, the result showed that this area had not been mapped as glacier area in 1978 and was not likely to have turned into glacier area during the 24-year period either. After a closer inspection this area was too far up-glacier to be debris, i.e. it was part of the accumulation basin of the glacier. Figure 6.1.2 a) and b) show a close up look of this area, both the classified results and the image displayed the way it was interpreted. This illustrates how easy it can get totally wrong if the interpreter make a wrong interpretation. For the glaciers in New Zealand such errors should be possible to avoid by the use of data like topographic maps, photographs, former inventories etc, as long as sufficient time for the interpretation is given. However, for a remote area in parts of the world where little information from the ground exist, nor aerial photographs, these errors can easily be large, obscuring the large picture of the interpretation. In such areas, information from digital elevation models made from satellite imagery can be extremely valuable for minimizing these kinds of errors and provide more information to the interpreter. Even so, the interpretation would still depend on the interpreters' glaciological understanding of the DEM info.

Another problem of the visual interpretation was to decide "when is a mountain face rocks and nunataks, and when is it part of the glacier below?" For the 1978 glacier inventory the definition was "if it contributed ice by flow, it was part of the glacier, but if disconnected and only contributed by winter snow avalanche the area was not part of the glacier. For the satellite interpretation areas where not withdrawn from the total glacier area unless it showed up as rock when displayed. Thus, meaning that if it was snow in the image it would also be glacier in the interpretation. Few of the highest mountain faces in New Zealand consists of clean rock (there are no granite walls in this area…). This means that even the faces which could be characterized as rock faces, there would almost always be some amount of snow. The comparison of the 1978 and 2002 rasters show many areas around the highest peaks

along the main divide as red (see figure 5.2.1), indicating that glaciers here have grown in the study period, something which is not likely the case. This would also be fairly easy to correct for where higher resolution data or ground data exist, but impossible if this is not the case, not even with a DEM. Also figure 6.1.2 c) and d) show a close up look of the areas around Mt Cook, that appear to be classified wrongly in the satellite image interpretation. All the red areas are mainly classified to be glacier because they were snow covered at the time of image acquisition, whereas in reality they were just snow covered rocks. Figure 6.1.3 show a photograph of this area taken from east towards the East face of Mt Cook in April 2005. This photographs is taken in late summer, when the face is at its most ice free showing large areas of bare rock. The arrow in figure 6.1.2 c) and d) points at an area that are most likely wrongly classified in the 1978 inventory and it actually illustrates the complexity of tracing glacier outlines. This area is in fact the site of a major rock avalanche from the summit of Mt Cook in 1991 (Chinn, personal communication) which blanketed the neve with debris. The change in mapped glacier areas are in fact changes (both burial and fresh additions) to this avalanche debris.
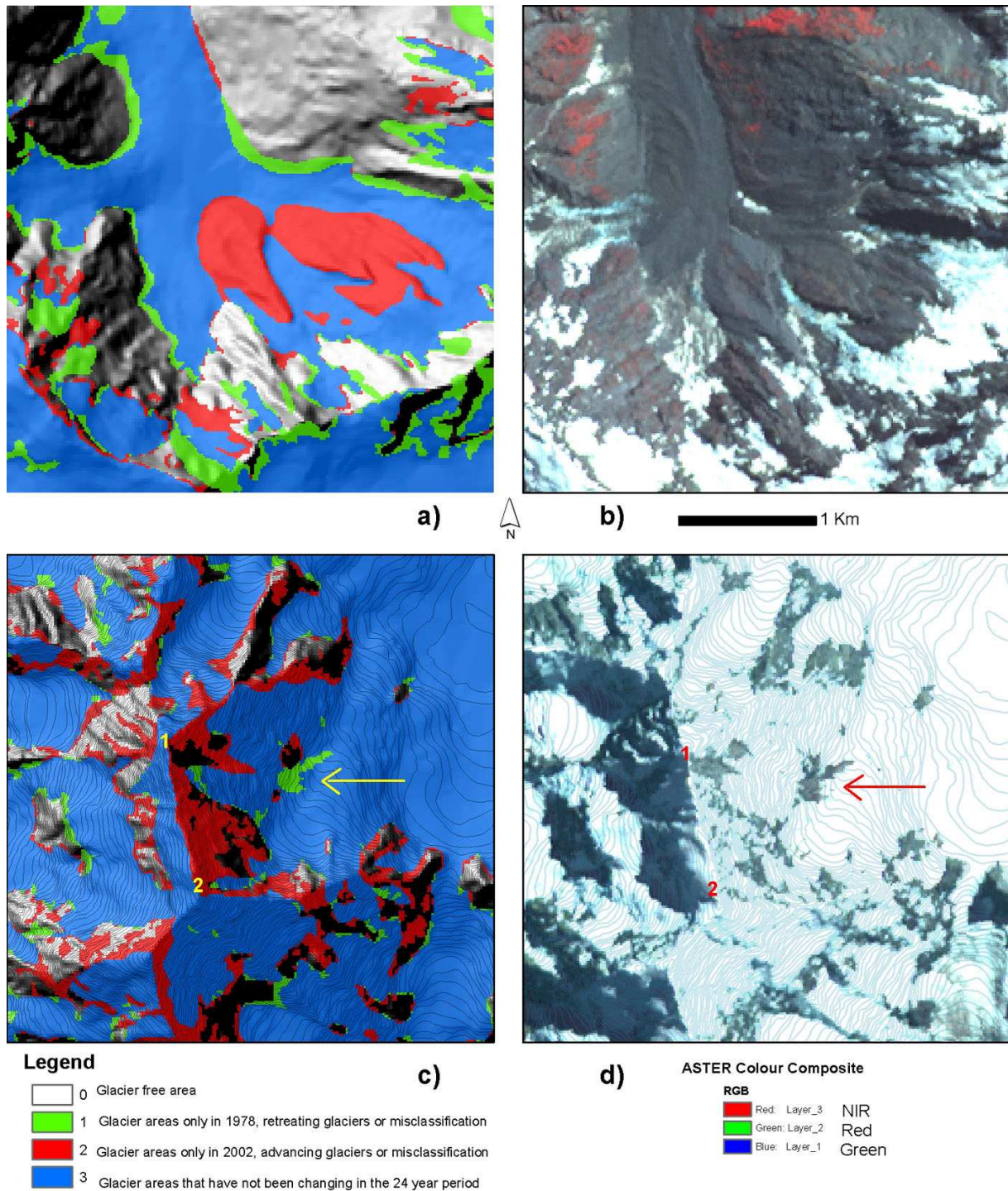
Figure 6.1.2. *Comparison of the 1978 and 2002 glacier inventories in the left windows compared to the original image displayed to delineate the 2002 glacierst. Windows a) and b) show Whymper glacier (for location in image see figure 5.2.1). The red area in the middle of window a) is very likely to have been misclassified in the digitizing of the satellite image. Window c) shows the sum of the 1978 and 2002 glacier inventories for Mt Cook and d) the image displayed as it was interpreted. 1 marks the High peak of Mt Cook (3754 m a.s.l.) and the source of the rock avalanche, and 2 marks the Middle peak (3717 m a.s.l). The arrow*

points at a spot on the East Face of Mt Cook (shown in figure 6.1.3) apparently misinterpreted in the 1978 inventory, but in fact is active rock avalanche debris, while some of the red areas could be wrongly interpreted in the 2002 inventory.

Figure 6.1.3. *Photograph of East face of Mt Cook taken from Langdale glacier in April, showing the face at its most ice free. 1 is the High peak (3754 m a.s.l), whereas 2 is the Middle peak (3717 m a.s.l). The ridge between the two peaks is often referred to as "the highest mile in New Zealand". This face in the satellite image can be shown in figure 6.1.2 c) and d).*

It is important to emphasise, that all these errors from the manual photo interpreting of the image would also have been errors, (most likely to a lot higher degree) by using automatic methods (see chapter 4 for comparison between automatic an manual methods).

6.1.3 Accuracy of the field data collection – comments for some of the glaciers studied

The first question about the field results would be; how precisely can glacier boundaries be recognised in field? The first though that is coming to mind is that this must be really easy. However, it is not necessarily very straight forward. How do you determine the exact boundary of a debris covered glacier when the debris is several meters and there is no indication of ice? How do you define the smaller glaciers extension when they are partly connected to seasonal snow patches? These are questions which had to be interpreted and answered as good as possible in field. The data from the differential GPS used for this study were later corrected to a base antenna, giving a theoretical sub-meter accuracy, meaning that possible inaccuracies in the field work would result from wrong interpretation and not the equipment used.

Jalf/Bauman

Baumann glacier on a saddle on a ridge is a sort of Dome glacier with Jalf as one of its 3 outlets. The problem with Baumann for boundary mapping is that even though it is a kind of a dome glacier it is surrounded by higher elevated terrain on 2 sides. These sides naturally have seasonal snow cover which survives some summers and disappears in others. This makes it hard to map the proper glacier outlines without mixing it with the seasonal snow cover in a positive balance year. At the time the fieldwork was conducted some seasonal snow was still present in the area, thus complicating the mapping (see figure 6.1.4). It was considered to dig some pits to see where we could find glacier ice under the snow, but since the top layer of the snow was heavy metamorphosed from the warm summer this turned out to be impossible with the equipment available. Instead, in the areas of doubt, an approximate line was drawn where the glacier outline was most likely to be situated. Because of this glaciers special characteristics, surrounded by higher elevated snow patches, this glacier is tricky for mapping, unless the particularly glacier year is very negative. With repeating annual satellite data or/and aerial photographs over a 20 year period snow patches directly connected to glaciers could easily be removed from a glacier map. This is again underlining that making accurate glacier maps from remote areas where neither field work, *in situ* data, repeating annual end-of-summer satellite imagery nor annual aerial photographs for more than a decade exist, has to rely on the assumption that the particular year chosen is a negative one. This

problem would occur in alpine areas where the majority of the glaciers are relatively small in area. Baumann glacier is terminates at a relatively high altitude near the snowline (around 1600 m a.s.l.). This is not a problem where the glacier runs down to much lower elevations allowing all surrounding snow-patches to melt during the summer, leaving the real glacier outline at the end of the ablation season.

Figure 6.1.4. *Where is the glacier boundary? Jalf/Bauman glacier. Photograph is taken from a snow patch which is not part of the glacier.*

Ridge glacier

Ridge glacier was easier to map than Jalf/Baumann, however the boundary was not obvious everywhere. In the most southern part of Ridge snow patches obviously not part of the glacier were connected to it (figure 6.1.5). Consequently finding the exact boundary between glacier ice and snow seemed more or less impossible, without drilling and taking density samples. The accuracy of the GPS outline in this particularly area is therefore highly questionable. On the higher elevations on the eastern part of the glacier the GPS was not able to record any data

at all because the cliffs above the glaciers caused limited sky of view, i.e. not enough satellites on the sky above the GPS device to record accurate positions. This was effectively and manually corrected later.

Figure 6.1.5 *Ridge glacier seen from the accumulation basin looking southwards. The snowpatches in the background of the image are just seasonal snow that would be classified as glaciers on a satellite image. Photograph Pete Sinden.*

Debris covered tongues

GPS measurements of the Hooker glacier (figure 6.1.6) were collected along both sides of the trunk, up to where the clean ice surface begins. The data was recorded in the through or depression between the screeslopes from the mountain sides and the glacier itself. It was also difficult to define exactly where the boundary of the glacier was. The depression might not necessarily represent the true boundary (e.g. sometimes ice was visible on the outer side of the depression, however, this is likely to have be dead ice). However, the uncertainty was in most cases though to be within one pixel (15 meters).

6.1.6 *Where is the glacier boundary? The photograph is showing the eastern side of Hooker glacier looking southwards towards its tongue.*

In spite of the problems in the field, the glacier outlines should for the majority of the glaciers be relative precise and for validation of the satellite imagery with a 15 m spatial resolution these results should be more than adequate.

6.1.4 Making a new glacier inventory from 2002

The location of New Zealand, with large oceans on all sides, makes the weather rough and the temperature and precipitation depends more on the directions of the wind rather than the season itself. The temperature will change dramatically when the prevailing winds change from north to south. No land masses are located between New Zealand and Antarctica, so winds from Antarctica reaches New Zealand without any modification from land barriers. So summers can fast turn into winters if the prevailing wind changes to southerly, allowing for

snow to fall in the middle of summer, thus obscuring glacier outlines. This has been the largest problem for the annual snowline survey, in addition to bad flying weather. In other parts of the world where there is a more distinct change between summer and winter, recording satellite imagery and aerial photographs at the very end of summer would be easier and more effective. At Alan's Basin at an elevation of 1750 m in the Craigieburn Range (north of the study area), peak snow accumulation varied between 230 mm and 1030 mm over a 12-year period (Fitzharris, 1999). This shows the strong variation in snow accumulation between one year and another, thus illustrating how much prevailing winds and weather circulations is influencing on the glacier states.

The year 2002 was a negative mass balance year (Chinn et al 2005), something clearly shown in table 6.1.1 and figure 6.1.7. In 2002 the general snowline measured from the index glaciers were 114 meters higher than the average. This clearly illustrates that a satellite image from 2002 was an optimal choice for updating the glacier inventory for parts of New Zealand. During the time spent in field in 2005 there was much more seasonal snow surrounding the glaciers compared to the satellite image, which would have made a photo interpretation of an ASTER image from 2005 much more complicated.

Year	Number of readings	Mean	Standard deviation
1977	15	-19	44
1978	40	38	51
1979	5	30	83
1980	32	-22	53
1981	36	-42	39
1982	41	7	44
1983	41	-131	64
1984	27	-109	64
1985	40	-77	45
1986	38	-16	45
1987	33	-37	39
1988	33	12	50
1989	49	-4	50
1090	2	239	
1991	1	-35	
1992	15	-125	79
1993	49	-135	69
1994	50	-67	42
1995	50	153	70
1996	48	-46	55
1997	45	-125	52
1998	50	43	70
1999	48	170	71
2000	46	145	62
2001	50	-93	51
2002	49	114	62
2003	49	-103	44
2004	45	-84	54

Table 6.1.1 *Mean annual values and standard deviations for ELAo departures from ELAo, for the Index Glaciers in New Zealand annual means and standard deviations. 2002 is highlighted (from Chinn et al, 2005).*
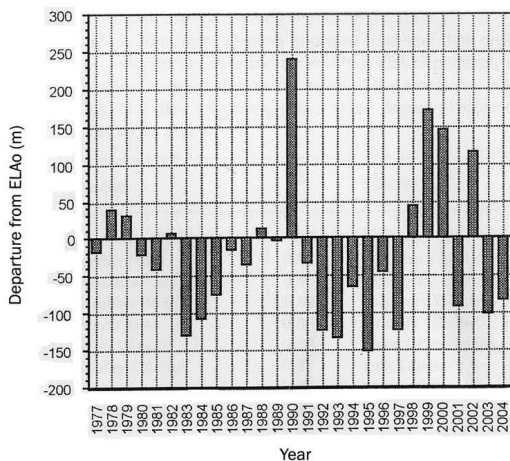
Figure 6.1.7 *Departure from the Mean ELA of the Index Glacier in New Zealand from 1977 to 2004.*

6.1.5 Accuracy of the 1978-2002 glacier area change calculation

Based on the discussions presented, there are reasons to believe that the calculation of glacier change in the area is fairly accurate. There are some misinterpretations in the two inventories, however, the overall pattern and magnitude of glacier retreat would not change significantly after a later refinement of these outlines. Corrections of Whymper glacier (figure 6.1.2) and other errors would not influence much on the percentage of area change in the region. The inaccuracy of the 2002 map is not believed to be larger than the 1978 maps, in spite of its lower spatial resolution. Comparison of the two (figure 5.4.1) shows that the 1978 inventory, have softer boundaries i.e. exhibiting a higher degree of generalisation compared to the 2002 glacier map. Smaller glacier polygons (less than 1 ha/ 1km² in area) should also be removed from the 2002 dataset, even though this would probably not change the total 2002 glacier area much. Overall the accuracy of these calculations should represent the true change well. Even though acquisition of field work from the same year as the image recording would have been and advantage, the field work from a different year can still be a good validation as long as eventual changes are taken into account and good interpretations are made in field.

6.2 Main problems for satellite based glacier extraction

6.2.1 The debris mapping problem, how to overcome this

For debris-covered ice, the spectral signature of the debris may prevail over the ice signature depending on the percentage of the debris-covered surface area. If the ice surface within a pixel is covered with debris by more than several ten percents of surface area it can hardly be separated from pixels of periglacial debris or bedrock using multispectral data (Kääb, 2005). Debris covered glacier tongues have commonly been manually subtracted from the classification as a post-classification step (e.g. Williams et al 1997).

Paul et al (2004) describe a semi-automatic method for delineating debris-covered glaciers. This method combined the advantages of automated multispectral classification for clean glacier ice and vegetation with slope information derived from a Digital Elevation Model

(DEM). The use of an ASTER-derived DEM revealed promising results. This method was tested by Paul & Kääb (2005) for glaciers on Cumberland Peninsula, Baffin Island in the Arctic Canada, but it did not work very well in this region. Manual delineation of debris cover was preferred in the end.

One question appearing after this study would be how can debris covered glacier tongues be mapped accurately from satellite imagery, even by using manual delineation, when it is near impossible to recognise their exact boundaries in field? However, as stated earlier, misinterpretation in the field should in the worst cases not deviate largely from the true boundary and should be within the number of a few pixels, as long as we make the assumption that the ice beneath the debris is glacier ice and not dead ice.

6.2.2 The shadow problem, how to overcome this

Snow in shadow is another problem for automatic extraction of glaciers because it tends to have similar reflectance properties as bright rock. Manual detection of these surfaces were relatively straight forward to map as long as good care was put into the interpretation, and topographic maps and other cartographic information were used. However, these areas were not necessarily easy to extract with the automatic methods, depending on the type of snow (clean snow versus dirty ice), steepness of the slope (snow in steeper slopes tended to be harder to extract). Most of the shaded clean snow could be relatively accurately delineated by using the lowest threshold tested for the band3/band4 ratio. However, this threshold would also include large areas which obviously not were glaciers, so care has to be taken if these results were to be used for an inventory. Paul & Kääb (2005) used a thresholded band3/band4 ASTER image in addition to an ETM scene for calculating glacier areas in Arctic Canada. In addition they used a threshold of ASTER band 1 which proved to be efficient for removing wrongly classified shadow pixels that were located over bare rock, due to the markedly higher reflection of shadowed ice and snow pixels.

The results from this study showed that when a low threshold was applied for the band3/band4 ratio, this method was able to detected most areas of shaded snow as long as the snow was clean. Dirty snow/ ice patches in shadow seemed to be left out. The NDSI also

proved to detect these areas relatively good, but not as good as the band3/band4 ratio. However, when choosing a threshold in order to include shaded snow, this often made large areas that was not classified as glaciers in the digitizing to be classified as glacier in the automatic methods.

6.2.3 Automatic extraction of glacier area in a satellite image versus manual approaches

Paul & Kääb (2005) studied glaciers on the Baffin Island, Arctic Canada and they found that with the ETM3/ETM5 method, nearly all lakes in the study were classified as glacier, independent of their turbidity. They were detached from the glaciers in the course of the basin delineation, as they are clearly visible in the background image. The same happened in this study when applying the NDSI. However, this was not a significant problem for the ban3/band4 ratio. As reported from Baffin Island, also in New Zealand the lakes are clearly visible in background image and the water bodies were therefore manually digitized on the background image and removed from the NDSI results. For the Baffin Island and the New Zealand setting we see that manual delineation of waterbodies have to be applied to the ETM3/ETM4 and the NDSI in order to get the results from these classifications representable.

Band ratios have been reported to be an especially simple, robust and fast method for glacier mapping over large areas (Paul 2002a; 2002b, Albert, 2002), which is also confirmed in this study. Here it appears that the band3/band4 ratio with a threshold around 2.0 is the most efficient. 3*3 median filter was efficient for removing noise in areas with dense vegetation, but did not influence the classification results largely. After a water mask was applied to the NDSI results for removing all water bodies, this method also revealed results similar to the ban3/band4 ratio. In some areas the NDSI could even be more efficient. For Franz Josef glacier area the NDSI showed slightly better overall accuracy than the band3/band4 ratio (tables 4.3.2 and 4.3.4) when no median filter was applied to the band3/band4 ratio. However, this was very marginal and a result of the special characteristics of the Franz Josef area, with much noise in the band3/band4 ratio (dense vegetation) which was not included in the NDSI. The confusion between the manual digitizing and the band3/band4 ratio and the NDSI is mainly due to debris cover of many of the glaciers in the area. It appears that if these debris

areas were removed from all the approaches, the confusion would not be large, thus indicating that these two automatic approaches give a sufficient extraction for large glacier area, where the broad picture of glacier area change is wanted and not much details for individual glaciers necessarily is needed as long as debris is removed manually.

6.3 The change of glacier area in New Zealand compared to other parts of the world

The result of this work shows a measured retreat of the glaciers within the study area of about 17 % in the period from 1978 to 2002. Similar results have been reported in other part of the world. For the new Swiss glacier inventory (Paul, 2003) the relative loss in glacier size from 1973-1998/9 was mapped to about 20%. However, in Switzerland glaciers smaller than 1 km² (100 ha) contributed to about 40% of the total loss although they cover only 15% of the area. About 18% of this change occurred from 1985 to 1999, illustrating a recent acceleration of the glacier retreat. This is in large contrast to the New Zealand situation where the largest glaciers by far have contributed to the largest ice loss.

In Norway, the maritime glaciers along the western coast with a large annual mass turnover had a large mass surplus between 1962 and 2000. Conversely, the continental glaciers with small summer and winter balances had a mass deficit over the same period (Andreassen et al, 2005). Since 2001, all monitored glaciers in Norway have shown a considerable mass deficit. Overall the Norwegian glaciers have retreated during the 20th century. Continental glaciers have, with few exceptions, retreated throughout the century, while many maritime glaciers have been through periods of advance and recession, although recession has been the main process (Andreassen, et al, 2005). A calculation of the total area of glacier recession in Norway has not been made to date (but is on its way…).

Paul & Kääb (2005) calculated a decrease in area for 225 glaciers in Cumberland Peninsula, Baffin Island in the Arctic Canada. They compared a Landsat ETM+ and an ASTER scene from August 2000 to manual delineation of Little Ice Age trimlines and moraines. They found

an average area loss of 11% in the time period. The relative loss of area increased towards smaller glaciers (if sizes are <10km²) and was more or less constant for larger glaciers.

Khromova et al (2006) assessed glacier recession in the eastern Pamir, Central Asia, by using historical data and space images from Russian satellites and ASTER. They found 7.8% decrease in glacier area during 1978-1990, and 11.6% in 1990-2001. In addition to decrease in glacier area and retreat of glacier fronts, they also found increased debris-covered area and the appearance of new lakes.

All these reports of glacier retreat are similar to what is found in this study, however, the reasons behind the recessions might be very different.

6.4 Reasons behind the recent changes of individual glaciers in New Zealand

Even though no new individual glacier map for the study area in New Zealand was made, visual inspection of the results shows that the smallest glaciers in New Zealand certainly don't contribute to the largest ice loss (figure 5.2.1, 5.3.1, 5.3.2, 5.4.1). In New Zealand the large heavily debris covered valley glacier have lost enormous areas over the last few decades, whereas some of the smaller glaciers might even have shown a small advance. The main clustering of these large valley glaciers is covered by the 2002 image, thus indicating that the area change for the study period is likely to be larger here compared to the rest of the glaciated areas in New Zealand. This means that if the 2002 glacier inventory was made not only for the central Southern Alps, but for the entire New Zealand, the total area change from 1978 would probably have turned out to be less than what the result from this work shows.

The low gradient heavy debris covered valley glaciers have a very long response time, thus have not until recently started to pull back from the position obtained during the Little Ice Age. Their insulating debris cover damps the response to climate forcing as it introduces inertia into the response of the glacier to negative mass balance (Chinn, 1991). With the development of proglacial lakes, these glaciers have shown a rapidly accelerating retreat

during the last decades as a result of lake calving. This calving is not directly linked to the present climate, so their fast recession is a not a result of warming in today's climate. On the contrary, Chinn (1999) reported of a reversal of the past century glacier – recession trend. During the 20-year period of photographing end-of-summer snowline positive balance had occurred in most years since 1980, and more recently all glaciers had shown positive balances (table 6.1.1 and figure 6.1.7).

Chinn (1988) writes as a comment to the NZ glacier inventory from 1978; "it happens that at present the interplay between climate and topography has placed a large number of our peaks just above the snowline, with the result that we have an unusually large number of small glaciers". He continues; "at present, we appear to be in a climate close to the most favourable for the maximum number of individual glaciers. Should the climate continue with present warming trend then many hundreds of these glaciers will disappear. Conversely, if the climate cools again and the snowline lowers, many hundreds of these small glaciers would coalesce to form larger glaciers, and although new small glaciers would form on peaks presently below the snowline, the total number of glaciers would eventually decrease". Even if there have been a large change in glacier area since Chinn wrote this, a decrease in the number of individual glaciers is not likely based on the results from the annual snowline survey (table 6.1.1 and figure 6.1.7). However, this is something which should be closer investigated.

Figure 5.3.1 and 5.3.2 gives a view on the change in glacier area for the western and eastern glaciers in the 24-year period. Only the two largest glaciers of the west coast glaciers have advanced, whereas all the other large glaciers have retreated. This could easily be interpreted as the western climate to be more favourable for glacier advance as opposed to east of the Main Divide. However, it might not be that simple. Chinn (2001) writes; "the notion that the "western" glaciers behave differently from the "eastern" glaciers that is frequently mentioned in literature is unfounded. This false impression arises from the many simplistic comparisons made between only two groups of glaciers that are of different types and have very different responses to climate. Frontal changes at the steep and exceptionally responsive Franz Josef and Fox Glaciers, which provide enhanced responses to climate within 5 to 8 years, have repeatedly been compared with the large, low-gradient valley glaciers of the Mount Cook area, which have slow, subdued response times in the order of 100 years." Fox and Franz Josef Glaciers have a very steep mass balance gradient and enormous accumulation basins compared to all the other glaciers presented in 5.3.1 and 5.3.2. An illustration of their

6. DISCUSSION

enormous accumulation basins is given in figure 6.4.1 and compared to the other main valley glaciers west of the Main Divide. A part of the accumulation basin of Fox glacier is also shown in figure 6.4.2. The reaction times for Franz Josef and Fox Glaciers are though to be less than a decade (Fizharris et al, 1999), something which is in large contrast to the rest of the large valley glaciers in New Zealand. In figure 6.4.1 we see that the 2 glaciers with largest accumulation basins have advanced (Fox and Franz Josef Glaciers), the ones with reasonable large basins seems to be stable (e.g; Spencer Glacier, Fritz Glacier, Salisbury Snowfield), while the valley glaciers with the smallest accumulation basins have shown a marked retreat (the glaciers in the small window in figure 6.4.1). The important thing to highlight is that the hypsometry (the distribution of glacier area over its altitudinal range) for Fox and Franz Josef Glaciers compared to the rest of the western valley glaciers are very different. The main part of the accumulation basins for these two glaciers are located above 2000 m a.s.l., while a very small part of the other valley glaciers are above the same elevation. This should make Fox and Franz Josef Glaciers very responsive to small changes in climate, much more than the other western valley glaciers. Chinn (2001) writes; "Franz Josef and Fox Glaciers are the best known, but perhaps the most unrepresentative of the New Zealand glaciers. They both occupy a high plateau feeding the only two valleys of Westland that are not incised back to the Main Divide; they descend to the lowest altitudes of all glaciers, and they have as short response time to climate fluctuations as any glacier in New Zealand".

Because of Fox and Franz Josef Glaciers fast reaction time scientists have tried to correlate their retreat and advance to climatic parameters. Hooker and Fitzharris (1999) found a strong link between atmospheric circulation changes, climate variables and glacier behaviour. Results from this study are shown in table 6.4.1. This table shows linkages between atmospheric system behaviour and positive or negative mass balance. Studies like this would not be possible for the other large valley glaciers, where the time would smoothen the climate signal from the glacier, thus not making it applicable for climate parameter correlation.
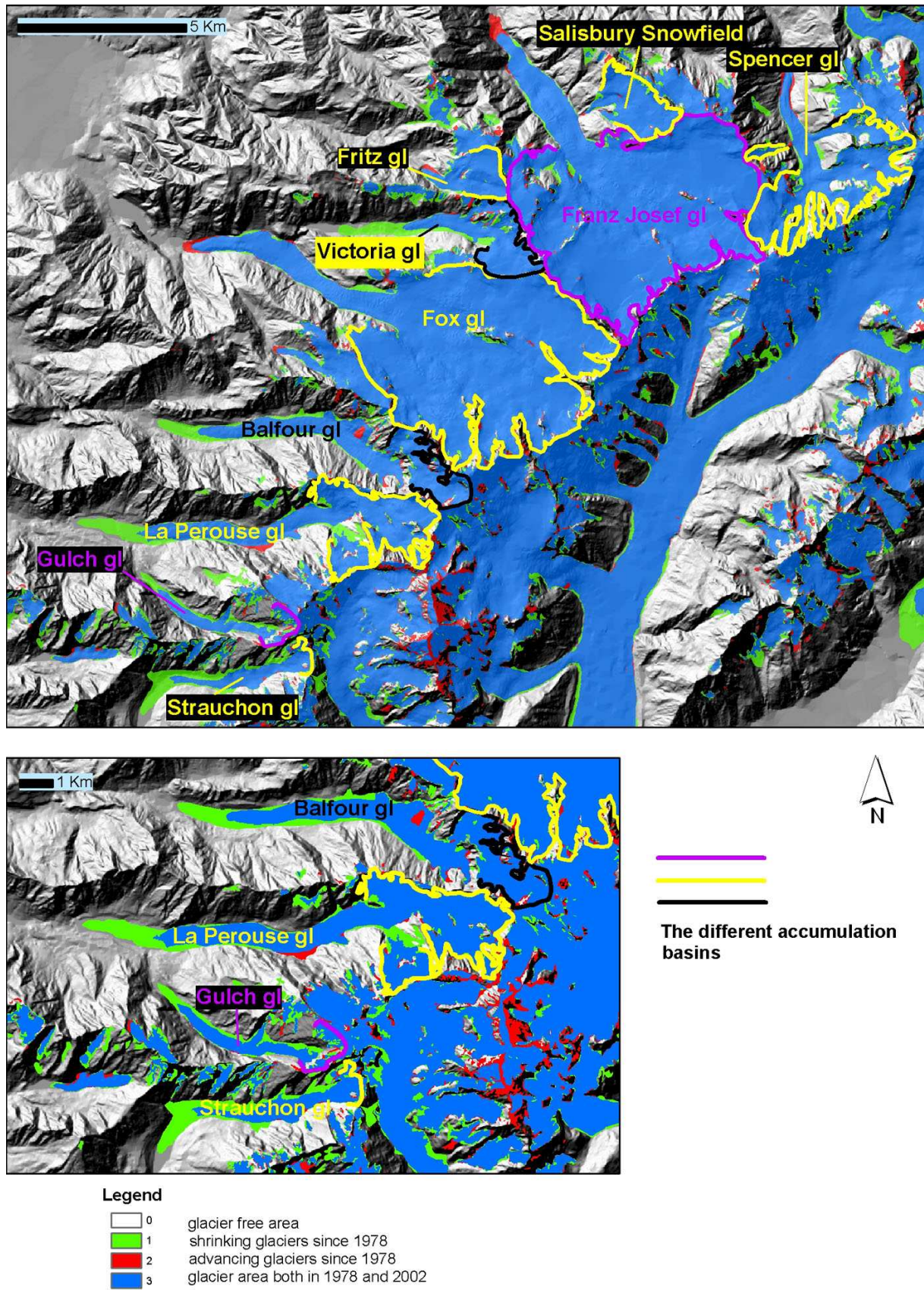
Figure 6.4.1 *Accumulation basins on the west coast glaciers, illustrating their large variance in size.*

Figure 6.4.2 *Northern part of the accumulation basin of Fox glacier, looking towards Tasman Sea in the west. The photograph is taken from Glacier Peak and shows less than 1/3 of the whole accumulation basin.*

Atmospheric system	Positive net balance Low snowline Glacier advance	Negative net balance High snowline Glacier retreat
Wind direction anomaly	southerly	northerly
Westerly air flow over the Southern Alps	stronger	weaker
700 hPa geopotential anomalies to the southeast of New Zealand	negative	positive
700 hPa geopotential anomalies in the southeast Pacific	positive	negative
Sub-tropical jet stream	stronger	weaker
Sea surface temperature anomalies near New Zealand	cool	warm
Sea surface temperature anomalies towards equatorial South America	warm	cool
Precipitation	increased	decreased
Air temperature during ablation season	lower	higher
Westerly air flow during ablation season	stronger	weaker
Position of main westerly zone	northwards	southwards
Position of the sub-tropical high pressure zone	northwards	southwards
Air flow anomalies during ablation season	southwesterly	northeasterly
Pressure anomaly over new Zealand in ablation season	negative	positive
Southern Oscillation Index (SOI)	negative	positive
Circulation phase	El Niño	La Niña

Table 6.4.1. *Climatological and circulation patterns influencing the mass balance of New Zealand glaciers (after Clare et al. 2002; Hooker and Fitzharris 1999; Chinn et al, 2005).*

6.5 Future research

The use of DEM for improving glacier extraction

The method for semi-automatic extraction of glacier debris described in Paul et al (2004) should be tested for the New Zealand environment as debris where found to be one of the most significant limitation for glacier mapping. This method combined the advantages of automated multispectral classification for clean glacier ice and vegetation with slope information derived from a DEM. Rott and Markl (1989) wrote that there is still a large potential from spectral data and its derivatives alone, but multidimensional classification including DEMs may be most promising since they best reflect the nature of high-mountain phenomena and processes. The increasing availability of suitable DEMs supports this trend (e.g. satellite-based photogrammetric DEM, development of LIDAR technology). Rott and Markl (1989) wrote that the manual application of expert knowledge for glacier delineation will decline gradually but never become redundant.

The ASTER-derived DEM in combination with GIS-based processing provides a wealth of additional possibilities, including automated 3-D glacier inventorying, particularly for regions outside the coverage of the SRTM DEM.

Volume calculation

From the 1978 inventory ice volumes have been estimated using formulas based on surface area and estimated thickness. Volume change is much more significant than glacier area, thus a calculation of volume would have been interesting. Because of the large amount of debris covered glacier, measuring ice volume will give a much more realistic estimate of what has happened to the glaciers. Tasman Glacier, along with the majority of the other large debris-covered valley glaciers, has downwasted by well over 100 m since LIAM (Hochstein et al, 1995) but has not started to retreat until recently when ice levels allowed proglacial lake to form (Chinn, personal communication). Thus, interpreting area change won't tell much about what's happened to the glacier levels. The complete story of what's happened to the glaciers, - the large, low-gradient valley glaciers which in 1978 looked as large as they were at the end of the little ice age, but were soon to collapse into proglacial lake explosion, could only have been told by measuring the change in surface elevation.

Making a new individual glacier map

For this work the total glacier area change within the boundary of the image was calculated. However, it would have been interesting to have calculated the new additional number of individual glaciers in the area. With such information it would have been easier to draw conclusions on aerial changes within the different size intervals. However, it was not possible to use ice divides from the 1978 inventory so new glacier divides would have had to be defined, - a time consuming job and was not prioritized in this work. A selection of representative glaciers should be selected according to various criteria (size, height, side and distance from the divide) to quantify changes for the medium-size or small-size glaciers.

Object oriented technique

This is a technique where spectral and spatial approaches can be combined to spatial and-spectral segmentations. This could be done by applying object-oriented image classifications with the software eCognition. This method has not yet been reported for glacier extraction and could have the potential to separate glacier debris from rocks and screeslopes if a DEM is fed into the classification.

Thermal bands

Kääb (2005) writes that inclusion of thermal bands for ice and snow applications has rarely been tested and should be investigated further. These are better recorded at night-time. There could be a potential of extracting debris from the information in these wavelengths due to the different temperature of debris over ice as opposed to rock and screeslopes.

More field studies

Khromova (2006) is underlining the importance of in situ studies and historical glaciological and climatic data in order to best asses glacier changes from satellite data. Thus, more fieldwork should be committed on the New Zealand glaciers to get a larger understanding for the processes going on today, for instance the rapid retreat of glaciers with proglacial lakes.

7. CONCLUSIONS

Conclusions for the work are divided into two separate sections, one for the methods tested and one for the change in glacier coverage within the study area in the 24-year period between 1978 and 2002. Lastly, a paragraph is included summarizing the outcome and the most crucial findings of this work.

7.1 Conclusions: methods

The most important conclusions from the methods tested are summarized and given in bullet points below:

- Orientation of the ASTER image, using only points collected in field, failed due to planimetric and altimetric clustering of these points. Combining these field collected points with points from the New Zealand topographic data base, well spread in elevation and position over the image, proved to be efficient.

- The initial test of supervised classification did not provide very promising results. There was considerable confusion between glacier ice and saturated snow within the glacier areas and in addition shaded vegetation was classified as glacier ice, and shaded snow was also poorly detected by the supervised classification. This underlines the importance of choosing appropriate training areas, and the difficulties involved when the output classes have similar spectral signatures.

- ASTER band3/band4 ratio (near infrared/shortwave infrared) proved to be the most efficient automatic classification, similar to reports from other studies (e.g. Paul, 2003), Applying a 3*3 median filter was efficient for removing noise in some areas with dense vegetation, but did not change the classified results significantly. The optimum threshold was around 2.0, which is in agreement with other studies (e.g. Paul, 2003).

127

- As expected, the band rationing excluded all debris covered glacier areas, as did the NDSI. Therefore, the overall accuracy of the classification increased with decreasing debris cover in the study areas tested.

- For the Normalized Differential Snow Index (NDSI) there was a large misclassification of water bodies, especially for turbid water bodies. This misclassification increased with decreasing thresholds. After manually masking out all the water bodies, the NDSI gave very close to similar results as the band3/band4 ratio. The optimum threshold for the NDSI was around 0.5.

- The manual delineation of lateral margins of Hooker glacier in the 2002 ASTER image exhibited a larger discrepancy in results than expected in comparison with the field work carried out in 2005. This glacier is not believed to have changed much along the lateral margins in these three years, confirming the difficulties involved in manual extraction of debris covered glaciers - even for debris covered glacier tongues in a deep valley.

7.2 Conclusions: Change in glacier area

The most important conclusions in the detection of area change in the study area between 1978 and 2002 are summarized and given in bullet points below:

- The glaciers in the study area show an overall area loss of about 17% during the 24-year period from 1978 to 2002. Glaciers west of the Main Divide of the Southern Alps lost about 14 % of their 1978 area, whereas glaciers east of the Main Divide lost about 18 % of their 1978 area. This overall retreat is in agreement with results reported from other parts of the world e.g. Switzerland (Paul, 2003), Pamir (Khromova et al, 2006), Baffin Island (Paul & Kääb, 2005), and Norway (Andreassen et al, 2005).

- The largest glaciers in New Zealand contribute to the greatest decrease in glacier area. This contradicts reports from other parts of the world (e.g Switzerland) where glaciers

smaller than 1 km² (100 ha) contributed to 40 % of the decrease in glacier area (Paul, 2003).

• The large, western, tropical, fast-flowing, maritime Fox and Franz Josef Glaciers have been fluctuating backward and forward in the study period, but show an overall advance of about 300 and 650 meters, respectively, in the study period.

• Many of the low-gradient, heavily debris covered valley glaciers have, since 1978, developed proglacial lakes and have shown a rapid retreat due to lake calving. Tasman glacier retreated more than 2 km in the study period, whereas the main, large, low-gradient, valley glaciers retreated between 1 and 2 km in this period. Fieldwork showed that Tasman glacier continued to retreat at approximately 100 m/a between the late summers of 2002 and 2005.

• The small, alpine, high-elevated glaciers showed only minor changes in the study period. Some showed a slight retreat, some showed a slight advance and some were approximately the same size as they were in 1978.

This study has stressed the large potential of glacier extraction from ASTER and other multispectral imageries, but at the same time underlined the problems involved. A ratio of band3/band4 (NIR/MIR) proved to be the most efficient automatic classification method, and when combined with the manual extraction of debris covered tonglly this should yield reasonably accurate results when working on a large scale. Despite the large climatological precipitation difference between glaciers west and east of the Main Divide, they show relatively similar area losses. The overall loss in the study area is similar to reports from other parts of the world. Large glaciers show the greatest area loss, whereas some of the small, alpine, high altitude glaciers even show signs of advance - something which is in agreement with reports of a positive trend in mass balance from the New Zealand annual snowline survey (Chinn, 2005). It is important to state that if all the glaciers that have developed proglacial lakes during the last decades were removed from the glacier area and from the area calculations, the changes in glacier area between 1978 and 2002 would have been minimal.

REFERENCES

REFERENCES

Anderton, P.W. (1973): The significance of perennial snow and ice to the water resources of the South Island, New Zealand. Journal of Hydrology (New Zealand) 12, 6-18

Albert, T. (2002): Evalutaion of remote sensing techniques for ice – area classification applied to the tropical Quelccaya ice cap, Peru. Polar Gography, vol 26 (3), 210-226

Andreassen, L.M., Elvehøy, H., Kjøllmoen, B., Engeset, R.V., Haakensen, N. (2005): Glacier mass-balance and length variation in Norway, Annals of Glaciology, vol. 42

Benn, D.I., Evans, D.J.A. (1998): Glaciers & Glaciation, Arnoldpublishers and Oxford University Press Inc, p 734

Benn, D.I. personal communication (December 05)

Brown, D.G., Lush, D.P., Duda, K.A. (1998): Supervised classification of types of glaciated landscapes using digital elevation data, Geomorphology, Vol 21, 233-250

Burrough, P.A., McDonnell, R.A. (2000(reprint from 98)): Principles of Geographical Information Systems – Spatial Information Systems and Geostatistics, Oxford University Press, 333p.

Chinn T.J., (1989): Glaciers of Irian Jaya, Indonesia, and New Zealand – Glaciers of New Zealand. Satellite imgage atlas of glaciers of the world, Edited by Richard S. Williams, Jr., and Jange G. Ferrigno. U.S. Geological Survey Professional Paper 1386-H-2, United States government printing office, Washington

Chinn, T.J. (1979): How wet is the wettest of the wet West Coast? New Zealand Alpine Journal, (I.E. Whitehouse, ed.), Vol. 32

Chinn, T.J (1988): Glaciers and the glacier inventory, New Zealand Alpine Journal, v.41

REFERENCES

Chinn, T.J., (1991): Glacier inventory of New Zealand. Institute of Geological and Nuclear Sciences, unpublished

Chinn, T.J., (1996): The New Zealand glacier responses to climate change of the past century. New Zealand Journal of Geology and Geophysics, 39, 415-28

Chinn, T.J.H., (1999): New Zealand glacier response to climate change of the past 2 decades, Global and Planetary Change 22 (1999) 155-168

Chinn, T.J., Salinger, M.J. (2001): New Zealand glacier snowline survey, 2000, NIWA Technical Report 98

Chinn, T.J.(2001): Distribution of the glacial water resources of New Zealand, Journal of Hydrology (NZ) 40 (2): 139-187, 2001

Chinn, T.J (2002): The proliferating glacier lakes – what's the story? New Zealand Alpine Journal

Chinn, T.J., Heydenrych, C., Salinger, M.J. (2005): Use of the ELA as a practical method of monitoring glacier response to climate in New Zealand's Southern Alps, Journal of Glaciology, Vol. 51, No. 172

Chinn, T.J., Winkler, S., Salinger, M.J. and Haakensen, N. (2005): Recent glacier advances in Norway and New Zealand: A comparison of their glaciological and meteorological causes, Geografiska Annaler, 87 A (1): 141-157

Chinn, T.J, personal communication

Clare, G.R., Fitzharris, B.B., Chinn, T.J.H., and Salinger, M.J. (2002): Interannual variation in end-of-summer snowlines of the Southern Alps of New Zealand, and relationships with southern hemisphere atmospheric circulation and sea surface temperature patterns, International Journal of Climatology, 22, 107-120

REFERENCES

Congalton, R.G. (1999): A review of assessing the accuracy of classifications of remotely sensed data, Remote Sensing of Environment, vol. 37, 35-46

Fitzharris, B.B., Chinn, T.J., Lamont, G.N. (1997): Glacier balance fluctuations and atmospheric circulation patterns over the Southern Alps, New Zealand, International Journal of Climatology, Vol. 17, 745-763

Fitzharris, B., Lawson., W., Owens. (1999): Research on glaciers and snow in New Zealand, Progress in Physical Geography vol.23, 4 469-500

Fitzharris, B.B., Hay, J.E., and Jones, P.D. (1992): Behaviour of New Zealand glaciers and atmospheric circulation changes over the past 130 years, Holocene 2,2 pp. 97-106
Fitzharris, B., personal communication, 2006.

Gao, B-C., Han, W., Tsay, S.C., Larsen, N.F. (1999): Cloud detection over the Arctic region using airborne imaging spectrometer data during the daytime, Journal of Applied Meteorology 37, 1421–29.

Gao, J., Liu, Y. (2001): Applications of remote sensing, GIS and GPS in glaciology: a review, Progress in Physical Geography 25 vol. 4 pp. 520–540

Gellatly, A.F. (1985): Historical records of glacier fluctuations in Mt Cook National Park, New Zealand: A century of Change, The Geographical Journal, Vol. 151, No. 1, March 1985, pp. 86-99

Gellatly, A.F., Norton, D.A. (1984): Possible warming and glacier recession in the South Island, New Zealand, New Zealand Journal of Science, 1984, Vol. 27: 381-388

Haeberli, W. (1995): Glacier fluctuations and climate change detection – operational elements of a worldwide monitoring strategy. World Meteorological Organisation Bulletin 44, 23 - 31

Hessel, J.W.D. (1983): Climatic effects on the recession of the Franz Josef Glacier, New Zealand Journal of Science, 1983, Vol. 26: 315-320

REFERENCES

Hochstein, M.P., Claridge, D., Henrys, S.A., Pyne, A., Nobes, D.C., Leary, S.F. (1995): Downwasting of the Tasman Glacier, South Island, New Zealand: changes in the terminus region between 1971 and 1993, New Zealand Journal of Geology and Geophysics, 1995, Vol. 38: 1-16

Hochstein, M.P., Watson, M.I., Malengreau, B., Nobes, D.C., Owens, I. (1998): Rapid melting of the terminal section of the Hooker Glacier (Mt Cook National Park, New Zealand), New Zealand Journal of Geology and Geophysics, 1998, Vol. 41: 203-218

Hooker, B.L., Fitzharris, B.B. (1999): The correlation between climatic parameters and the retreat and advance of Franz Josef Glacier, New Zealand, Global and Planetary Change 22, 39-48

Hugh Kieffer, personal communication (Feb, 06).

IPCC, Climate Change 2001: Working Group 2, Impacts, Adaption and Vulnerability, Summary for Policymakers Edited by James J. McCarthy, Osovaldo F.Canziani, Neil A. Leary, David J. Dokken, Kasey, S.White

Jacobs, J.D., Simms, E.L., Simms, A. (1997): Recession of the southern part of Barnes Ice Cap, Baffin Island, Canada, between 1961 and 1993, determined from digital mapping of Landsat TM, Journal of Glaciology, vol. 43, 98-102

Jon Ove Hagen, personal communication.

Kääb A (2002): Monitoring high-mountain terrain deformation from repeated air- and spaceborne optical data: examples using digital aerial imagery and ASTER data, ISPRS Journal of Photogrammetry & Remote Sensing vol. 57 (1-2) 39-52

Kääb, A., (2005): Remote Sensing of Mountain Glaciers and Permafrost Creep, Zürich Universität, pp 264

Kääb, A., Huggel, C., Fischer, L., Guex, S., Paul, F., Roer, I., Salzmann, N., Schlaeffli, S., Schmutz, K., Schneider, D., Strozzi, T., Weidmann, Y. (2005): Remote Sensing of glacier-

REFERENCES

and permafrost-related hazards in high mountains: an overview, Natural Hazards and Earth System Sciences, 5, 527-554

Kääb, A., Huggel, C., Paul, F., Wessels, R., Raup, B., Kieffer, H., Kargel, J. (2002): Glacier monitoring from ASTER imagery: Accuracy and applications, Proceedings of EARSeL-LISSIG-Workshop Observing our Cryosphere from Space, Bern, March 11 – 13.

Kargel, J.S., Abrams, M.J., Bishop, M.P., Bush, A., Hamilton, G., Jiskoot, H., Kaab, A., Kieffer, H.H., Lee, E.M., Paul, F., Rau, F., Raup, B., Shroder, J.F., Soltesz, D., Stainforth, D., Stearns, L., Wessels, R. (2005): Multispectral imaging contributions to global land ice measurements from space, Remote Sensing of Environment 99 (2005) 187 – 219

Khromova, T.E., Osipova, G.B., Tsvetkov, D.G., Dyurgerov, M.B., Barry, R.G. (2006): Changes in glacier extent in the eastern Pamir, Central Asia, determined from historical data and ASTER imagery, Remote Sensing of Environment 102, 24-32.

König, M., Winther, J.-G., Isaksson, E. (2001): Measuring snow and glacier ice properties from satellite, Reviews of Geophysics, 39 (1), 1-27.

Lambrecht, A., Würländer, R., Kuhn, M. (2005): The new Austrian glacier inventory: a tool for the analysis of modern glacier change, Geophysical Research Abstracts, Vol. 7, 03097

Lamont, G.N., Chinn, T.J., Fitzharris, B.B. (1999): Slopes of glacier ELAs in the Southern Alps of New Zealand in relation to atmospheric circulation patterns, Global and Planetary Change 22, 209-219

Liestøl, O., (2000): Glaciology, second edition, Unipub forlag 2000, 123 pp

Massonnet, D., Feigl, K.L. (1999): Radar interferometry and its application to changes in the earth's surface, Reviews of Geophysics, 36, 4, 441-500

NASA, 2004. Aster Mission. http://asterweb.jpl.nasa.gov/mission.asp, (read October, 2006)

Nesje, A., (1995): Brelære, Høyskoleforlaget AS – Norwegian Academic Press

REFERENCES

New Zealand's Snow and Ice Research Group, Proceedings from the 3rd annual workshop held at Harihari, Westland 15th-17th January 2005-01-18. Proceedings compiled by Becky Goodsell, Department of Geography, University of Canterbury

O'Shea, B.E. (1954): Ruaphehu and the Tangwai disaster. New Zealand Journal of Geology and Geophysics 36, 1974 - 89

Oerlemans, J. (1989): A projection of future sea level, Climatic Change 15, 151-174

Paterson, W.S.B., (1994): The physics of glaciers, Butterworth – Heinemann, 481pp

Paul, F. (2002a): Changes in glacier area in Tyrol, Austria, between 1969 and 1992 derived from Landsat 5 Thematic Mapper and Austrian Glacier Inventory data. International Journal of Remote Sensing, vol. 23 (4), 787-799

Paul, F. (2002b): Combined technologies allow for rapid analysis of glacier changes. EOS, Transaction, American Geophysical Union, 83 (23), 253, 260, 261

Paul, F. (2003): The New Swiss Glacier Inventory 2000 - Application of Remote Sensing and GIS, PhD Thesis, Department of Geography, University of Zurich, 198 pp, 203

Paul, F., Huggeli, C., Kääb, A. (2004): Combining satellite multispectral data and a digital elevation model for mapping debris-covered glaciers, Remote Sensing of Environment vol. 89, 510-518

Paul, F., Kääb, A. (2005): Perspectives on the production of a glacier inventory from multispectral satellite data in Arctic Canada: Cumberland Peninsula, Baffin Island, Annals of Glaciology, vol. 42

Paul, F., Kääb, A., Maisch, M., Kellenberger, T., Haeberli, W., (2001): The new remote sensing derived Swiss glacier inventory: 1. Methods, 4th International Symposium on remote Sensing in Glaciology, Maryland, revised version

PCI Geomatics http://www.pcigeomatics.com/products/ecognition.html (read January, 2007)

REFERENCES

Pohl, C., Van Genderen, J.L. (1998): Multisensor image fusion in remote sensing: concepts, methods and applications, International Journal of Remote Sensing, 19 (5), 823-854

Purdie, J., Fitzharris, B. (1999): Processes and rates of ice loss at the terminus of Tasman Glacier, New Zealand, Global and Planetary Change 22, 79-91

Rott, H., Markl, G. (1989): Improved snow and glacier monitoring by the Landsat Thematic Mapper. Proceedings, Workshop on Landsat Thematic Mapper applications, ESA, SP-1102, 3-12

Salinger, M.J., Heine, M.J., Burrows, C.J. (1983): Variations of the Stocking (Te Wae Wae) Glacier, Mount Cook, and climatic relationships, New Zealand Journal of Science, Vol. 26, 321-338

Sara, W.A. (1968): Franz Josef and Fox Glaciers, 1951 – 1967, New Zealand Journal of Geology and Geophysics, 11, 768-80

Sidjak, R.W., Wheate, R.D. (1999): Glacier mapping of the Illecillewaet ice field, British Columbia, Canada, using Landsat TM and digital elevation data int. j. remote sensing, 1999, vol. 20, no. 2, 273-284

Toutin, T. (2002): Three-Dimensional Topographic Mapping With ASTER Stereo Data in Rugged Topography, IEEE Transactions on Geoscience and Remote Sensing, Vol. 40, No.10, October 2002

Toutin, T. (2003): Block bundle adjustment of Ikonos in-track images. International Journal of Remote Sensing, 24 (4), pp.851-857

Toutin, T. (2004). Review article: Geometric processing of remote sensing images: models, algorithms and methods. International Journal of Remote Sensing, 25 (10), pp.1893-1924.

REFERENCES

Tyson, P.D., Sturman, A.P., Fitzharris, B.B., Mason, S.J. and Owens, I.F., (1997): Circulation changes and teleconnections between glacial advances on the west coast of New Zealand and extended spells of drought years in South Africa. International Journal of Climatology, 1499-1512

Walsh, S.J., Butler, D.R., Malanson, G.P. (1998): An overview of scale, pattern, process relationships in geomorphology: a remote sensing and GIS perspective. Geomorphology, vol. 21, 183-205.

Warrick, R.A. and Oerlemanns, J., (1990): Sea level rise. In Houghton, J.T., Jenkins, G.J. and Ephraums, J.J., editors, Climate Change. The IPCC assessment Cambridge: Cambridge University Press, 257-81.

Wessels, R., Kargel, J.S. and Kieffer, H.H. (2002): ASTER measurement of supraglacial lakes in the Mount Everest region of the Himalaya. Annals of Glaciology, vol. 34, 399-408

Williams Jr., R.S., Hall, D.K., Sigurdsson, O., Chien, J.Y.L. (2006): Comparison of satellite-derived with ground-based measurements of the fluctuations of the margins of Vatnajökull, Iceland, 1973-1992, Annals of Glaciology, 24, 72-80

World Glacier Monitoring Service http://www.geo.unizh.ch/wgms/

Zemp, M., Haeberli, W., Hoelzle, M., Paul, F. (2006): Alpine glaciers to disappear within decades?, Geophysical Research Letters, vol. 33, no. 13, L13504, doi:10.1029/2006GL026319

Zeng, Q., Cao, M., Feng, X., Liang, F., Chen, X., Sheng, W. (1983): A study of spectral reflection characteristics for now, ice and water in the north of China, In: Goodison, B., ed., Hydrological applications of remote sensing and remote data treansmission, IAHS, 145, 451-462.

APPENDIX

List of Abbreviations

A.S.L	Above Sea Level
ASTER	Advanced Spaceborne Thermal Emmision Reflection Radiometer
CP	Check Point
DEM	Digital Elevation Model
ELA	Equilibrium Line Altitude
EOS	Earth Observer
ETM+	Enhanced Thematic Mapper Plus
GCP	Ground Control Point
GIS	Geographic Information System
GPS	Global Positioning System
IKONOS	Greek for *image*
IPCC	Intergovermental Panel of Climate Change
LIA	Little Ice Age
LIAM	Little Ice Age Maximum
LIDAR	Light detection and ranging
LINZ	Land Information New Zealand
NDSI	Normalised Difference Snow Index
NOAA	National Oceanic and Atmospheric Administration
NZMG	New Zealand Map Grid
NZTM	New Zealand Transverse Mercator
RMSE	Root Mean Square Error
VHR	Very-high Resolution
VIS	Visible
VNIR	Visible and Near Infrared
SPOT	Systeme probatoire pour l'observation de la terre
SRTM	Shuttle Radar Topography Mission
SWIR	Shortwave Infrared
TIR	Thermal Infrared

APPENDIX

List of figures

APPENDIX

APPENDIX

List of tables

Chapter 6 DISCUSSION